OPTIMIZATION OF SOLAR PANEL TILT ANGLES BY ISOTROPIC AND ANISOTROPIC MODELS FOR TURKEY

GÜNEŞ PANELİ EĞİM AÇILARININ İZOTROPİK VE ANİZOTROPİK MODELLERLE TÜRKİYE İÇİN OPTİMİZASYONU

ZEYGÜL TANHAN

DOÇ. DR A. UFUK ŞAHİN

Supervisor

Submitted To

Graduate School of Science and Engineering of Hacettepe University

As A Partial Fulfillment to The Requirements

For The Award of The Degree of **Master of Science**

In Civil Engineering

2022

ABSTRACT

OPTIMIZATION OF SOLAR PANEL TILT ANGLES BY ISOTROPIC AND ANISOTROPIC MODELS FOR TURKEY

Zeygül TANHAN

Master of Science, Department of Civil Engineering
Supervisor: Assoc. Prof. Dr. A. Ufuk ŞAHİN
August 2022, 97 pages

The energy resources used in the world may be insufficient in many aspects such as economic changes and living conditions in the development of countries. The popularity of renewable energy sources is increasing with the increase in the problems arising from the use of non-renewable energy sources. Solar energy plays a significant role in meeting the worldwide energy supply as a clean, reliable and accessible energy source. Achieving maximum gain from solar panels, which form the basis of solar energy, depends on geographic location, solar energy model applied and obtaining accurate data. Determining the tilt angle of the panels provides maximum efficiency from solar energy. In this study, monthly, annual and seasonal optimum tilt angles for all provinces of Turkey were obtained by using 12 isotropic and anisotropic solar radiation models. The data in the calculations are taken from satellite-based sources for the period from the beginning of 2001 to the end of 2020. In order to examine the accuracy of solar radiation models, monthly, seasonal and annual values of tilt angles were investigated. It has been observed that the optimum mean annual tilt angle obtained by using different radiation models varies between 28° and 48°. When the seasonal mean optimum tilt angles are analyzed, it is observed that the optimum tilt angles for summer and spring seasons mostly vary

between 20°-25°, 39°-53° for autumn and 46°-72° for winter. As a result of the analysis made with the real field data taken for the province of Izmir, it can be concluded that the Perez model is a suitable model for İzmir. The optimum panel inclination angles obtained in this thesis study are expected to be a literature study that guides the panel optimization for 81 provinces in Turkey, while obtaining the maximum efficiency.

Keywords: optimization, optimum tilt angle, solar energy, radiation, isotropic model, anisotropic model

ÖZET

GÜNEŞ PANELİ EĞİM AÇILARININ İZOTROPİK VE ANİZOTROPİK MODELLERLE TÜRKİYE İÇİN OPTİMİZASYONU

Zeygül TANHAN

Yüksek Lisans, İnşaat Mühendisliği Bölümü
Tez Danışmanı: Doç. Dr. A. Ufuk ŞAHİN
Ağustos 2022, 97 sayfa

Dünyada kullanılan enerji kaynakları ülkelerin gelişmesinde ekonomik değişiklikler ve yaşam şartları şeklinde birçok açıdan yetersiz kalabilmektedir. Yenilenemez enerji kaynaklarının kullanmasıyla doğan problemlerin artmasıyla yenilenebilir enerji kaynaklarının popülerliği artmaktadır. Güneş enerjisi temiz, güvenilir ve erişebilir bir enerji kaynağı olarak dünya çapındaki enerji arzını karşılayabilmek için önemli bir rol oynamaktadır. Güneş enerjisinin temelini oluşturan güneş panellerinden maksimum kazancı elde etmek coğrafi konuma, uygulanan güneş enerjisi modeline ve doğru verileri elde etmeye bağlıdır. Panellerin eğim açısının belirlenmesi, güneş enerjisinden maksimum verim elde etmeyi sağlamaktadır. Bu çalışmada, Türkiye'nin tüm illeri için aylık, yıllık ve mevsimlik optimum eğim açıları izotropik ve anizotropik olmak üzere 12 tane güneş ışınımı modeli kullanılarak elde edilmiştir. Hesaplamalardaki veriler 2001

yılının başından 2020 yılının sonuna kadar olan dönem için uydu tabanlı kaynaklardan alınmıştır. Güneş ışınımı modellerinin doğruluğunu inceleyebilmek için eğim açılarının aylık, mevsimlik ve yıllık değerleri araştırılmıştır. Farklı radyasyon modelleri kullanılarak elde edilen Optimum ortalama yıllık eğim açısının 28° ile 48° arasında değiştiği gözlemlenmiştir. Mevsimsel ortalama optimum eğim açıları analiz edildiğinde yaz ve ilkbahar mevsimleri için optimum eğim açılarının çoğunlukla 20°-25° arasında, sonbahar için 39°-53°, kış için 46°-72° arasında değiştiği gözlemlenmiştir. İzmir ili için alınan gerçek saha verileriyle yapılan analiz sonucunda Perez modelinin İzmir ili için uygun bir model olduğu sonucuna varılmıştır. Bu tez çalışmasında elde edilen optimum panel eğim açılarının, Türkiye'deki 81 il için panel optimizasyonu sağlanırken maksimum verimi elde etmesinde yol gösteren bir literatür çalışması olması öngörülmektedir.

Anahtar Kelimeler: optimizasyon, optimum eğim açısı, güneş enerjisi, ışınım, izotropik model, anizotropik model

ACKNOWLEDGMENTS

To my esteemed advisor to Assoc. Dr. A. Ufuk ŞAHİN, he guides me through my graduate education and thesis work, always encourage me with his positive attitude, and enabled me to look differently with his vast and unique knowledge and I am proud to work with and be a student of him,

To my family, who have always been by my side, who have always supported the decisions I have made, who have encouraged me not only during this work process, but throughout my entire life, and who have given me all kinds of financial and moral support, and to my fiancé, İsmail Bozoklu, who has always been by my side, who has not spared me his motivation and support in this work,

I express my endless gratitude and thank you.

Zeygul Tanhan

August 2022, Ankara.

TABLE OF CONTENTS

LIST OF FIGURES

LIST OF TABLES

SYMBOLS AND ABBREVIATIONS

Symbols

φ	Latitude Angle
δ	Declination Angle
n	Day Number of Year
θ_Z	Zenith Angle
ω	Hour Angle
β	Tilt Angle
α	Altitude Angle
t_s	Solar time
r	Correlation Coefficient
θ	Incidence Angle
ρ	Ground Albedo
max	Maximum
min	Minimum
I_{SC}	Solar Constant
w_s	Sunset hour angle
I	Instantaneous Total Radiation
I_0	Instantaneous Extraterrestrial Radiation
$I_{0\beta}$	Instantaneous Extraterrestrial Radiation on Inclined Surface
I_β	Hourly Global Solar Radiation on Inclined Surface
I_b	Beam Radiation
$I_{b\beta}$	Beam Radiation on Inclined Surface
I_d	Diffuse Radiation
$I_{d\beta}$	Diffuse Radiation on Inclined Surface
I_r	Reflected Radiation from Surface

H_0	daily extraterrestrial radiation in outside the atmosphere on horizontal surface
P_1	Sun Disc's Locality
P_2	Radiation in The Horizon Region
K	Clearness Index
ε	Discrete of Clearness
°	Degree
$°C$	Celcius
%	Percentage

Abbreviations

BM	Bugler's Model
BAM	Badescu Model
BSR	Beam Solar Radiation
DSR	Diffuse Solar Radiation
EUROSTAT	European Statistical Office
HDKR	Hay-Davies-Klutcher-Rendl
HM	Hay's Model
IEA	International Energy Agency
KLM	Klucher's Model
KM	Koronakis Model
LJM	Liu and Jordan's Model
MBE	mean bias error
MENR	Ministry of Energy and Natural Resources
MPE	mean percentage error
NSE	Nash-Sutcliffe Efficiency
OPA	Optimum Tilt Angle

PM	Perez’ Model
POWER	Prediction Of Worldwide Energy Resources
PV	Photovoltaic
RM	Reindl’s Model
RMSE	root mean squared error
SUM	Steven and Unsworth’s Model
TCM	Temps & Coulson’s Model
TM	Tian’s Model

1. INTRODUCTION

1.1. Energy

Energy is one of the main needs for human lives. Unfortunately, the world is a place where demands are infinite while supplies are insufficient. The unbalance between supply and demand for energy, the guarding and controlling the energy-lines can be typical examples of conflict reasons among the countries. To manage these problems, the energy sources should more than the existing level or alternative energy sources could be invented or discovered. According to the projections for annual energy demand under different scenarios, which was prepared by International Energy Agency (IEA), by 2040, global natural gas demand will be expected to increase by 31% to provide 17% of total energy consumed worldwide, and global oil demand will be expected to increase by 21% to provide 35% of total energy consumed as shown in Figure 1.

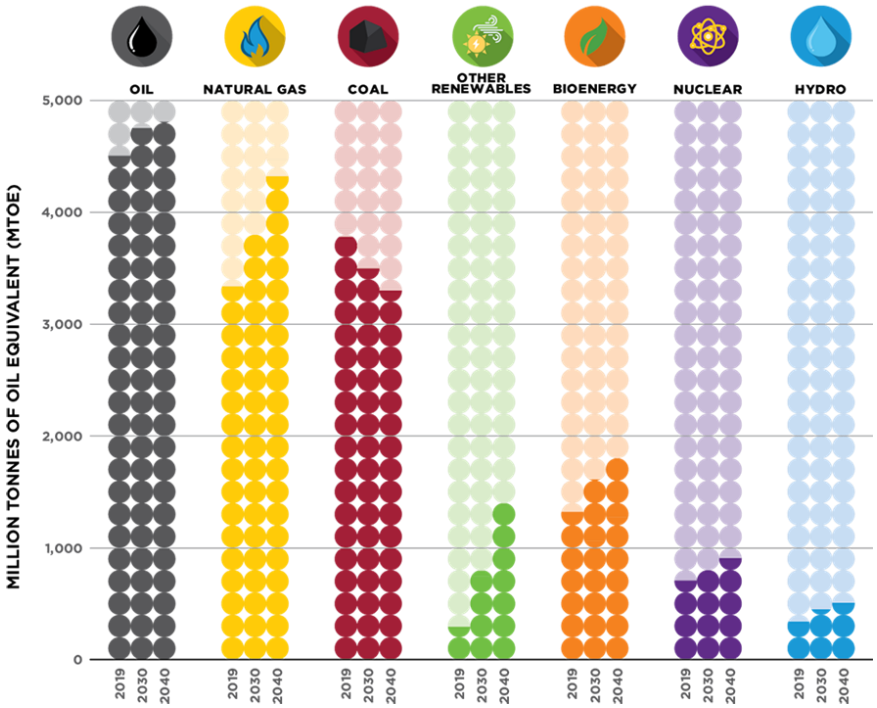

Figure 1 The Global Potential Energy Demand (The International Energy Agency (IEA))

The energy can be simply obtained from renewable and non-renewable energy sources. Figure 2 shows the world electricity generation by fuel in years between 1971 and 2019. The use of coal shows the dominant behavior about 35% and 40% and remains almost constant for given term. As seen, in 2013, the share of renewable energy in electricity production exceeded that of natural gas, and the difference between the two continued to increase. In 2019, renewable sources provide approximately 27% of electricity production, but it is seen that it is significantly higher than natural gas. The rate of nuclear energy remained stable at 10% after 2010, while oil ratio is 20% in 1970 it decreased to about 3% in 2019.

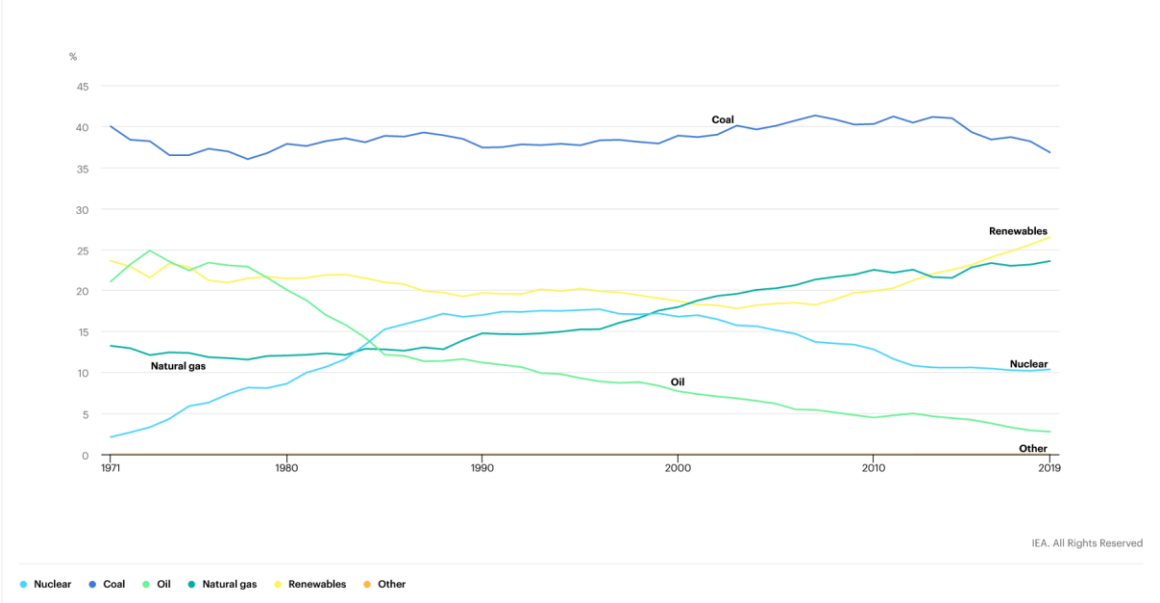

Figure 2 World Electricity Generation by Fuel in 1971-2019 (IEA)

The disposal of hazardous waste induced by non-renewable energy sources such as coal, oil, natural gas, and nuclear energy may harm to the environment. For instance, the coal can be regarded as rare source in the world, which is unevenly distributed with various qualities over the world's land. To obtain the sufficient energy from coal may need mining operation, transportation and processing. The energy production from fossil fuels is about 80 % of the world. These activities increase the carbon footprint of energy production from the coal and seems unfriendly process to the environment.

Worldwide carbon dioxide emissions from the use of fossil fuels in 2019 were 38 gigatons in 2019. The increasing carbon footprint brings on more greenhouse gases in the atmosphere. This issue can result in climate change and imbalance in the Earth's energy. As a result, non-renewable energy sources may also speed up the global warming that is the one of the most recent global issues threaten to all humanity. In order to reduce carbon dioxide emissions caused by the use of fossil fuels, people have started to prefer renewable energy sources, which are alternative energy sources. As can be seen in Figure 3, renewable energy sources have been used with a significant increase since 2010 in order to meet the electricity production demanded worldwide.

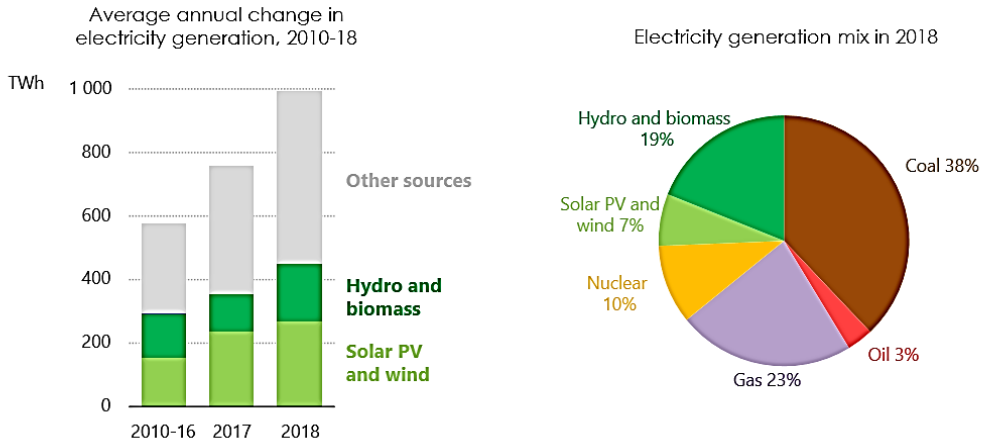

Figure 3 Electricity Production by Energy Sources (BP,2018)

Renewable energy offers sustainable and environment friendly solutions for the generation of electricity. Solar wind, hydroelectric, geothermal, hydrogen, ocean and biomass are renewable energy sources. Among the other sources, it is seen that renewable energy sources met almost 26% of electricity production needs in 2018. The Solar Photovoltaic (PV) and wind systems approximately has a noteworthy change about 430 TWh although it was near 300 TWh between 2010 and 2016 years.

The distribution of the total electrical energy produced in Turkey in 2018 is shown in Figure 4. When this distribution is analyzed, it can be seen that renewable resources have 50%, solid fuels 42%, oil 3% and natural gas 1%.

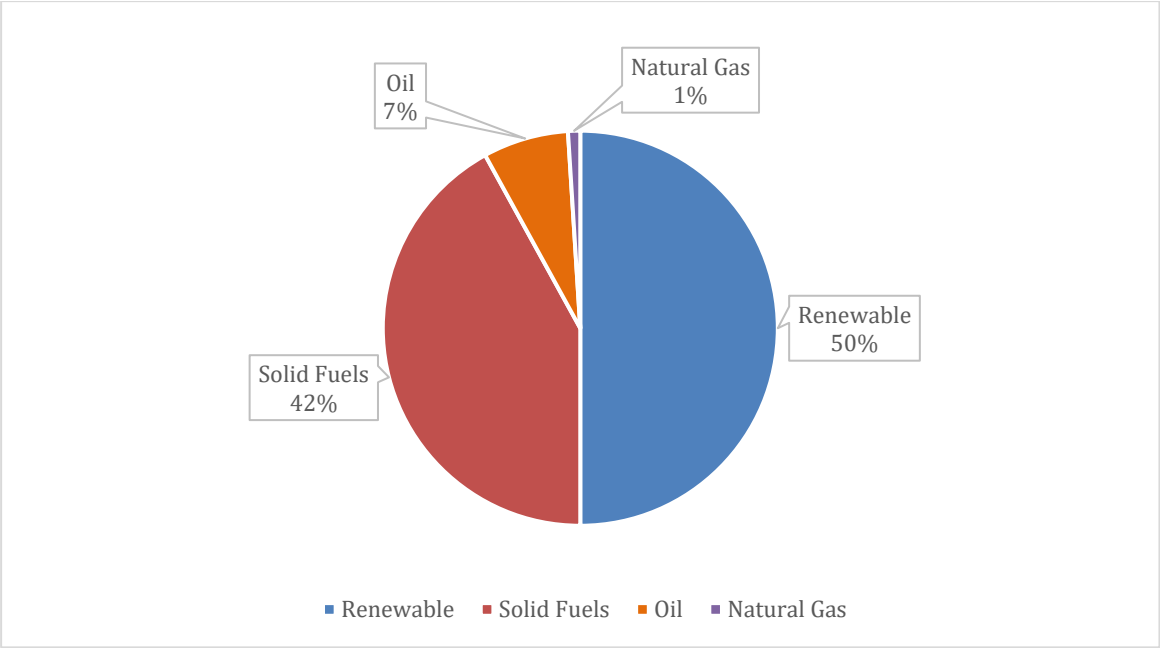

Figure 4 The total electrical energy production in 2018, Turkey (EUROSTAT)

By the end of 2018, Turkey's electricity consumption was 304,166.9 GWh, and the total of electricity supplied by renewable energy sources was 98,741.3 GWh. According to this the ratio of electricity supplied by renewable energy sources to gross electricity consumption was 32.5%. According to the European Statistical Office (EUROSTAT), when the gross electricity consumption data of EU-28 countries in 2017 is analyzed, the rate of electricity produced from renewable energy sources was 32.1%. As can be seen in the Table 1, distribution of electricity producing by renewable energy sources in 2018 for Turkey is 60.70% for hydraulic, 20.20% for wind, 7.53% for geothermal, 3.67% for biomass, and 7.90% for solar.

Table 1 Distribution of electricity producing by renewable energy sources in 2018 for Turkey (EUROSTAT)

SOURCE	PRODUCTION (GWh)	PERCENTAGE (%)
HYDRO	59.938,4	60,70
WIND	19.949,2	20,20
GEOTHERMAL	7.431,0	7,53
BIOMASS	3.662,9	3,67
SOLAR	7.799,8	7,90
TOTAL	98.741,3	100

1.2.Solar Energy

Solar energy systems, as a clean and sustainable renewable energy source, are one of the most effective alternative solutions to the increasing global warming problem. The first use of energy in the world was started with an idea which was put forward by scientist Socrates in B.C 470-399. The idea was depending on to build the southern walls of the buildings higher and to get the maximum heating efficiency from the sun in winter months. The use of solar energy continued in the 1500s with the solar pump powered by Salama de Caus. In 1868, Ericsson operated a machine with steam from solar energy. The first photovoltaic cells were discovered by Edmond Becquerel, moreover, photovoltaic panels came to life in 1893 with the invention of Charles Fritts. The introduction of solar energy to power satellites in 1958 is also an important application of solar systems. Subsequently, the oil crisis in 1973 is one of the biggest reasons for the acceleration of the trend towards solar energy. Oil prices started to increase with the oil crisis and the countries could not maintain the supply-demand balance in energy. For the sake of overcoming the lack of energy, many investor countries have turned to alternative energy sources, especially solar and wind energy. Considering the Figure 5, it could be argued that the trend towards solar energy systems has started to increase worldwide.

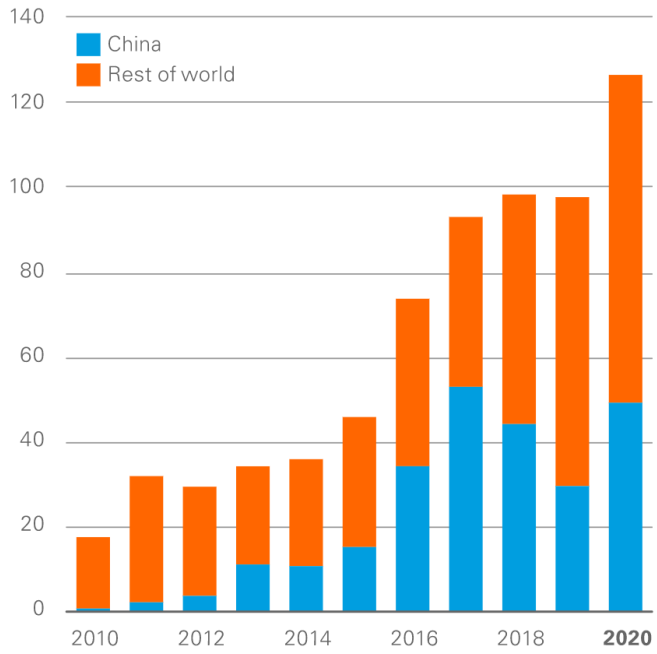

Figure 5 Annual Change of Solar Capacity, GW(BP,2021)

Solar energy is widely used worldwide and the increase in the share of solar energy use in the last 10 years can be seen in the Figure 5. While China is a leader in this regard, Japan, Germany, the USA, Italy, the United Kingdom and India are in the first place in terms of installed power. The change in the use of solar energy from renewable energy sources by years is given in the Figure 6 for Turkey. The amount of solar energy, which reached approximately 1600 Mtoe in 2018, will increase even more in the coming years. As you can be seen, there has been a noticeable increase since 2010. Until 2014, solar energy in Turkey was only used for generating hot water, drying etc. in residences and industry. After 2015, in addition to these, it has started to be used for electricity generation. This development has led to a rapid increase in the utilization of solar energy after 2015, as can be seen in Figure 6.

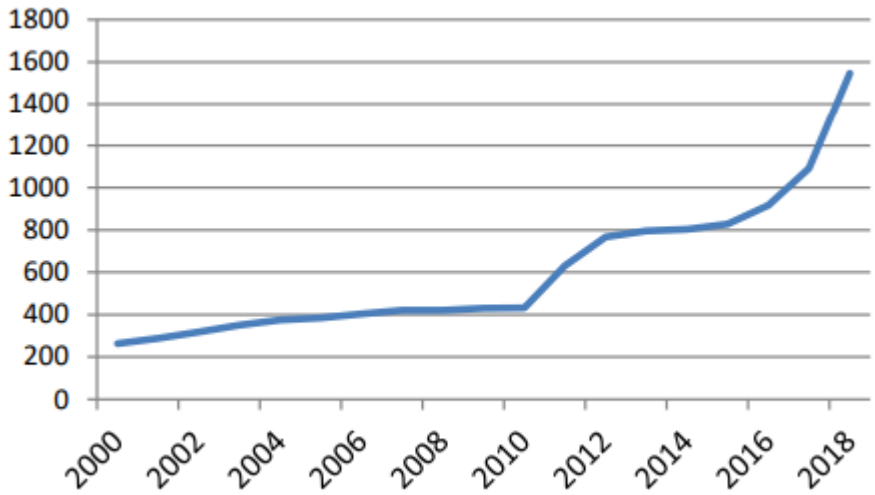

Figure 6 Change in the Amount of Solar Energy Utilized in Turkey by Years (Mtoe)

According to data from the Ministry of Energy and Natural Resources in Turkey, the annual sunshine duration of 2,741 hours, annual total solar radiation was measured as 1,527 kWh / m²year and the Global Radiation Values of Turkey is shown in Figure 7. It can be interpreted as the solar radiation in the southern region of Turkey is higher than in northern regions as seen in Figure 5. On December 2020, solar energy-based electricity installed power in Turkey is 6,667 MW, and the ratio in total electricity generation is 3.6%.

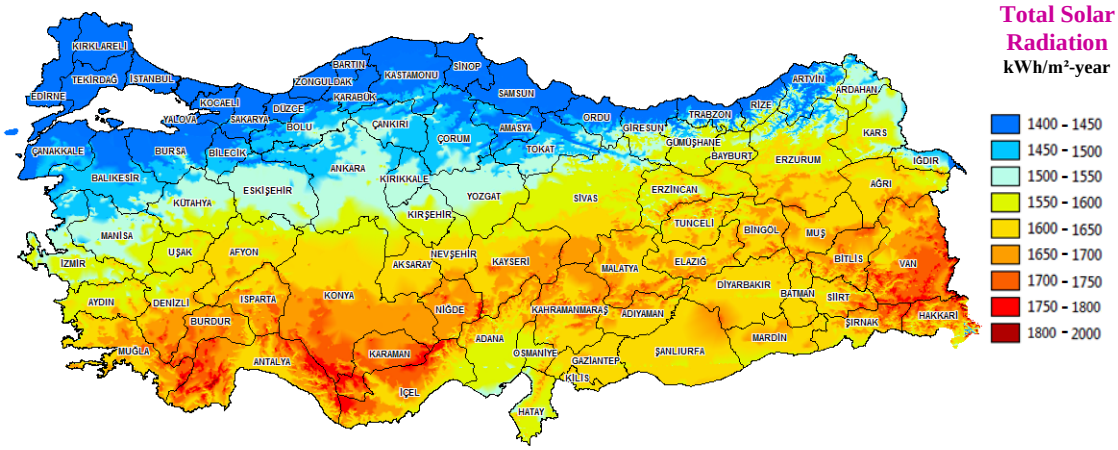

Figure 7 Solar Energy Map, Turkey (MENR)

There are the Global Radiation Values of Turkey presented in Figure 8. In the May, June, July and August months, the radiation values are higher than other months in case of daily values. The December has the smallest daily radiation with 1.59 kWh/m²- day.

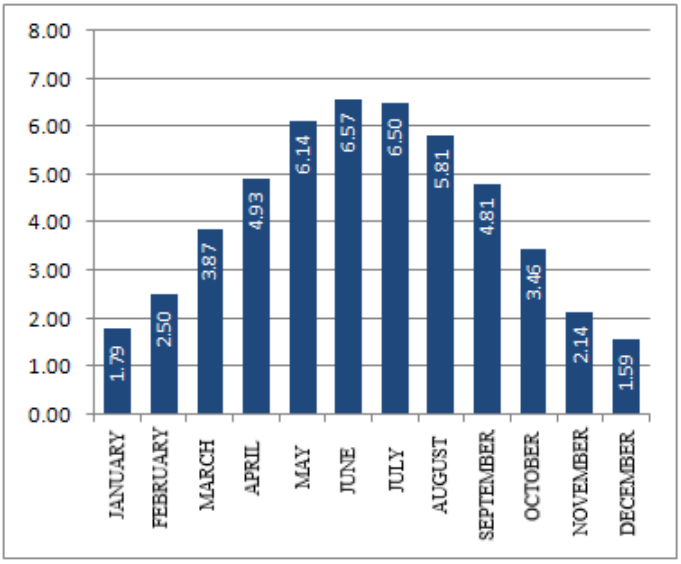

Figure 8 Global Radiation Values of Turkey (kWh/m2-day) (MENR)

There are many parameters that affect the efficiency of solar energy systems. Solar radiation intensity, panel properties and climatic conditions such as ambient temperature, wind speed, altitude, evapotranspiration can affect the efficient of the solar panels. The shady place where the solar panel is placed reduces the efficiency of solar energy. In addition, the direction of the panels also affects the efficiency, for example, for Turkey, more efficiency is obtained from the panels facing south. Overheating of the solar panels affects the decrease in the efficiency of the energy it will produce. In regions with hot climates, solar panels are mounted a little higher than the ground, providing a continuous air flow and preventing the panels from overheating. Besides that, seasons are another factor affecting panel efficiency, as the duration of sun benefiting varies.

The tilt angle is the angle of inclination between the panel surface and the horizontal plane. Tilt angle of the PV panel is one of the most important factors affecting the efficiency of increasing solar energy systems worldwide. The optimum tilt angle (OTA)

ensures maximum solar radiation which means more generation. The OTA may vary by region and seasons and the angle uses in fixed and tracking panel applications. There are many of studies, which are will be mentioned in literature review section, has conducted for OTAs in different regions. The angles are obtained as daily, monthly, seasonally, and yearly. Generally, the seasonal and monthly angles are acquired more useful in order to increasing the effectiveness of solar systems. Besides the calculations of the OTAs, the improvement of various mathematical models that examine the diffusion of extraterrestrial radiation values from the sun due to the atmosphere is also frequently found in the literature.

1.3.Literature Review

In this section, there are studies on the OTA and calculation of solar radiation in the literature. Isotropic and anisotropic radiation models were used in these studies. First, to explain the difference between the two radiation models, isotropic models suppose the volume of diffuse solar radiation (DSR) is uniform over the vault of heaven. Therefore, scattered radiation falling on an inclined surface originates from the part of the sky dome that it sees. Anisotropic models suppose DSR in the district around the sun and diffuse component isotopically reflected from the rest of the vault of heaven.

Ulgen and Hepbaslı (2002) used the climatic parameter defined as clearness index that the monthly average hourly clearness index for Izmir, Turkey (38° 24' N, 27° 14' E) by making field measurements revealed a formula that gives the index of regression analysis in form of polynomial relationship. The monthly average daily global solar radiation and the hourly total radiation on a horizontal surface were obtained by using Duffie and Beckman (1982) model. The monthly average daily hours of bright sunshine values were between 3.54 and 12.28. As a result of the regression analysis, the monthly average daily clearness index varied between 0.41 and 0.66 for a 5 year with an annual average value of 0.55. When the studies were taking into consideration it can be stated that predicting the I_d/I ratio for Izmir by these models is acceptable.

Ogulata T. and Ogulata N. (2002) estimated the monthly horizontal DSR and BSR by using meteorological measured data of Adana, Turkey. (37° 00' N, 35° 20' E). The global DSR was obtained by using clearness index. Based on calculations, the monthly average daily global radiation is 18.51 MJ/m²-day in July and 5.13 MJ/m²-day in December. The maximum global solar radiation is obtained in July. The hourly global radiation is higher when compared with the hourly DSR and BSR.

Kacira et al. (2004) conduct a study to determine OTAs and optimization of the face of photovoltaic panels by mathematical models for Sanliurfa, Turkey. (37°08' N,38°46' E) The study was based on the experiment that two single-crystalline photovoltaic panels,120 W peak power for each, were mounted on the roof of the Solar Energy Research Center located at Harran University. One of the PV panels was set up at a constant inclination angle of 14 ° and facing south. The second panel was equipped with a two-axis solar tracking system that follows the azimuth and altitude angles of the sun during the day. The research was determined that the maximum value was 61° in December while the minimum value was 13° in June according to monthly OTA results. The gain solar radiation obtained by the two-axis solar tracking system is 34.6% and south faced panels have daily average solar radiation of 29.3%. The study has underlined the effectiveness of the two-axis solar system should be compared with the amount of power generation and life cycle cost.

Mediavilla et al. (2005) performed a comparison of measured data and DSR on the inclined surface with 10 radiation models. The measured data are taken from an area of Valladolid, Spain that has south faced surface with 42° inclination. Hourly and daily DSR values were obtained, preferably, by using the Muneer model (1990) and the Reindl model (RM) (1990). When compared the result of the isotropic model, Temps-Coulson model (TCM) (1977), and measured values, a significant difference between data could be observed. For the DSR on a tilted surface, the characteristics of the work field must be considered in order to produce the most accurate results. Therefore, the data obtained from the Perez model (PM) (1990) has not given the most reliable results due to the parameters were not specifically calculated for the area in this study. The verification of results made with three statistical parameters which are RMSE, MBE, and Stone's t-

statistics. The most accurate model for this case found that the Hay model (HM) (1979), the Muneer (1990) model and the Willmott model (1982) had the most approximate results.

Menges et al. (2006) have analyzed the global solar radiation models in literature for Konya, Turkey. (37° 52' N, 32° 29' E). The study was conducted to determine the suitability of monthly global radiation values for models according to latitude, longitude, altitude, and climatic parameters by using more than 50 mathematical models in the literature. The verification of models was ensured by statistical error tests, which are percentage error, MPE, MBE, RMSE, R, and NSE. The result of statistical analysis showed that Ertekin and Yaldiz (1999) model was most accurate for the estimation of global solar radiation on a horizontal surface for Konya. When the measured global radiation values compared to predicted values, the analysis was establishing a straight line. Therefore, the model is convenient for the meteorological and geographical data of this location.

Senpınar (2006) researched for Elazıg, Turkey (38° 40' N, 39° 14' E) to obtain monthly OTA. The optimum angle of each day during the year was calculated by using MATLAB. Approximate monthly optimum angles were found with the obtained daily data. Senpınar presented that seasonal and annual optimum angle can be found in line with monthly data. According to research, the optimum angle is 34.82° for annual, 57.76° for winter, and 19.52° for summer. When these values are analyzed, it will be more advantageous to use optimum values that change according to the seasons instead of annual optimum value because there is a significant difference between winter and summer months.

Bulut and Buyukalaca (2007) have studied a model to evaluate daily global radiation by using measured data from 68 locations in Turkey throughout 10 years. The validity of the model is predicted for Adana, Ankara, Erzurum, Izmir, and Istanbul. The model calculated on a trigonometric function with one dependent parameter that is the day of the year. The model is correlated with the model in literature which is Kılıc and Ozturk (1983) model. The accuracy of the model tested by statistical analysis and coefficient (r)

is changed between 0.62 and 0.90. The model is valid for finding monthly global solar radiation for Turkey in the long term. The estimated and measured data has a high accuracy relationship.

Ertekin et al. (2008). calculated the optimal tilt angles by improving an equation that based on the latitude and day of the year. The study performed at 158 different locations in Turkey in order to make a comprehensive analysis. In the study, the regression analyzes that depending on the latitude and day of the year was conducted by using monthly average daily amount of global and DSR on a horizontal plane. The monthly OTAs were calculated based on the empirical model by Tasdemiroglu and Sever (1991) while they estimated by the improved equation over Turkey. The verification has resulted in as R2 of 98.8% with RMSE of 2.06°. Similarly, the seasonal and annual OTAs were obtained. The results showed that the OTAs showed a significant seasonal tendency with respect to the maximum amount of daily insolation. The highest OTAs observed on autumn and winter months although the lowest tilt angles obtained in summer.

El-Sebaii et al. (2010) analyzed the solar radiation on horizontal and tilted surfaces for Jeddah, Saudi Arabia. (21°42' N,39°11' E) Monthly averages daily radiation was calculated based on meteorological parameters sunshine hour, daily average ambient temperature, humidity, and cloudiness ratio. The estimations performed on the isotropic model, Liu and Jordan (1961) (LJM), and anisotropic model, Klucher (KLM) (1979). According to the results of the analysis, LJM (1961) has presented more accurate values than the KLM (1979). The study was argued that the gain of solar energy can be increased by set up the PV panels southward and OTAs in winter

($\varphi + 15$) and in summer ($\varphi - 15$) where φ is latitude degree.

Benghanem (2011) studied on optimization of tilt angle and direction of surface for Madinah, Saudi Arabia. The measured hourly global and DSR has used to calculation solar radiation on a inclined surface. Throughout the calculations, the panel surface has accepted as facing to the equator. The isotropic models and anisotropic models conducted to get OTA for all months and all stations by using MATLAB. The seasonally OTAs have found as 37° and 12° for winter and summer, respectively. The use of a yearly average

tilt angle was caused loss of energy amount of 8%. The research offered that using the yearly fixed OTA of panels is more efficient about manufacturing and installation costs.

Bakırcı (2012) presented an article with a correlation equation that function of the declination angle to obtain the monthly OTAs. The study was based on eight provinces of Turkey which are Adana, Ankara, Diyarbakir, Erzurum, Istanbul, Izmir, Samsun, and Trabzon. The average daily radiation was estimated by the isotropic model, LJM(1961). The relationship is expressed in linear, parabolic, and cubic equations. The OTAs vary between 0° in June and 65° in December for all over Turkey. Monthly solar energy values have minimum values during December. Yearly collected energy was calculated by using monthly, seasonal, and yearly optimum angles. The results show that when using a monthly average tilt angle, the gain energy has the maximum value. (i.e., The yearly collected energy for Adana lined up from 5635.86 to 6483.11 MJ/m²-year) The equations of OTA S_{opt} which depend on the declination angle was developed for Turkey. The equations give the minimum errors with respect to other equations according to the statistical test result. The determination coefficient is R^2=0.9958. By results, the equations have successful results for each province.

Stanciu C. and Stanciu D. (2014) have a comparative study on solar radiation models to determine OTAs and gain solar radiation on flat plate panels in different geographical locations. Absorbed solar radiation on flat plate panels was calculated with instantaneous solar radiation obtained by Hottel and Woertz model (1942), LJM(1961), and HDKR model. The Hotel and Woertz model (1942) was defined as the easiest way and the results are as precise as HDKR model that is the more complex model. The OTAs estimated from the LJM(1961) and HDKR model were close to each other although result of the Hottel and Woertz model (1942) was different. The difference between the maximum absorbed solar energy at the annually fixed angles and the monthly OTA was determined, which was less than 4% for all latitudes. Therefore, fixing a constant value for the annual tilt angle suggested as more efficient than using monthly tilt angles.

Ajder et al. (2018) studied annual, seasonal, and monthly OTAs of PV panels were calculated for different climatic regions. The study was performed for fixed-tilt angles for

seven locations which are on the same latitude of America with the help of mathematical models by MATLAB. Calculations were developed by the isotropic models that are LJM(1961) model and Duffie and Beckman (1982) model. When regarding the only radiation data, the OTA of fixed- PV panels is different for locations that in different climatic zones but on same latitude. This result underlines the importance of meteorological data. Also, when PV panels positioned for the seasonal optimum angle the gain energy increased between 1.75% and 3.34% concerning annual. Likewise, if the monthly optimum angle is used in place of the annual optimum angle the producted energy is approximately 4.19% for seven different locations. The research emphasized if meteorological data as cloudiness, humidity temperature, etc. are considered with solar radiation the result will be different.

Smith et al. (2016) described the integrated radiance method to calculate global radiation under all-sky conditions. The method is used with atmosphere, clouds, ozone, albedo, and aerosol input measurements to obtain irradiance on a tilted surface, horizontal surface, and OTAs for 27 locations. Verification is performed for horizontal and inclined radiation against high-quality pyranometer data. The estimated annual horizontal by the model has differences of MBE of +0.56% and RMSE of 6.69%. The optimal tilt angles are steeper than estimations of Muneer (1990) for European and African countries. The model can be applied anywhere on the surface since satellite, cloud and atmospheric data are available worldwide.

Berisha et al. (2017) analyzed the OTAs and the gain in the solar energy by estimations for south-facing panels in Pristina. The optimal tilt angles were estimated monthly, seasonal, and annually with reference to LJM isotropic model (1961). The annual OTA for Pristina location obtained as 34.7°. When the panel mounted at seasonally, monthly, and annually OTA, the gain in solar energy predicted as 21.35%, 19.98%, 14.43%, respectively. The maximum solar energy was obtained using a monthly OTA. The seasonally optimum angle results in energy losses about 1.13% and annual energy losses reached 5.7%.

Maleki et al. (2017) conducted a comprehensive review study that examines the mathematical models to evaluate the direct, diffuse and reflected solar radiation on both horizontal and inclined planes. The study upholds that research latitude, which depends on location, is an important parameter for radiation models to make accurate estimating of solar radiation. The clearness index was played a major role throughout the computations. The finding DSR on the inclined surface the most accurate isotropic models are LJM (1961) and Koronakis model (KM) (1986). Besides that, anisotropic models which are the PM (1990), TCM (1977), KLM (1979), and Bugler Model (BM) (1977) have the most accurate results.

Kallioglu et al. (2017) carried out a study that determined the optimum panel angle for each month of Gaziantep, Turkey (37° 3' N, 37° 22' E) by using meteorological radiation data on the horizontal plane. OTAs calculated as 52°, 19°, 5°, and 44° respectively for winter, spring, summer, and autumn months. The maximum and minimum monthly OTAs are 0° and 57°, respectively. The annual OTA was determined as 30°. In the light of results, the monthly changes of tilt angles, increases the annual productivity up to 14% and annual gain radiation reaches up to 4951 W/m². In this region where the months of December and January are 80% closed, the panel angles should be adjusted according to these months. Therefore, they suggest that the PV panel's angle should change with respect to monthly/seasonally to obtain maximum energy from solar energy systems.

Danandeh and Mousavi G. (2018) reviewed many models that suitable for estimate solar irradiance on horizontal and tilted surfaces. The main approaches to finding OTAs have performed for different provinces of Iran. On the calculation of DSR, the global irradiance data and environmental conditions were considered. The one of them of main approaches is the search-based approach and the other is the direct approach. The direct approach based on the idea that panels fixed to the south face on the north face and panels fixed to the north face on the south face. This approach has accomplished with radiation models that LJM(1961) and Hottel and Woertz (1942). Accurate models and OTAs have selected for many countries of Europe, Australia, Asia, America, and Africa. The global irradiance for cities of Iran has determined by OTA calculations. In the light of results, a relation was detected between the HM (1979) and Skartveit and Olseth model (1987).

Cağlar (2018) offered monthly OTAs for Adana, İstanbul, Ankara, and Erzurum provinces in Turkey. The purpose of this study was to minimize the effects of time and region on the OTAs and productivity of solar collectors. To shed light upon the idea, the cities were selected from four different degree-day regions in Turkey. To compare results, the theoretical method and Hottel and Woertz model (1942) were used to calculating the daily and monthly OTAs. The results from the theoretical method show that the maximum tilt angle was determined as 56° for Erzurum in December. On the other hand, the minimum angle was obtained as 12° for Adana in June. The results found with the Hottel and Woertz method (1942) are always higher for all four cities, the difference was increased to 19.3% in winter months with large OTAs and decreased to 4% with the tilt angle decreasing in summer. The OTA has higher values due to the low declination angle in winter, and in summer it has lower values as the declination angle increases and the sun rays are vertical to the tropic of cancer. It has been concluded that the differences between the cities are caused by the difference in latitude and altitude values and that the geographical features of the region are an essential factor in the different inclination angles.

Table 2 Comparison and Summary of Literature Review

	NAME	LOCATION	USED MODEL	OBTAINED PARAMETERS
1	Cağlar (2018)	Adana, İstanbul, Ankara, And Erzurum	Hottel And Woertz Model (1942)	The Daily and Monthly Optimum Tilt Angles
2	Danandeh And Mousavi G.(2018)	Iran	Liu And Jordan (1961) And Hottel And Woertz (1942). Hay Model (1979) And Skartveit And Olseth Model (1987).	The Global İrradiance, Optimum Tilt Angles
3	Kallioglu Et Al. (2017)	Gaziantep	Liu And Jordan Model (1961)	Monthly, Seasonal, Annual Optimum Tilt Angles
4	Maleki Et Al. (2017)		Liu And Jordan Model (1961),Koronakis Model (1986), Perez (1990), Temps-Coulson (1977), Klucher (1979), And Bugler (1977)	Direct, Diffuse and Reflected Solar Radiation On Both Horizontal And İnclined Planes

5	Berisha Et Al. (2017)	Pristina	Liu And Jordan İsotropic Model (1961).	Optimal Tilt Angles Were Estimated Monthly, Seasonal, And Annually
6	Smith Et Al. (2016)	27 Locations	Muneer (1990)	İrradiance On A Tilted Surface, Horizontal Surface, And Optimum Tilt Angles
7	Ajder Et Al. (2018)	America	Liu And Jordan (1961) Model And Duffie And Beckman (1982) Model	Annual, Seasonal, And Monthly Optimum Tilt Angles
8	Stanciu C. And Stanciu D. (2014)	Different Locations on Earth	Hottel And Woertz Model (1942), Liu And Jordan Model (1961), And HDKR Model	Determine Optimum Tilt Angles and Gain Solar Radiation On Flat Plate Panels
9	Bakırcı (2012)	Adana, Ankara, Diyarbakir, Erzurum, Istanbul, Izmir, Samsun, And Trabzon.	Liu And Jordan (1961).	The Monthly Optimum Tilt Angles
10	Benghanem (2011)	Madinah, Saudi Arabia		Optimization Of Tilt Angle
11	El-Sebaii Et Al. (2010)	Jeddah, Saudi Arabia.	Liu And Jordan (1961), And Anisotropic Model, Klucher (1979).	The Solar Radiation On Horizontal And Tilted Surfaces
12	Ertekin Et Al. (2008).	At 158 Different Locations İn Turkey	Tasdemiroglu And Sever (1991).	Optimal Tilt Angles
13	Bulut And Buyukalaca (2007)	Adana, Ankara, Erzurum, Izmir, And Istanbul		Daily Global Radiation
14	Senpınar (2006)	Elazıg, Turkey		Obtain Monthly Optimum Tilt Angle
15	Menges Et Al. (2006)	Konya, Turkey	More Than 50 Mathematical Models	Monthly Global Radiation
16	Mediavilla Et Al. (2005)	Valladolid, Spain	10 Radiation Models	Diffuse Solar Radiation On The İnclined Surface
17	Kacira Et Al. (2004)	Sanliurfa, Turkey	Mathematical Model And By A Computer Package.	Optimum Tilt Angles
18	Ogulata T. And Ogulata N. (2002)	Adana, Turkey.		Monthly Horizontal Diffuse And Direct Radiation
19	Ulgen And Hepbaslı (2002)	For Izmir, Turkey	Duffie And Beckman (1982)	Monthly Average Daily Global Solar Radiation And The Hourly Total Radiation On A Horizontal Surface

According to the summary literature review shown above also in Table 2, analyzes based on various mathematical models were made for Turkey. Many of these studies have examined the OTA based on the isotropic model for DSR values. However, the literature discussed in this study did not cover the applicability of anisotropic models for Turkey. In this way, the optimum panel tilt angle will be calculated.

1.4.Scope Of Thesis

As a merit of this study, the OTA, which is the tilt angle of solar PV panels, was investigated. As mentioned before, the OTA is one of the most important parameters affecting the efficiency of panels and solar energy systems. The OTA is the tilt angle at which the panels can receive the maximum radiation. As can be seen in the literature review chapter, the OTA has been examined for some provinces of Turkey, but not for the whole of Turkey. In this study, the OTAs of 81 provinces in Turkey investigated monthly, seasonally and annually. In order to comprehensively detail the OTA values, 4 isotropic diffuse model and 8 anisotropic diffuse models are used. Besides, Maximum efficiency was expressed with geographical and climatic dependencies using anisotropic models. The existence of a new mathematical model was investigated with multivariate regression analysis. Common mathematical optimization methods used to calculate the tilt angle values and the obtained value will be created for a yield map for the whole of Turkey. For this purpose, solar radiation data is available from the NASA Worldwide Energy Resources Estimate for 20 years of Meteorological and Solar Monthly and Annual Climatology values (January 2001 - December 2020).

1.5.Thesis Organization

This thesis manuscript was organized in five chapters. In introduction part, the main topic and scope of the thesis were mentioned. In the last part of this section, a comprehensive literature review including the optimization and applications of solar panels will be presented In the theoretical background section, solar geometry will be introduced, and the detailed information will be given about the correlations which are used over the methodology. Furthermore, the theoretical all radiation models including isotropic and anisotropic models used for various regions and climates will be shown. In the optimization models chapter, OTAs for each province obtained by using mathematical

optimization methods with isotropic and anisotropic models the statistical correlations of data will be obtained in the sequel. The results obtained in the results and discussions section will be demonstrated in detail. The results of optimization models by using MATLAB will be interpreted in the last section and recommendations will be made for coming studies.

2. METHODOLOGY

In this section, first of all, solar geometry will be explained and angles used in solar geometry will be defined. Solar radiation will be defined and solar radiation types will be presented with their formulas. Afterwards, 12 isotropic and anisotropic radiation models used in this study will be explained. The Golden - Ratio Search Algorithm to be used to obtain the OTAs will be explained. It will be mentioned how the radiation data used in the calculations in the thesis were obtained from NASA. How the obtained data will be used and the flow of the thesis can be seen in the flowchart given in the Figure 9 below.

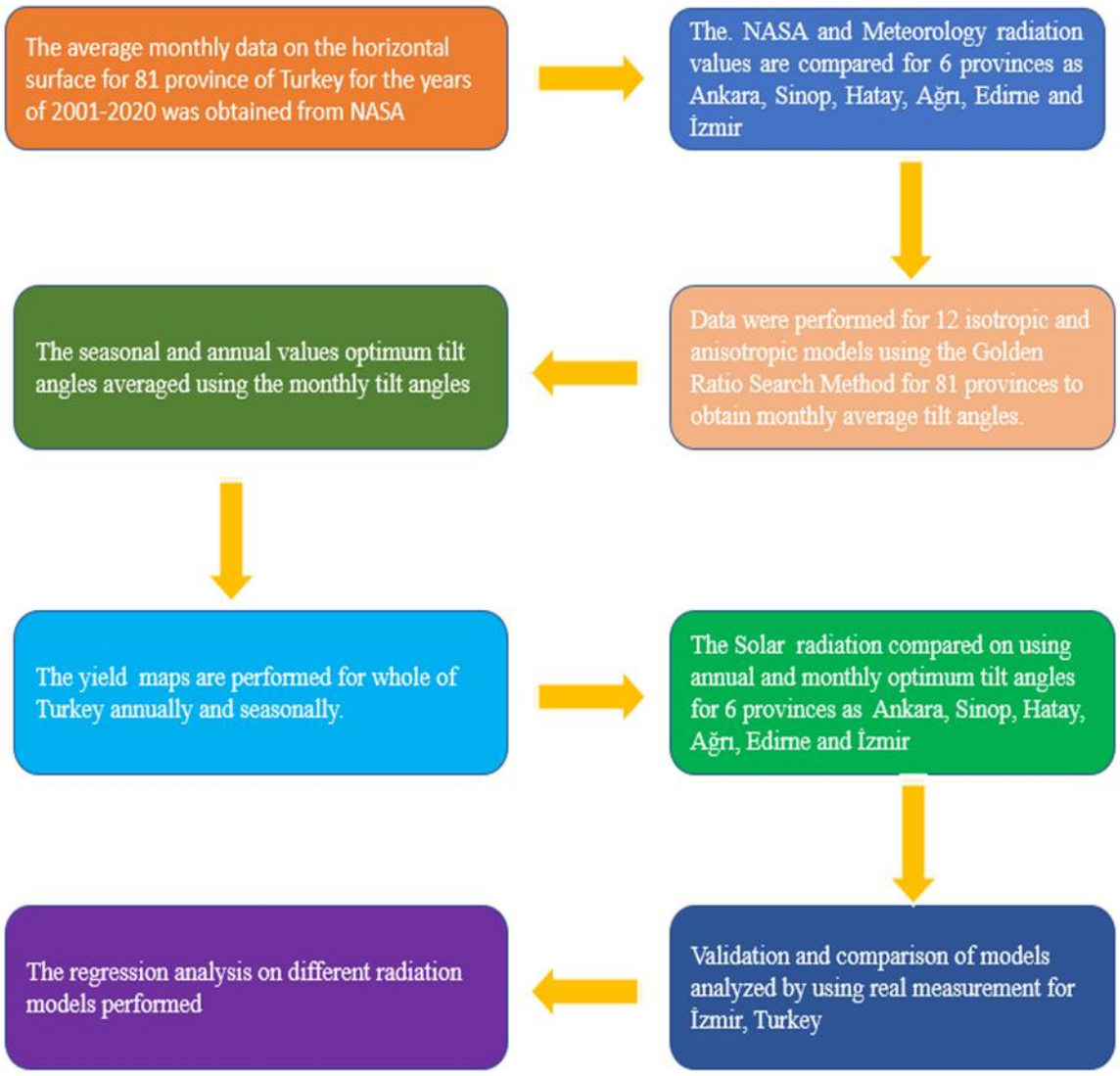

Figure 9 The Flowchart of Thesis Methodology

2.1. Solar Geometry

The solar geometry made up with solar angles for finding the solar radiation values on a fixed or moving panel. The main solar angles were enlightened in chapter and the schematic representation of angles can be seen in Figure 10.

2.1.1. Latitude Angle (ϕ)

The latitude angle is the angle between the lines towards the center of the earth and the equatorial plane. The southern hemisphere was considered negative while the northern hemisphere was positive and the latitude angle is assumed to vary between - 90° and 90°.

2.1.2. Declination Angle (δ)

The declination angle is the angle of the sun's rays with the equator. It occurs while the Earth makes an angle of 23.45 degrees with the orbital plane. It varies with minimum -23.45° in winter solstice for northern hemisphere, 22 December, and maximum 23.45° in summer solstice for northern hemisphere, 22 June. The autumnal equinox and vernal equinox are events that occurs when the sunlight come to the equator at steep angles twice a year. Therefore, declination angle is 0° on 23 September, autumnal equinox, and 20 March, vernal equinox. The declination angle can be calculated by Cooper (1969):

$$\delta = 23.45 \sin\left(360 \frac{284+n}{365}\right) \tag{2.1}$$

where n is the day number starting from January 1.

2.1.3. Zenith Angle (θ_z)

The zenith angle is can be defined as the angle between the direction of the sun lights and the steep axis of the horizontal plane. The zenith angle is 0 degrees at noon while 90 degrees at sunset and sunrise. Zenith angle can be obtained by Duffie and Beckman (1982):

$$\cos\theta_z = \cos\delta \cos\phi \cos w + \sin\delta \sin\phi \tag{2.2}$$

where δ is declination angle, ϕ is latitude angle and ω is hour angle in degrees.

2.1.4. Tilt Angle (β)

Tilt angle is the angle of inclination between the panel surface and the horizontal plane and it is an important parameter that affects the solar energy systems about gained energy. Tilt angle changes between $0° \leq \beta \leq 180°$.

2.1.5. Azimuth Angle (γ)

The azimuth angle is the projection of vertical axis of the surface on horizontal plane in the south direction. It is varying from south as negative in east direction and positive in west direction. It is assumed as $0°$ on the south-faced surface whereas $180°$ at noon. $-180 \leq \gamma \leq 180$.

It can be calculated from equation:

$$\gamma = \cos^{-1}[(\sin(\alpha)\sin(\phi) - \sin(\delta)) / (\cos\alpha)\cos(\phi)] \quad (2.3)$$

where α is the solar altitude angle.

2.1.6. Solar Altitude Angle (α)

Solar altitude angle is the angle between the sun's direct beam and the horizontal plane. It is also defined as the height of the sun from the horizon line. The minimum value of altitude angle is $0°$ at sunset and sunrise. The maximum angle is at noon with $90°$. Altitude angle is component of zenith angle and it can be expressed as:

$$\alpha = 90 - \theta_Z \quad (2.4)$$

2.1.7. Hour Angle ω

The hour angle is an angular displacement occurred by the earth rotating $15°$ per hour around its axis and it is defined as the angle between the longitude of the selected region and the longitude of the sun lights. The hour angle is $0°$ at noon and it was assumed as negative in the mornings and positive in afternoons. The hour angle can be calculated from equation:

$$\omega = 15(t_S - 12) \tag{2.5}$$

where t_S is solar time and it is taken as 12 at noon.

2.1.8. Incidence Angle (θ)

The sun's angle of incidence is the angle formed between the normal of the surface and the direct sun radiation on that surface. If the surface of the panel is perpendicular to the direct radiation the θ is $0°$, if they are parallel θ becomes $90°$. The incidence angle can be obtaining with following equation:

$$\theta = \cos^{-1}(\sin\delta \sin(\phi - \beta) + \cos\delta \cos\omega \cos(\phi - \beta)) \tag{2.6}$$

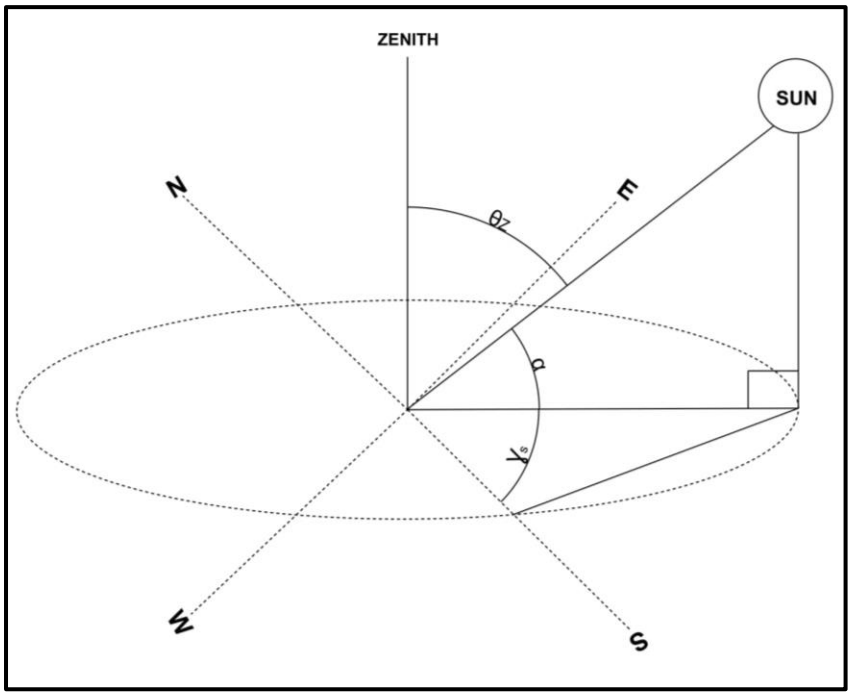

(a)

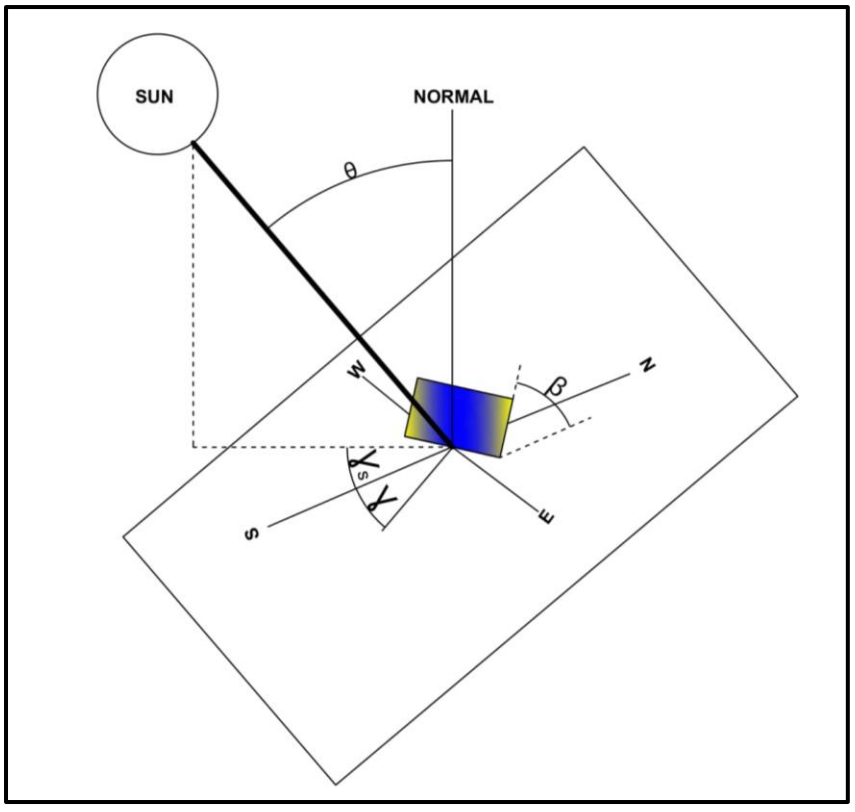

(b)

Figure 10 The Solar Angles on Inclined Surface

2.2 Solar Radiation

2.2.1. Extraterrestrial Solar Radiation

One of the key points of making the most efficient use of solar energy is the solar radiation that occurs on the earth. The position of the sun changes as the Earth rotates around its axis and in the ellipse orbit around the sun. The distance between the Earth and the sun is approximately 1.495 x 10^{11} m, when considering that it changes according to the seasons. All the solar radiation emitted from the sun could not reach the earth's surface. Approximately 45% of incoming solar radiation arrives at the earth, while 55% reflects from the atmosphere and returns to space. Some of the solar radiation entering the atmosphere is used to heat the surface, and almost 30% is reflected from the clouds into space. The daily extraterrestrial radiation in outside the atmosphere on horizontal surface H_0 can be expressed as:

$$H_0 = \frac{24x3600I_{sc}}{\pi}\left[1+0.033\cos\left(\frac{360n}{365}\right)\right]x\left[\cos\phi\cos\delta\sin\omega_s+\frac{2\pi\omega_s}{360}\sin\phi\sin\delta\right] \quad (2.7)$$

where n is the number of the days which start from 1 January, I_{sc} is the solar constant that solar radiation of all wavelengths perpendicular to a plane per unit time in outside of the atmosphere and it defined as 1366 W/m². The ω_s is sunset hour angle as

$$\omega_s = \cos^{-1}(-\tan\phi\tan\delta) \quad (2.8)$$

The instantaneous extraterrestrial radiation I_0 which was used for the calculation of radiation in period between two different hours can be computed as

$$I_0 = \frac{12x3.6}{\pi}I_{sc}\left(1+0.033\cos\left(\frac{360n}{365}\right)\right)x\left((\sin\phi\cos\delta)x(\sin\omega_2-\sin\omega_1)+\frac{\pi(\omega_2-\omega_1)}{180}(\sin\phi\sin\delta)\right)$$

(2.9)

2.2.2. Solar Radiation on a Horizontal Plane

The solar radiation on a horizontal surface can be classified into two categories namely, beam solar radiation (BSR) and diffuse solar radiation (DSR). BSR (I_b) is the radiation generated by the sun rays coming directly, without any diffusion, from the sun on a normal surface in a unit area. The BSR on a horizontal surface could be acquired by equation,

$$I_b = I_{bN} \cos\theta_z \tag{2.10}$$

where I_{bN} is direct normal radiation which measures with a pyrheliometer.

The total solar radiation on the horizontal plane (I_T) can be simply obtained by summation of BSR and DSR. The DSR (I_d) can be defined as solar radiation on a surface by scattering or reflecting from the dust particles, water vapor cloud. The correlation developed by Orgill and Hollands (1977) can be one of the common methods that enable us to obtain DSR using the clearness index, K_t.

$$\frac{I_d}{I} = \begin{cases} 1.0 - 0.249K_t & K_t < 0.35 \\ 1.557 - 1.84K_t & 0.35 < K_t < 0.75 \\ 0.177 & K_t > 0.75 \end{cases} \tag{2.11}$$

The clearness index (K_t) is a definition indicating the clearness of the atmosphere with a low value in cloudy weather and high value in the clear sky. While its value varies between 1 and 0 it can be expressed by the ratio of instantaneous total radiation (I) to instantaneous extraterrestrial radiation (I_0).

$$K_t = \frac{I}{I_0} \tag{2.12}$$

The hourly global solar radiation on an inclined surface (I_β) classified into three components, namely, the BSR $(I_{b\beta})$, the DSR on inclined surface $(I_{d\beta})$ and the reflected radiation from surface (I_r) which is simplified as

$$I_\beta = I_{b\beta} + I_{d\beta} + I_r \tag{2.13}$$

The hourly direct radiation on an inclined surface $(I_{b\beta})$ can be defined by Iqbal (2012) as

$$I_{b\beta} = r_b I_b \tag{2.14}$$

Where r_b is a coefficient factor that ratio of extraterrestrial radiation on inclined surface $(I_{0\beta})$ to on horizontal surface (I_0).

$$r_b = \frac{I_{0\beta}}{I_0} \approx \frac{\cos\theta}{\cos\theta_z} \tag{2.15}$$

The determination of reflected radiation (I_r) can be provided as,

$$I_r = I_t \rho \left(\frac{1-\cos\beta}{2} \right) \tag{2.16}$$

where ρ is world's ground albedo.

The DSR on the inclined surface ($I_{d\beta}$) can be evaluated with I_d by means of isotropic and anisotropic models. The methodology of this study will substantiate both isotropic and anisotropic models using radiation data.

2.2.3. Diffuse Radiation Models

2.2.3.1. Isotropic Models

Isotropic radiation models (IRM) are used to obtain DSR, and it is assumed that the radiation is entirely uniformly distributed in calculations. The summary of the models can be seen in Table 5.

1. **Badescu Model**

Badescu (2002) proposed the model that used for DSR on inclined surface. The expression:

$$I_{d\beta} = \left(\frac{3 + \cos\ 2\beta}{4} \right) \times I_d \tag{2.17}$$

2. **Koronakis' Model**

Koronakis (1986) presented a model which valid for vertical south faced plane to calculate the 66.7% of DSR.

$$I_{d\beta} = \frac{1}{3}\left(\frac{1}{2 + \cos\beta} \right) \times I_d \tag{2.18}$$

3. Liu and Jordan's Model

LJM(1961) isotropic sky model commonly preferred in many studies. The DSR equation:

$$I_{d\beta} = \left(\frac{1+\cos\beta}{2} \right) \times I_d \tag{2.19}$$

4. Tian's Model

The Tian (2001) DSR model as follows:

$$I_{d\beta} = \left(1 - \frac{\beta}{180} \right) \times I_d \tag{2.20}$$

2.2.3.2. Anisotropic models

The anisotropic diffuse models (ARM) assume sky conditions which specifically change according to research location and area. In this case, the results of anisotropic models can be deemed more realistic for many areas. The summary of the models can be seen in Table 5.

1. Bugler's Model

Bugler (1977) introduced an anisotropic model to literature by considering the angular height of the sun. The model expression is:

$$I_{d\beta} = \left(\frac{1+cos\beta}{2} \left(I_d - 0.05 \frac{I_{b\beta}}{cos\theta_z} \right) \right) + 0.05 I_{b\beta} cos\theta \tag{2.21}$$

2. Temps & Coulson's Model

Temps and Coulson (1977) added two terms to LJM's isotropic model and the adjusted anisotropic model is:

$$I_{d\beta} = \frac{1}{2} I_d (1 + cos\beta) P_1 P_2 \tag{2.22}$$

$$P_1 = 1 + cos^2\theta (sin^3\theta_z) \tag{2.23}$$

$$P_2 = 1 + sin^3\left(\frac{\beta}{2}\right) \tag{2.24}$$

where P_1 represents the sun disc's locality, and P_2 defines the radiation in the horizon region.

3. Hay's Model

The Hay model (1979) is proposed by Hay and Davies with two main assumptions that source DSR. these are presented with anisotropy function, f_{Hay}. The DSR calculation is:

$$I_{d\beta} = I_d \left[f_{Hay} \left(\frac{cos\theta}{cos\theta_z} \right) + \left(\frac{1 + cos\beta}{2} \right) (1 - f_{Hay}) \right] \tag{2.25}$$

$$f_{Hay} = \frac{I_b}{I_0} = \frac{I_H - I_d}{I_0} \tag{2.26}$$

4. Reindl's Model

Reindle (1990) has developed an anisotropic model to the idea of the HM (1979) based on DSR on the horizon region. The model includes the modification index, f_R, which represent the relation between radiation and cloudy sky. The expression of DSR model is:

$$I_{d\beta} = I_d \left[f_{Hay} \left(\frac{cos\theta}{cos\theta_z} \right) + \left(\frac{1+cos\beta}{2} \right) (1 - f_{Hay}) \left(1 + f_R sin^3 \left(\frac{\beta}{2} \right) \right) \right] \quad (2.27)$$

$$f_R = \sqrt{\frac{I_b}{I_H}} \quad (2.28)$$

5. Klucher's Model

The Klucher's anisotropic model (1979) is a modified model of TCM (1977) and LJM (1961). The Klucher (1979) argues that LM (1961) useful for fully cloudy sky conditions while cannot provide correct results for partly sky conditions. In the light of that a function, f_k, proposed by Klucher to TCM (1977) thus the DSR equations formed as:

$$I_{d\beta} = I_d \left[\frac{1}{2} \left(1 + cos \left(\frac{\beta}{2} \right) \right) \right] \left[1 + f_k cos^2\theta \ \ sin^3\theta_z \ \right] \left[1 + f_k sin^3 \left(\frac{\beta}{2} \right) \right] \quad (2.29)$$

$$f_k = 1 - \left(\frac{I_d}{I_H} \right)^2 \quad (2.30)$$

6. Klucher and Reindl, and Hay and Davies (HDKR) Model ' Model)

HM (1979), Davies, KLM (1979), and RM (1990) proposed an anisotropic model named as the HDKR model. The model was based on KLM's horizon region diffusion assessment and the equation defined as follows:

$$I_{d\beta} = I_d \left[\left(\frac{1+cos\beta}{2} \right) (1 - f_{Hay}) \left(1 + f_R sin^3 \left(\frac{\beta}{2} \right) \right) \right] \quad (2.31)$$

7. Steven and Unsworth's Model

Steven and Unsworth (SUM) (1980) proposed the anisotropic model as:

$$I_{d\beta} = I_d \left[\left(0.51 \left(\frac{\cos\theta}{\cos\theta_z} \right) \right) + \left(\frac{1+\cos\beta}{2} \right) - \frac{1.74}{1.26\pi} \left\{ \sin\beta - \beta\frac{\pi}{180}\cos\beta - \pi\sin^2\frac{\beta}{2} \right\} \right] \quad (2.32)$$

8. Perez' Model

Perez model (1990) is a numerical analysis method to estimate the DSR, which is categorized in three as isotropic background, horizon zones and circumsolar. The expression is:

$$I_{d\beta} = I_d \left[\frac{1+cos\beta}{2} \ 1-F_1 \ + F_1 \frac{a_1}{a_2} + F_2 sin\beta \right] \quad (2.33)$$

where a_1 and a_2 corresponds to the angles of the circumsolar region.

$$a_1 = max \ \ 0, cos\theta \quad (2.34)$$

$$a_2 = \max \ \ \cos 85°, \cos\theta_z \quad (2.35)$$

F_1 represents the circumsolar coefficients and F_2 is the dimensionless horizon brightness the equations are as follows and the brightness coefficients are given in Table 4:

$$F_1 = \max\left\{ 0, \left[F_{11} + F_{12}\Delta + F_{13}\theta_z \left(\frac{\pi}{180} \right) \right] \right\} \quad (2.36)$$

$$F_2 = \left[F_{12} + F_{22}\Delta + F_{23}\theta_z \left(\frac{\pi}{180} \right) \right] \quad (2.37)$$

$$\Delta = m\frac{I_d}{I_0} \quad (2.38)$$

where m is the air mass, I_d is DSR on horizontal surface and I_0 is extraterrestrial radiation. Air mass is the path length that light takes in the atmosphere normalized to the shortest possible path length. Air Mass measures the decrease in the power of light as it passes through the atmosphere and is absorbed by air and dust.

$$m = \frac{1}{cos\theta_z} \tag{2.39}$$

In the Table 3 the data of ε which is the function of direct radiation (I_b) and DSR (I_b) is given.

$$\varepsilon = \frac{\frac{I_d + I_b}{I_d} + 5.535\, x\, 10^{-6}\theta_z^3}{1 + 5.535\, x\, 10^{-6}\theta_z^3} \tag{2.40}$$

Table 3 Sky Clearness Range

ε discrete	Lower Bound	Upper Bound
1 Overcast	1	1.065
2	1.065	1.230
3	1.230	1.500
4	1.500	1.950
5	1.950	2.800
6	2.800	4.500
7	4.500	6.200
8 Clear	6.200	∞

Table 4 Brightness coefficients for irradiance

ε discrete	F_{11}	F_{12}	F_{13}	F_{21}	F_{22}	F_{23}
1.000	-0.008	0.588	-0.062	-0.06	0.072	-0.022
1.065	0.130	0.683	-0.151	-0.019	0.066	-0.029
1.230	0.330	0.487	-0.221	0.055	-0.064	-0.026
1.500	0.568	0.187	-0.295	0.109	-0.152	-0.014
1.950	0.873	-0.392	-0.362	0.226	-0.462	0.001
2.800	1.132	-1.237	-0.412	0.288	-0.823	0.056
4.500	1.06	-1.6	-0.359	0.264	-1.127	0.131
6.200	0.678	-0.327	-0.25	0.156	-1.377	0.251

Table 5 Summary of Radiation models

	NAME OF THE MODEL	**INPUT PARAMETERS**	**POINT**
A-ISOTROPIC MODELS			
1	Badescu (2002)	Diffuse radiation on inclined surface	Assuming sky radiance is isotropic
2	Koronakis (1986)	Diffuse radiation on inclined surface	Assuming sky radiance is isotropic
3	Liu and Jordan (1961)	Diffuse radiation on inclined surface	Assuming sky radiance is isotropic
4	Tian (2001)	Diffuse radiation on inclined surface	Assuming sky radiance is isotropic

B-ANISOTROPIC MODELS			
1	Bugler (1977)	Diffuse radiation on inclined surface, Beam radiation on inclined surface, Zenith angle, Incidence Angle	Fraction of the direct beam radiation
2	Temps and Coulson (1977)	Diffuse radiation on inclined surface, Zenith angle, Incidence Angle	Horizon brightening of the daytime sky
3	Hay model (1979)	Diffuse radiation on inclined surface, Beam radiation on inclined surface, instantaneous extraterrestrial radiation	Fraction of the direct beam radiation
4	Reindle (1990)	Diffuse radiation on inclined surface, Beam radiation on inclined surface, instantaneous extraterrestrial radiation	Circumsolar brightening and horizon brightening
5	Klucher (1979)	Diffuse radiation on inclined surface, Beam radiation on inclined surface, instantaneous extraterrestrial radiation	Assumes as cloudy sky varies from clear to overcast

6	HDKR (Hay (1979), Davies, Klucher (1979), and Reindl (1990))	Diffuse radiation on inclined surface, Beam radiation on inclined surface, instantaneous extraterrestrial radiation	Incorporates isotropic diffuse, circumsolar radiation and horizontal brightening.
7	Steven and Unsworth (1980)	Diffuse radiation on inclined surface, Beam radiation on inclined surface, Zenith angle, Incidence Angle	Assumes as cloudy sky varies from clear to overcast
8	Perez model (1990)	Diffuse radiation on inclined surface, Angles of the circumsolar region, dimensionless horizon brightness, air mass, Diffuse radiation on horizontal surface, Extraterrestrial radiation, Sky clearness index	The model assumes three sky regions with different diffuse radiation intensities: the circumsolar region, the region over the horizon line and the rest of the sky which is isotropic.

2.3 Golden-Ratio Search Algorithm and Optimization

Golden ratio search method Kiefer (1953) is an algorithm used to find the minimum and maximum values of a function within a specified range. For a single mode function with an extremum inside a range, it will find the extreme point, converge to one of them for a range containing multiple external points. The golden ratio method is generally considered to be accurate but slow technique because it works by iteratively narrowing the range of values in the specified range. The technique maintains function values in the ratio of 2-φ: 2φ-3: 2-φ for four points with three gap widths where φ is golden ratio.

The Golden-Ratio Search Method, illustrates on Figure 11, application steps can be simplified as,

1. The f(x), which denotes that the function to be reduced, should be determined, the period {X1,X4} should be specify with F1 and F4 which are functional values.
2. The internal point and F2 that functional value of internal point should be evaluated. The interval lengths identified by ratio as r:c or c:r. The r is r = φ − 1 and c is c = 1 − r where φ represents the golden ratio.
3. Using the triple it should be determined whether the convergence criteria are met. If so, at least X of these three must be estimated from that triplet and returned.
4. From the triple system, the internal point and the functional value of this point are calculated. The three ranges found will be obtained in the ratio c:cr:c.
5. The three points to base on for the next iteration will be the point where F has the minimum and the two points nearest to the value in X.
6. Return and repeat step 3.

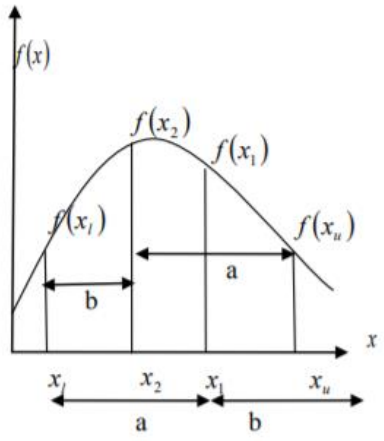

Figure 11 Example of Golden -Ratio Search Method

As an application of the equation,

For to determine the maximum of a function f (x) in Figure 12,

Determine x_1 and x_u that are enclose the maximum of the f(x).

Step 1:

Define the x_1 and x_2 ,which are two intermediate points, as,

$$x_1 = x_1 + d$$
$$x_2 = x_u + d$$

where $d = \frac{\sqrt{5}-1}{2}(x_u - x_1)$

Step 2:

Determine the $f(x_1)$ and $f(x_2)$

There are two cases as,

First case is when $f(x_1) > f(x_2)$ to evaluate the x_1

$$x_1 = x_2$$
$$x_2 = x_1$$
$$x_u = x_u$$
$$x_1 = x_1 + \frac{\sqrt{5}-1}{2}(x_u - x_1)$$

Second case is when $f(x_1) > f(x_2)$ to evaluate the x_2

$$x_1 = x_1$$
$$x_u = x_1$$
$$x_1 = x_2$$
$$x_2 = x_u + \frac{\sqrt{5}-1}{2}(x_u - x_1)$$

Step 3:

If $x_u - x_1 < \varepsilon$ (a sufficiently small number) the maximum value reaches at $\frac{x_u + x_1}{2}$ then stop iterating go to step 2.

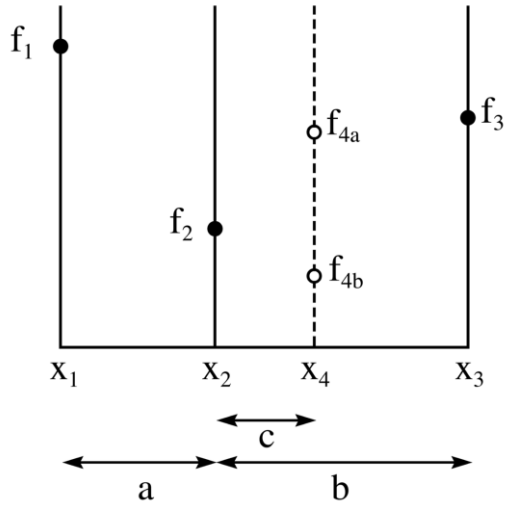

Figure 12 The Golden Ratio Search Method

As the mathematical formulations of the models were given in the previous section, the common feature of the models is the tilt angle, which is important in converting the DSR values on the horizontal surface to those on the inclined surface. Thus, the total solar radiation on the inclined surface can be maximized as,

$$\max_{\beta} I_{\beta T}\ \ \beta\ = I_b \frac{\tan\delta \sin\ \ \phi-\beta\ +\cos\omega\cos\ \ \phi-\beta}{\tan\delta\sin\phi+\cos\omega\cos\phi} + I_T\rho\left(\frac{1-\cos\beta}{2}\right)+I_d\chi\ \ \theta,\theta_z,\beta,\eta \tag{2.41}$$

where χ denotes the diffuse models that may require the additional model characteristic input η. χ can be defined by models as,

in Badescu Model (BAM) where the input parameter of the model is DSR on inclined surface and the model assuming sky radiance is isotropic,

$$\chi=\left(\frac{3+\cos(2\beta)}{4}\right) \tag{2.42}$$

in KM where the input parameter of the model is DSR on inclined surface and the model assuming sky radiance is isotropic,

$$\chi = \frac{1}{3}\left(\frac{1}{2+\cos\beta}\right) \tag{2.43}$$

in LJMwhere the input parameter of the model is DSR on inclined surface ,

$$\chi = \left(\frac{1+\cos\beta}{2}\right) \tag{2.44}$$

in Tian Model (TM) where the input parameter of the model is DSR on inclined surface and the model assuming sky radiance is isotropic,

$$\chi = \left(1-\frac{\beta}{180}\right) \tag{2.45}$$

in BM where the input parameters of the model are DSR on inclined surface, BSR on inclined surface, zenith angle, incidence angle,

$$\chi = \frac{1}{I_d}\left[\left(\frac{1+cos\beta}{2}\left(I_d - 0.05\frac{I_{b\beta}}{cos\theta_z}\right)\right) + 0.05 I_{b\beta} cos\theta\right] \tag{2.46}$$

in TCM where the input parameters of the model are DSR on inclined surface, zenith angle, incidence angle

,

$$\chi = \frac{1}{2}(1+cos\beta)(1+cos^2\theta(sin^3\theta_z))\left(1+sin^3\left(\frac{\beta}{2}\right)\right) \tag{2.47}$$

in HM where the input parameters of the model are DSR on inclined surface, BSR on inclined surface, instantaneous extraterrestrial radiation,

$$\chi = \left[\frac{I_b}{I_0} \left(\frac{cos\theta}{cos\theta_z} \right) + \left(\frac{1+cos\beta}{2} \right) \left(1 - \frac{I_b}{I_0} \right) \right] \tag{2.48}$$

in RM where the input parameters of the model are DSR on inclined surface, BSR on inclined surface, instantaneous extraterrestrial radiation,

$$\chi = \left[\frac{I_b}{I_0} \left(\frac{cos\theta}{cos\theta_z} \right) + \left(\frac{1+cos\beta}{2} \right) \left(1 - \frac{I_b}{I_0} \right) \left(1 + \sqrt{\frac{I_b}{I_H}} sin^3 \left(\frac{\beta}{2} \right) \right) \right] \tag{2.49}$$

in KLM Model where the input parameters of the model are DSR on inclined surface, BSR on inclined surface, instantaneous extraterrestrial radiation,

$$\chi = \left[\frac{1}{2} \left(1 + cos \left(\frac{\beta}{2} \right) \right) \right] \left[1 + \left(1 - \left(\frac{I_d}{I_H} \right)^2 \right) cos^2\theta (sin^3\theta_z) \right] \left[1 + \left(1 - \left(\frac{I_d}{I_H} \right)^2 \right) sin^3 \left(\frac{\beta}{2} \right) \right] \tag{2.50}$$

in HDKR Model where the input parameters of the model are DSR on inclined surface, BSR on inclined surface, instantaneous extraterrestrial radiation,

$$\chi = \left[\left(\frac{1+cos\beta}{2} \right) \left(1 - \frac{I_b}{I_0} \right) \left(1 + \sqrt{\frac{I_b}{I_H}} sin^3 \left(\frac{\beta}{2} \right) \right) \right] \tag{2.51}$$

in SUM where the input parameters of the model are DSR on inclined surface, BSR on inclined surface, zenith angle, incidence angle,

$$\chi = \left[\left(0.51 \left(\frac{\cos\theta}{\cos\theta_z} \right) \right) + \left(\frac{1+\cos\beta}{2} \right) - \frac{1.74}{1.26\pi} \left\{ \sin\beta - \beta \frac{\pi}{180} \cos\beta - \pi \sin^2 \frac{\beta}{2} \right\} \right] \tag{2.52}$$

in PM where the input parameters of the model are DSR on inclined surface, angles of the circumsolar region, dimensionless horizon brightness, air mass, DSR on horizontal surface, extraterrestrial radiation, sky clearness index,

$$\chi = \left[\frac{1+cos\beta}{2} \; 1 - F_1 \; + F_1 \frac{a_1}{a_2} + F_2 sin\beta \right] \tag{2.53}$$

For instance, the reduction coefficients f_{Hay} and f_R are appeared in HKDR model or categorized sky condition may be inserted in PM as explained above. Knowing the I_b and I_d for a given location and specific time, Eq. (2.41) only depends on the tilt angle β which is bounded by an interval of 0° and 90°. Being derivative-free algorithm, the golden-ratio search and parabolic interpolation method was performed to find the optimum β values. The golden ratio search is a simple space search algorithm, which is especially used for unimodal function. The idea behind the algorithm is based on narrowing the searching interval. This is achieved by selecting two the points inside the searching interval, which keep the golden ration for each iteration (Kiefer,1953). The golden-ratio search was hybridized later with parabolic interpolation to enhance the efficiency of the algorithm. In the hybrid method, the new points selected in the searching interval are evaluated by constructing a quadratic polynomial which yields faster convergence (Chapra and Canale,2015) (Brent,1973). The maximum 103 iterations were implemented, and the algorithm was terminated with a tolerance of 1×10^{-8}.

Although a number of population-based algorithms such particle swarm optimization, differential evaluation, cuckoo search (i.e. (Yang and Deb,2009), (Kennedy and Eberhart,1995)) could be performed, the golden-ratio search was preferred due to its simplicity, the computation effort and the converge speed and requiring no additional

parameters that are necessary to tweak the performance of the algorithm used. In this study, the golden-ratio search-based optimization procedure generally gave the result of the tilt angle in a few iterations.

2.4 Geographic and Solar Radiation Data and Processing

Turkey is located in a geographic region that occupying partially in Europe and partially in Asia. The geographic coordinates of Turkey which are nearly the south-east part of Europe defined as 36°- 42° N latitude and 26°-45° E longitude. Turkey is administratively divided into 81 provinces on approximately 783.562 km² area. The 47 of provinces located at 39 ° N latitude and higher, while the remaining 34 provinces are between 36 °N and 39 ° N. According to Turkish State Meteorological Service (TSMS), the average daily sunshine duration of Turkey was about 6.8 hours for a period of 1988-2017, the minimum 6.37 hours in 1998 and maximum 7.30 hours in 1990. The annual averaged global solar radiation was measured as 4.4 kWh/m2 /day for a period of 2004-2018 as seen in Figure 14. The southern region of Turkey receives more solar radiation that increases the solar energy capacity due to geographical location when compared to the northern part. The monthly average solar radiation data of each province were obtained from the website of NASA Prediction Of Worldwide Energy Resources (POWER) by using the latitude and longitude of each province of Turkey. The POWER project was established with the goal of improving existing renewable energy datasets, reaching clearest data and creating new datasets from new satellite systems. The main application areas of the POWER project are renewable energy, sustainable buildings and agroclimatology. The data archive used for Renewable Energy is designed to provide access to parameters custom help the design of solar and wind powered renewable energy systems.

The solar data for different provinces of Turkey was obtained and processed in steps as,

1. The average monthly data on the horizontal surface for each province of Turkey for the years of 2001-2020 was downloaded from the database in website of NASA Prediction Of Worldwide Energy Resources. NASA data is available on the https://power.larc.nasa.gov/data-access-viewer/ website. Its use has been developed in 2 different ways. As seen in the Figure 13, the location can be reached by entering the latitude and longitude values of a location or the location

can be selected using the cursor. Data sets are selected for the desired date range. CSV is chosen as the output format. By choosing Solar Fluxes and Related for the search parameter, 81 data sets were reached to be used for analysis for 81 provinces.

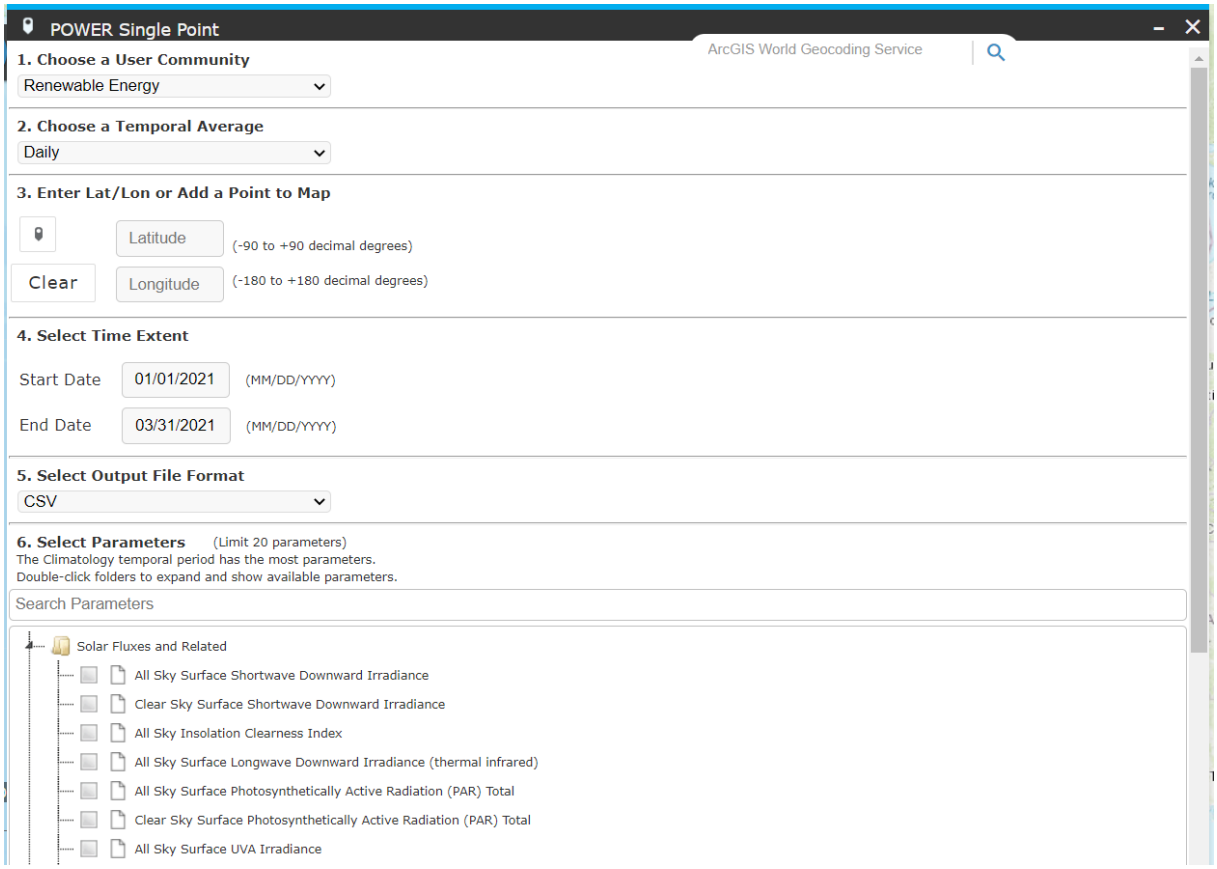

Figure 13 NASA POWER Data Access Viewer Screen

The parameters that obtained by the NASA are;

- Average Declination for Climatological Month (Degrees)
- Average Solar Noon Time for Climatological Month (Hour)
- All Sky Insolation Clearness Index (dimensionless)
- Cloud Amount (%)
- Top-Of-Atmosphere Shortwave Downward Irradiance (kW-hr/m^2/day)
- Average Sunset Hour Angle for Climatological Month (Degrees)
- All Sky Surface Albedo (dimensionless)

- All Sky Surface Shortwave Downward Direct Normal Irradiance (kW-hr/m^2/day)
- All Sky Surface Shortwave Downward Irradiance (kW-hr/m^2/day)
- All Sky Surface Shortwave Diffuse Irradiance (kW-hr/m^2/day)
- Daylight Average Of Hourly Cosine Solar Zenith Angles for Climatological Month (Degrees)
- Average Cosine Solar Zenith Angle At Mid-Time Between Sunrise And Solar Noon for Climatological Month (Degrees)

2. The monthly data were converted to seasonal and annual data.
3. The declination angle for each location were computed using Eqs. (2.1).
4. Since some models requires the daily extraterrestrial radiation therefore, it was taken from NASA data.
5. Data were performed for 12 isotropic and anisotropic models using the Golden Ratio Search Method for 81 provinces to obtain monthly average tilt angles.
6. The seasonal and annual values were also averaged using the monthly tilt angles.

Figure 14 Annual Averaged Global Solar Radiation of Turkey (MENR)

In this study, NASA data was used as an alternative to the radiation data of the Meteorology directorate. In order to compare the data of both sources, 6 provinces from different regions of Turkey were selected. NASA and Meteorology radiation values of these provinces are shown in the Table 6. The difference between the two data can cause serious changes in the angle of inclination, thus the efficiency of the PV panel.

Table 6 The Radiation Value of NASA and TSMS

	ANKARA		SİNOP		HATAY		AĞRI		EDİRNE		İZMİR	
	TSMS	**NASA**	**TSMS**	**NASA**	**TSMS**	**NASA**	**TSMS**	**NASA**	**TSMS**	**NASA**	**TSMS**	**NASA**
JAN	2.07	1.95	1.92	1.48	2.45	2.20	2.12	2.30	1.87	1.69	2.18	2.16
FEB	2.84	2.92	2.66	2.21	3.30	3.04	2.63	3.26	2.41	2.49	2.87	2.88
MAR	4.05	4.15	3.57	3.50	4.63	4.46	3.96	3.92	3.48	3.66	4.00	4.23
APR	5.23	5.43	4.86	5.04	5.42	5.72	5.28	4.60	4.92	5.08	5.39	5.55
MAY	6.34	6.42	5.82	6.03	6.96	6.92	6.27	5.84	5.27	6.21	6.42	6.70
JUN	6.60	7.27	6.17	7.09	7.65	7.89	7.36	7.30	6.67	6.80	7.04	7.58
JUL	6.70	7.60	6.36	7.14	7.14	7.77	7.09	7.31	4.77	7.09	6.64	7.91
AUG	5.95	6.77	5.72	6.21	6.35	6.95	6.15	6.66	6.13	6.38	6.34	7.06
SEP	4.71	5.40	4.29	4.64	5.27	5.77	4.99	5.50	4.55	4.76	4.93	5.57
OCT	3.31	3.73	2.91	2.97	3.97	4.15	3.54	3.62	2.91	3.13	3.52	3.96
NOV	2.37	2.58	2.13	1.88	2.93	2.91	2.37	2.32	1.94	1.97	2.48	2.69
DEC	1.92	1.75	1.66	1.34	2.32	2.10	1.38	1.79	1.50	1.47	1.89	1.95

The comparison of the values of 6 provinces is given in the Figure 15. As can be seen, the R2 values of NASA and Meteorology values vary between 0.90 and 0.99. These values show that both sources are compatible with each other.

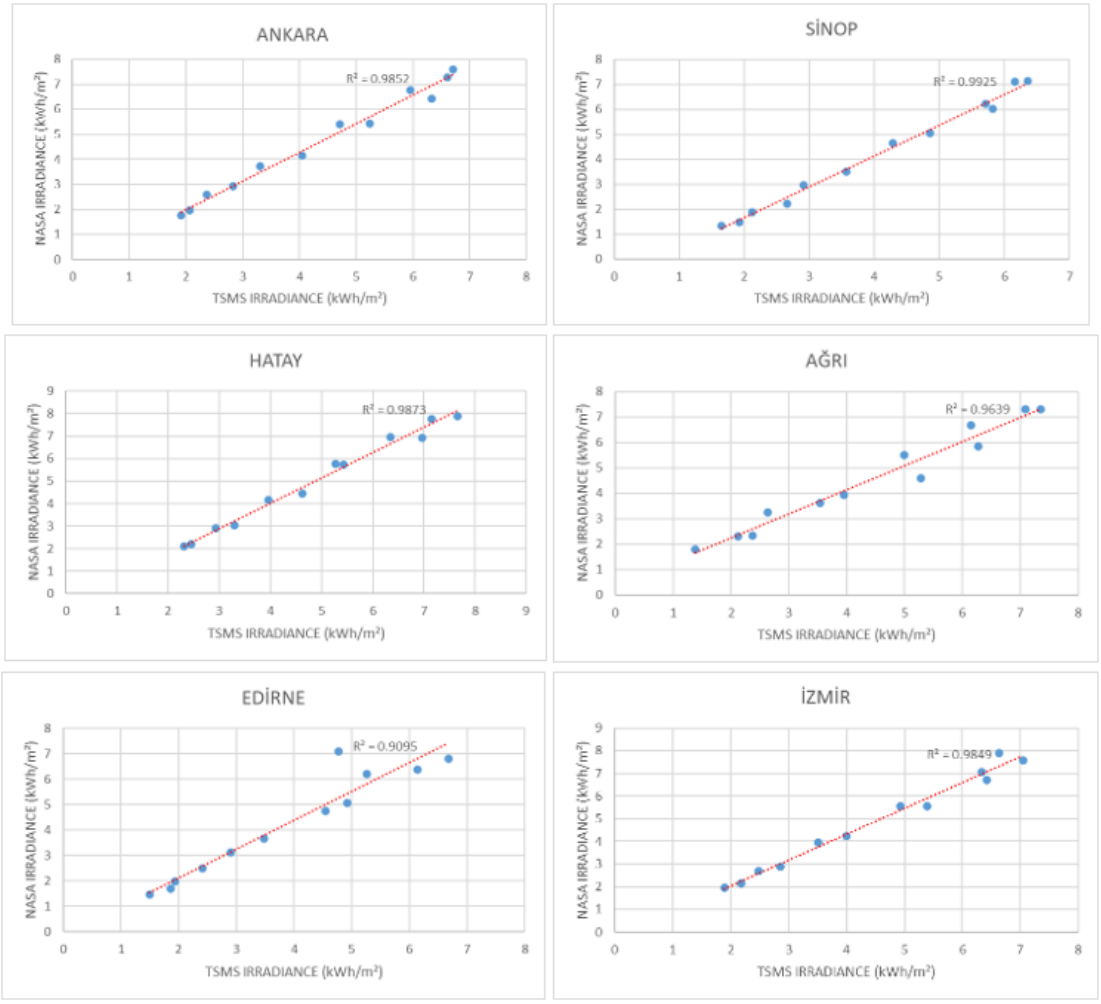

Figure 15 The Radiation Data Comparison of NASA and TSMS

3. RESULTS AND DISCUSSION

The models have performed to obtain the annual, seasonal, and monthly variations of tilt angles. In this part of the study, the results are presented beside the validation and comparison of results are shown according to the ground solar data. A sensitivity analysis has conducted to define parameters that have a significant effect on the tilt angles of PV panels.

3.1. Annual Variation

As aforementioned in the geographic and solar radiation and processing section, the monthly BSR and DSR values for 81 provinces of Turkey for 2000-2020 years used to obtained optimum monthly tilt angles for each province. The maximization correlation, Eq. 2.41, was performed on 12 models which include isotropic and anisotropic models. The analysis has solved for 12 months and 81 provinces in sum 11664 times and acquired annual OTAs presented in Figure 16.

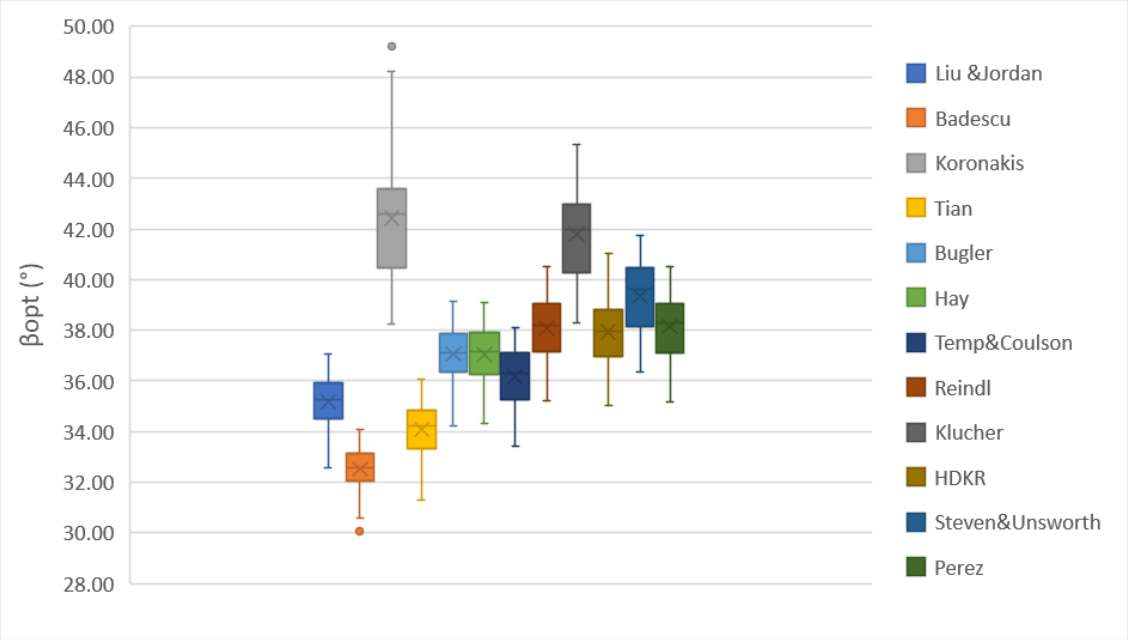

Figure 16 Annual optimum tilt angles variation for 81 provinces of Turkey

Each radiation model used for tilt angle values for different provinces and as can be seen in Figure 7, for Turkey located between the 36 ° and 42 ° latitudes, the annual OTA of analysis can be interpreted to scattered in 30 °- 48 ° range.

The annual OTAs obtained from the comprehensive analysis have implemented on t-Test which is the most applied statistical hypothesis test. Firstly, the significant differences in means of used radiation models aimed to define by t-Test. In the results of the t-Test analysis, the HM results in median as μβopt= 37.16° meanwhile, BM method has μβopt=

36.94°, in median as can be seen in Table 7. The medians of both methods are statistically equal, and a significant difference could not to seen. Also, the statistical similarity can be seen between RM and PM method with value μβopt = 38.17°as μβopt = 38.28°, respectively. The mean values of BM (μβopt = 37.05°) and PM (μβopt = 37.04°) models are same. On the other hand, the sign test which is a statistical method that qualifies the differences of paired data with zero medians was studied on methods. According to sign test, each method has different results which are not same or similar statistically.

Table 7 The Annual Optimum Tilt Angles

	OPTIMUM TILT ANGLES (βopt)			
	MAX	**MIN**	**MEDIAN**	**MEAN**
Liu &Jordan	37.07	32.57	35.24	35.17
Badescu	34.08	30.06	32.57	32.52
Koronakis	49.22	38.26	42.59	42.43
Tian	36.09	31.29	34.25	34.08
Bugler	39.12	34.23	37.13	37.05
Hay	39.11	34.33	37.16	37.04
Temp&Coulson	38.09	33.42	36.29	36.17
Reindl	40.53	35.21	38.17	38.09
Klucher	45.34	38.31	41.98	41.78
HDKR	41.01	35.04	37.97	37.93
Steven&Unsworth	41.76	36.36	39.61	39.35
Perez	40.52	35.18	38.28	38.14

It has already been mentioned that latitude is a parameter that contributes to the change of the optimum inclination angle and will be used in optimizations. As known, latitude changes with location, Figure 17 - Figure 28 present the variation of the OTAs which are obtained by using 12 radiation models, isotropic and anisotropic, along the latitudes of Turkey. According to the implemented analysis results shown in Figure 17 - Figure 28 , KM, an isotropic model, KLM, RM, SUM, PM, which are anisotropic models, show a linear relationship with latitude. On the contrary, the BAM and TM results are scattered and disprove the linearity of the latitude parameter by changing values between 30°-36°.

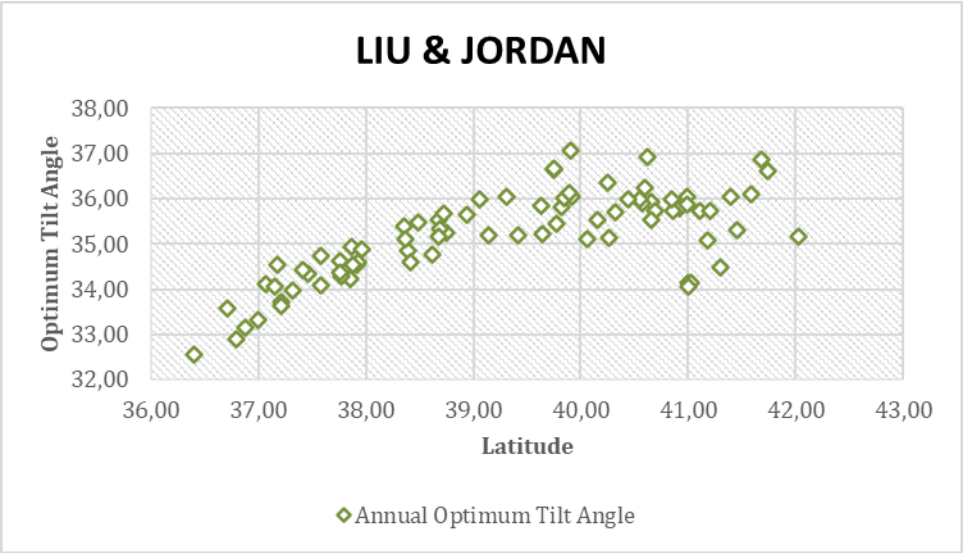

Figure 17 The optimum tilt angle variation with the latitudes by Liu & Jordan model

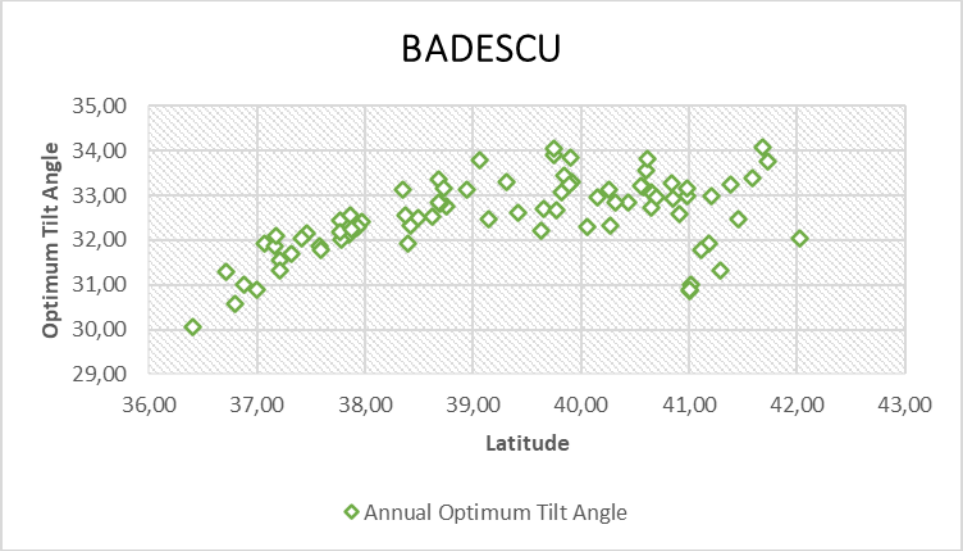

Figure 18 The optimum tilt angle variation with the latitudes by Badescu model

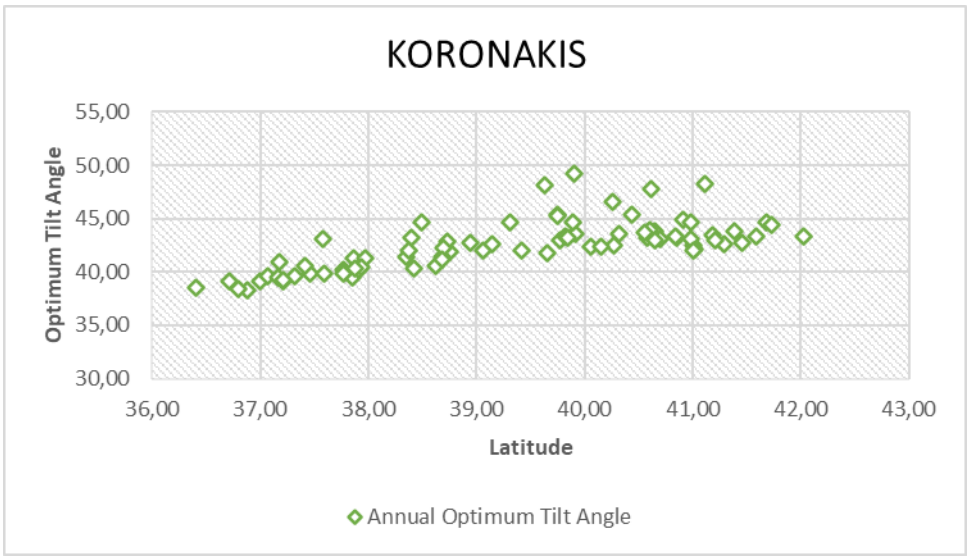

Figure 19 The optimum tilt angle variation with the latitudes by Koronakis model

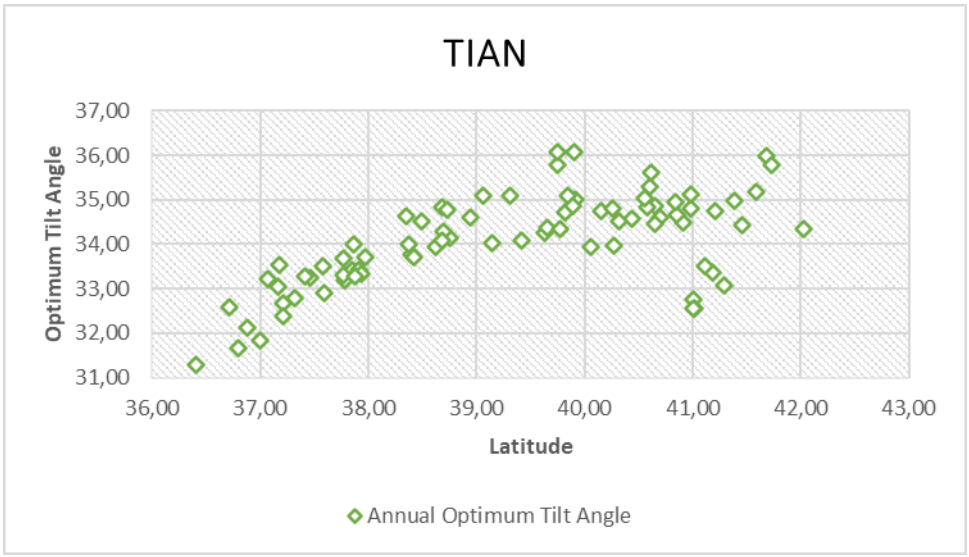

Figure 20 The optimum tilt angle variation with the latitudes by Tian model

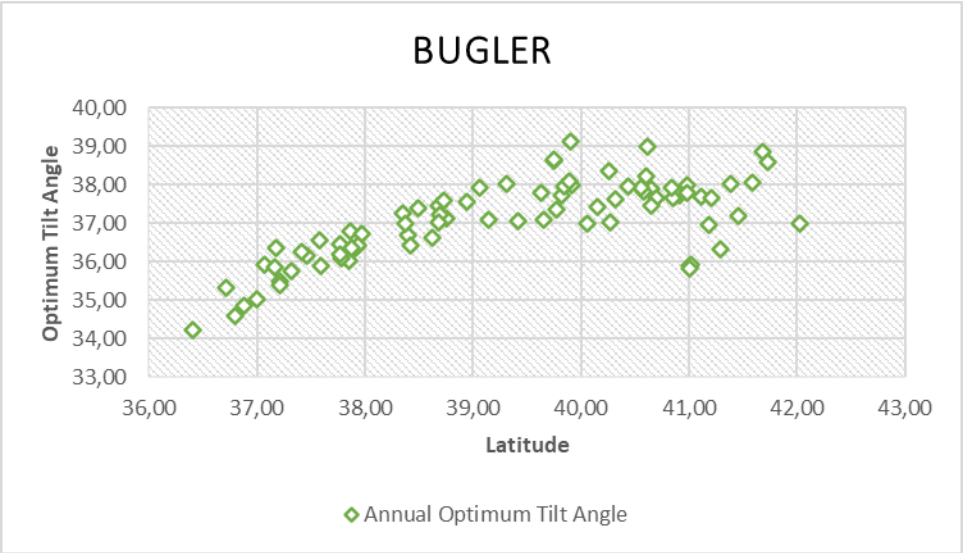

Figure 21 The optimum tilt angle variation with the latitudes by Bugler model

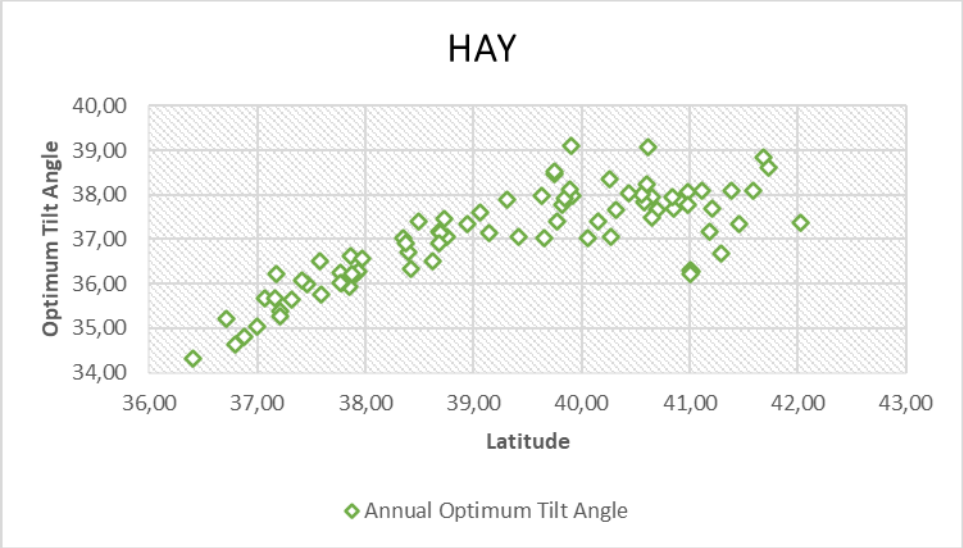

Figure 22 The optimum tilt angle variation with the latitudes by Hay model

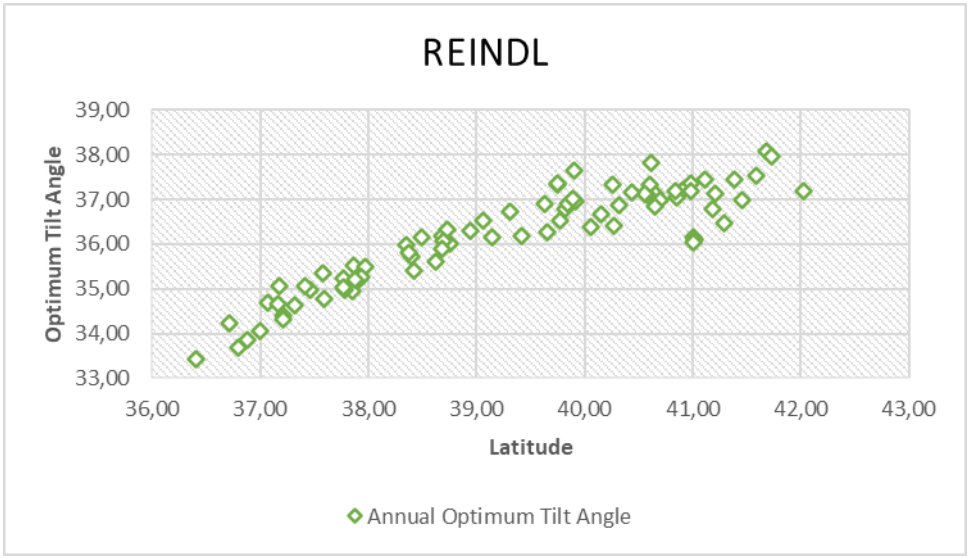

Figure 23 The optimum tilt angle variation with the latitudes by Reindl model

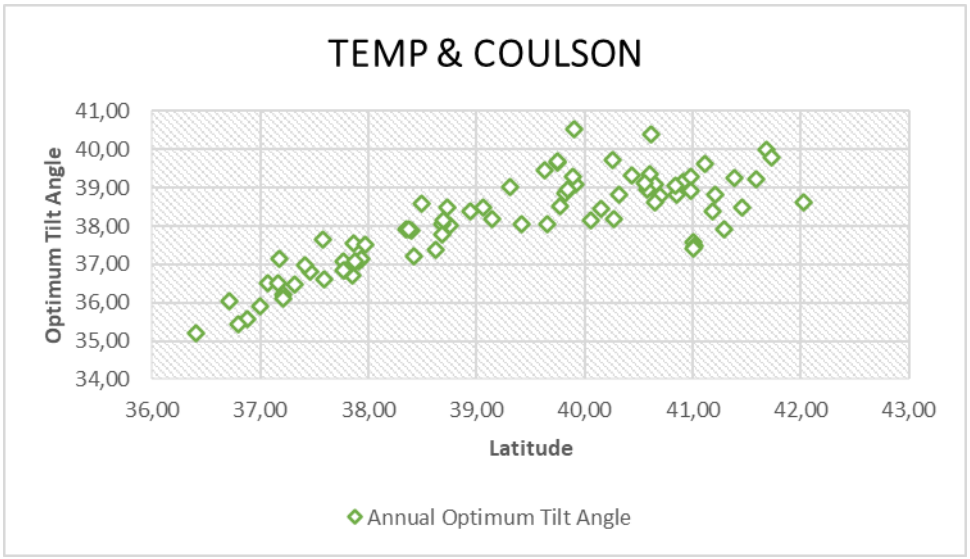

Figure 24 The optimum tilt angle variation with the latitudes by Temps & Coulson model

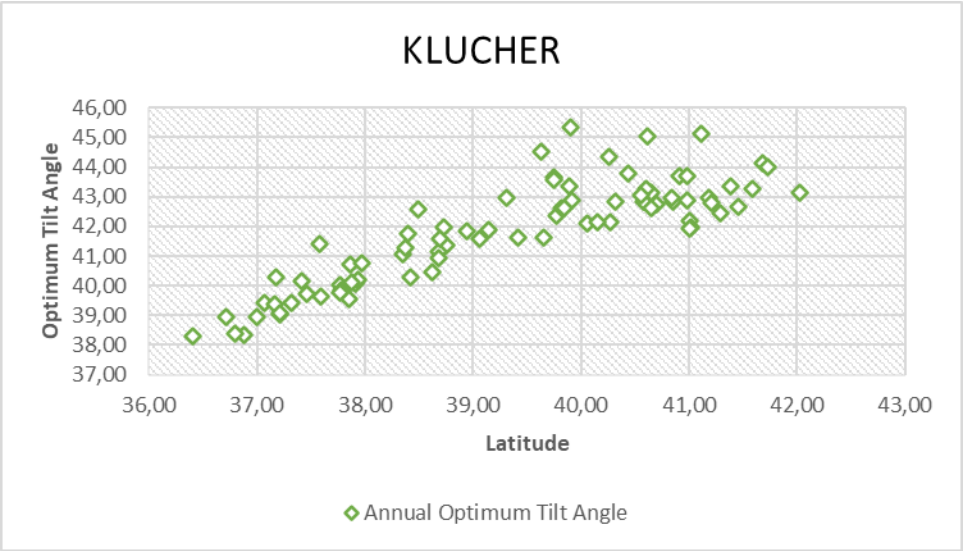

Figure 25 The optimum tilt angle variation with the latitudes by Klucher model

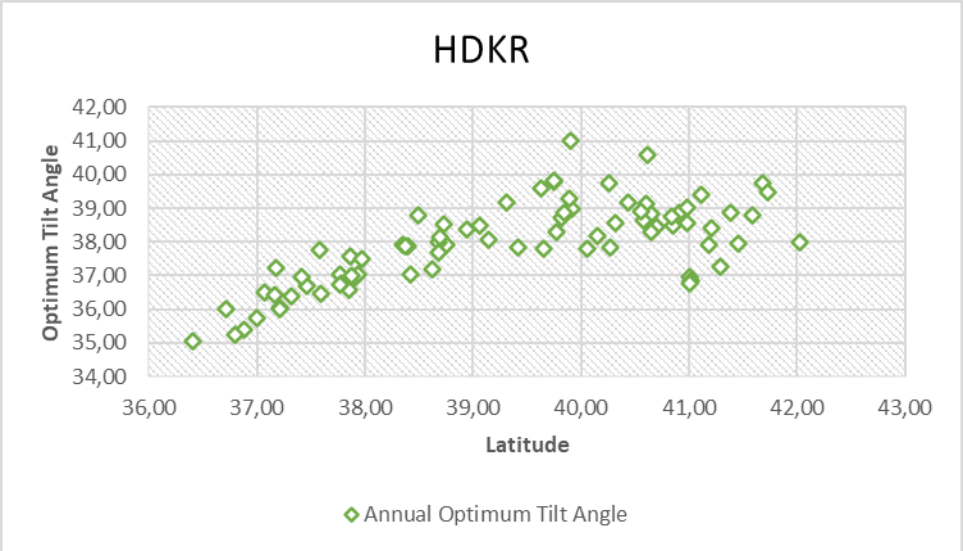

Figure 26 The optimum tilt angle variation with the latitudes by HDKR model

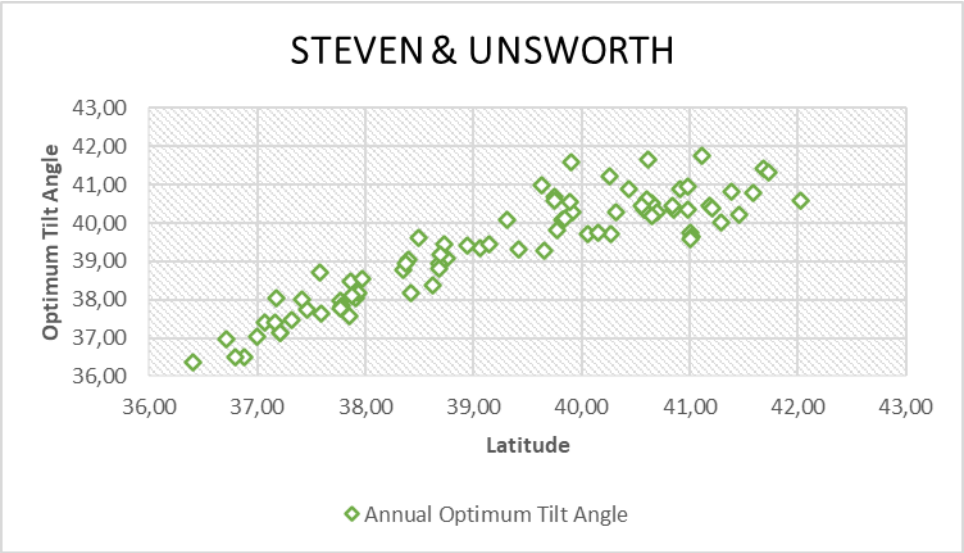

Figure 27 The optimum tilt angle variation with the latitudes by Steven & Unsworth model

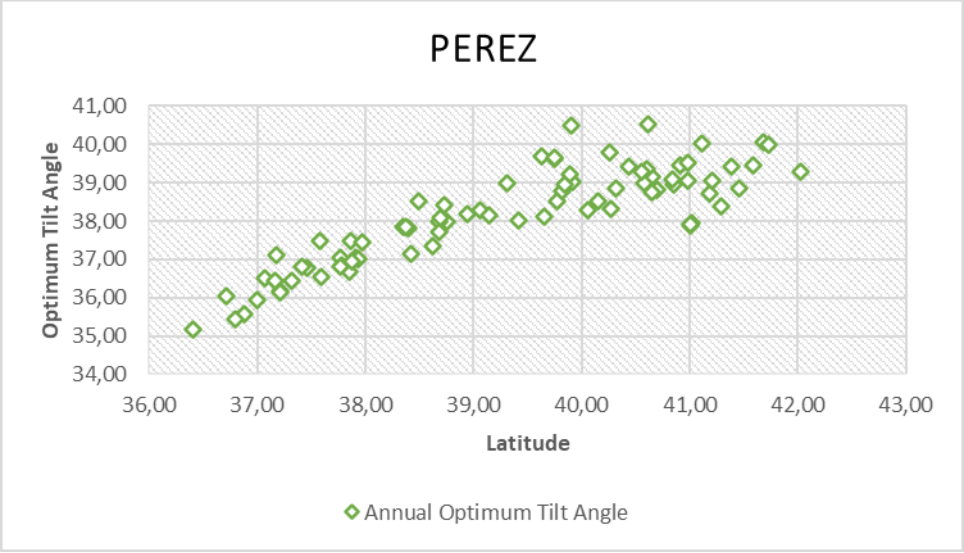

Figure 28 The optimum tilt angle variation with the latitudes by Perez model

The annual OTA is increased with the latitude, it can be observed that the angle increases toward the north of Turkey in Figure 29. Although the anisotropic models with the exception of KLM and HDKR look the same in terms of trend that the variation of OTA

according to latitude, the scatter in the figures appears to be different. The reason for this can be said that the characteristics of the models are different from each other. Among the isotropic models, the maximum average tilt angles are obtained with KM, those are maximum of 49.22° for Erzurum (ϕ= 39.904 °) and minimum of 38.26° for Antalya (ϕ= 36.884°). On the contrary, BAM gives the minimum ones, which are 30.06° for Hatay (ϕ= 36.402°) and the maximum is 34.08° for Edirne (ϕ=41.676°). For anisotropic models, KLM is able to produce higher tilt angles (the maximum is 45.34° for Erzurum with ϕ=39.904 ° and the minimum is 38.31° for Hatay) whereas HM performs the minimum averages, those are 39.11° for Erzurum as a highest value and 34° for Hatay as the lowest value. Although most methods show an increasing trend in tilt angles with latitudes, some deviations observed in figure could be explained by the quality of radiation data, topographic and local geographic properties.

The annual OTAs obtained as a result of the 12 models have been mapped by QGIS in order to see their distribution over Turkey more clearly and are shown in the Figure 29 and Figure 40. As we mentioned before, the importance of the effect of latitude on the OTA, the latitude value increases from the south to the north of Turkey, and it is seen that the OTA value increases with the increase in the latitude.

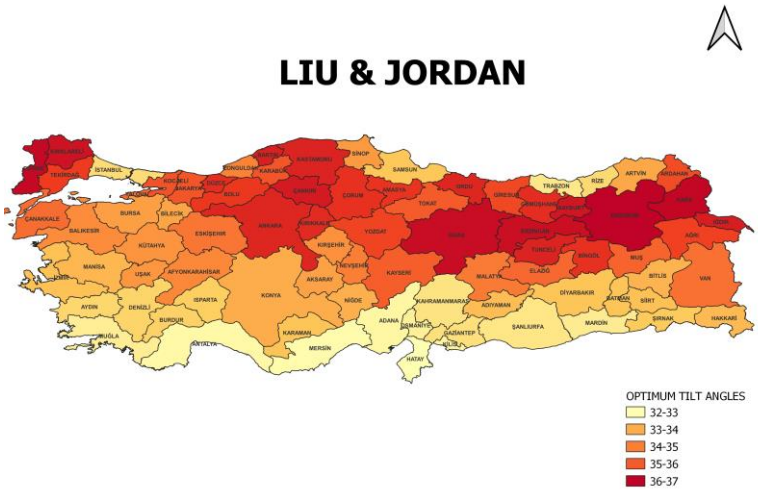

Figure 29 The Map Modelling of Annual Optimum Tilt Angles of Turkey by Liu and Jordan Model

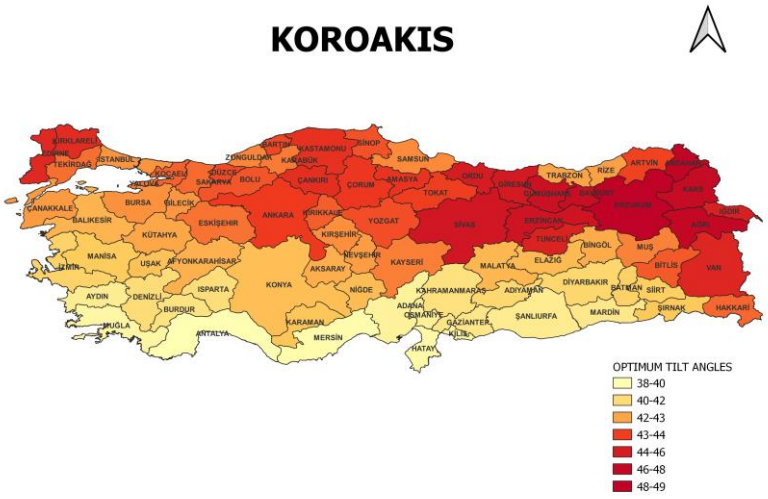

Figure 30 The Map Modelling of Annual Optimum Tilt Angles of Turkey by Koronakis Model

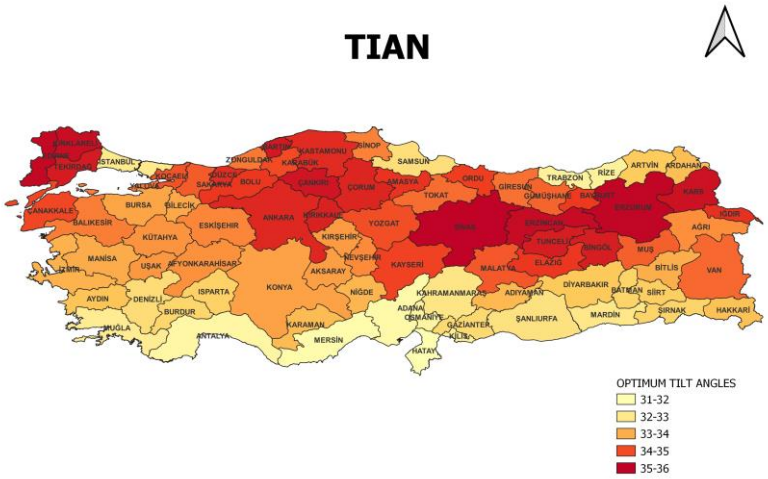

Figure 31 The Map Modelling of Annual Optimum Tilt Angles of Turkey by Tian Model

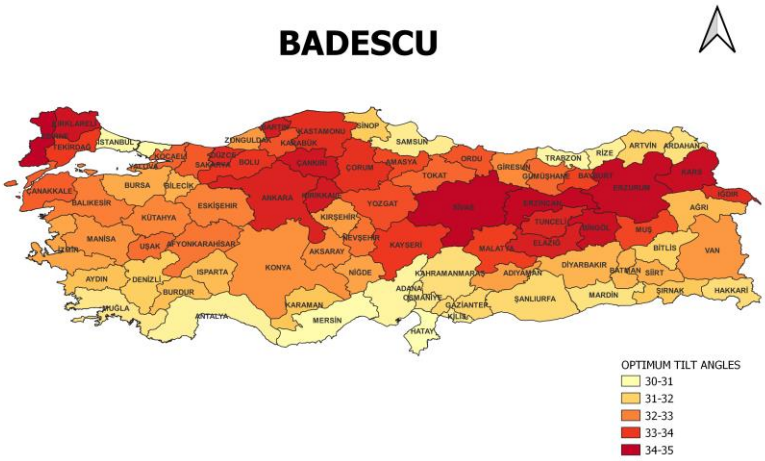

Figure 32 The Map Modelling of Annual Optimum Tilt Angles of Turkey by Badescu Model

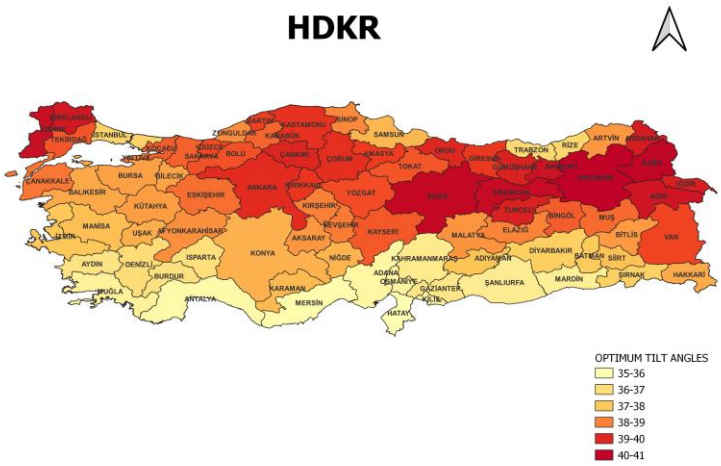

Figure 33 The Map Modelling of Annual Optimum Tilt Angles of Turkey by HDKR Model

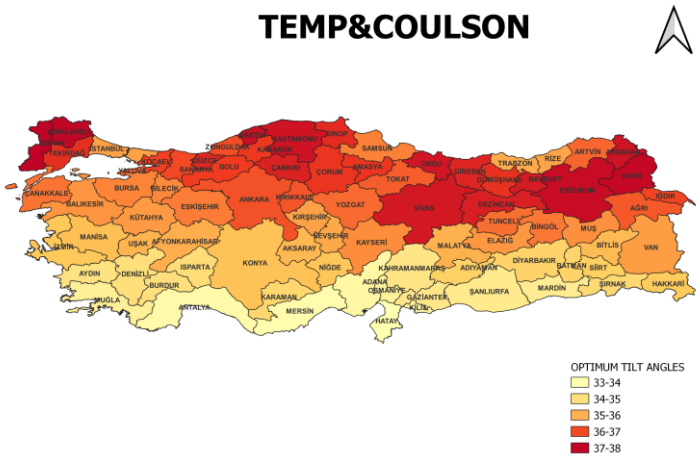

Figure 34 The Map Modelling of Annual Optimum Tilt Angles of Turkey by Temps & Coulson Model

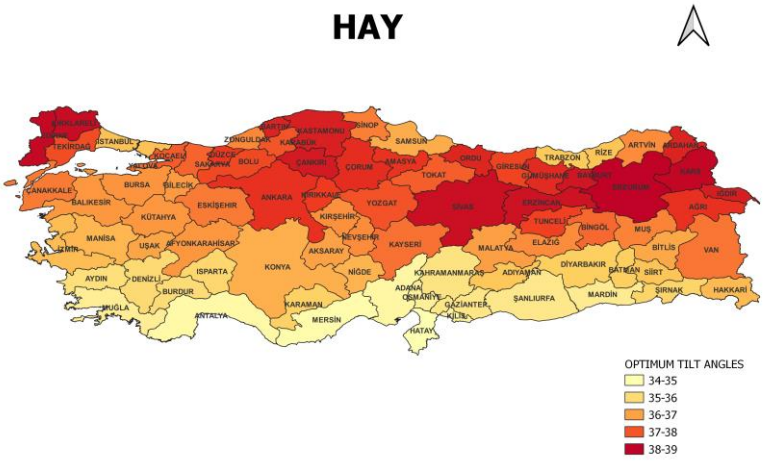

Figure 35 The Map Modelling of Annual Optimum Tilt Angles of Turkey by Hay Model

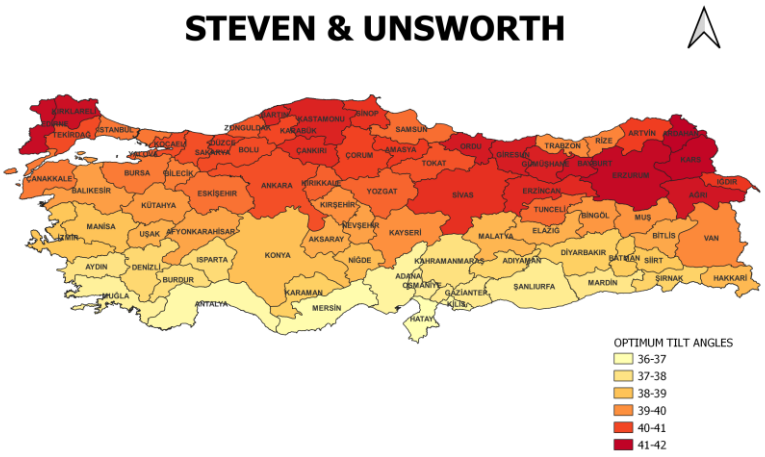

Figure 36 The Map Modelling of Annual Optimum Tilt Angles of Turkey by Steven & Unsworth Model

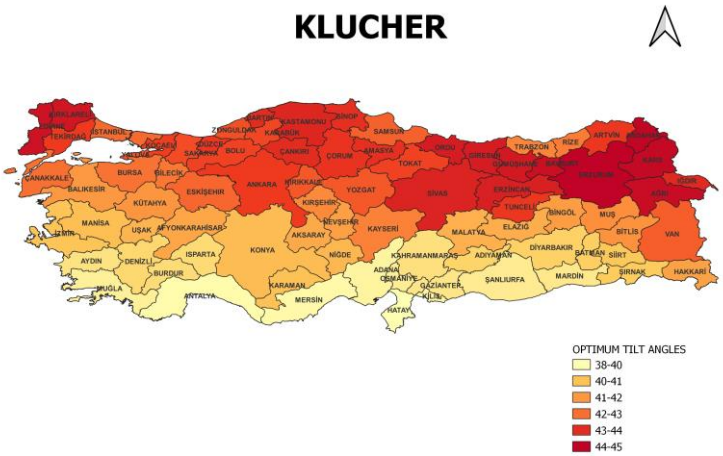

Figure 37 The Map Modelling of Annual Optimum Tilt Angles of Turkey by Klucher Model

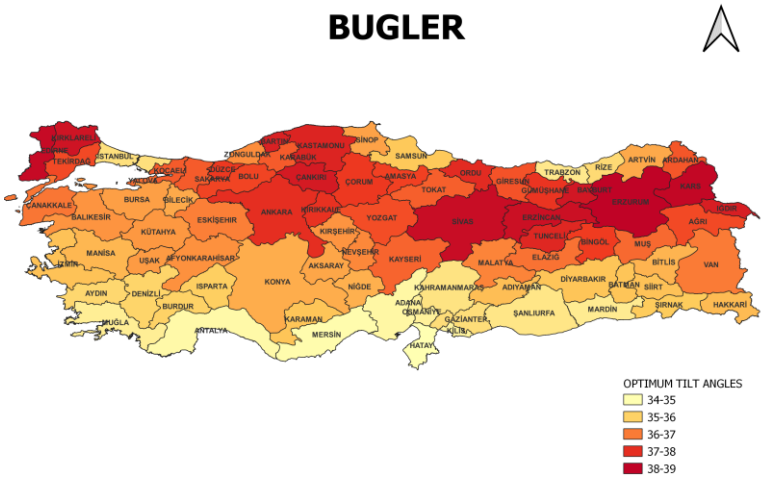

Figure 38 The Map Modelling of Annual Optimum Tilt Angles of Turkey by Bugler Model

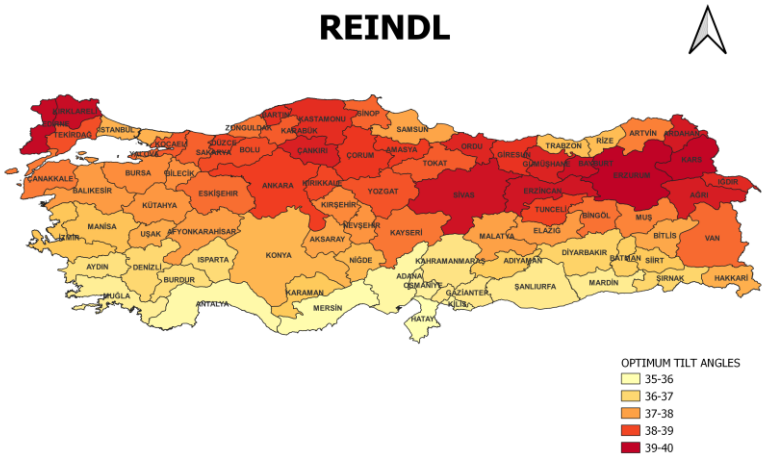

Figure 39 The Map Modelling of Annual Optimum Tilt Angles of Turkey by Reindl Model

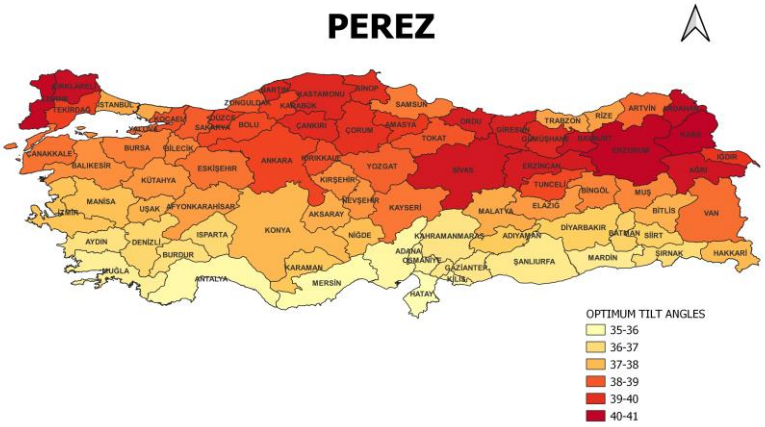

Figure 40 The Map Modelling of Annual Optimum Tilt Angles of Turkey by Perez Model

As can be seen from the color change on the map, the dark color represents the high OTA value. As, Koronakis, an isotropic model, KLM and SUM, which are anisotropic models, show a linear relationship with latitude the maps are almost same and the south of Turkey is in light colors and north-east of Turkey is in dark colors. As can be seen, the angles are higher in the Eastern Anatolia Region of Turkey. The reason for this may be errors in the measurements of the data obtained from NASA. If we had real measurement field data, more precise results could be obtained.

3.2. Seasonal Variation

The OTAs were obtained seasonally to by using 12 radiation models with data taken over 81 provinces of Turkey. The results in Figure 43 can be interpreted as the average tilt angles differ in 20°-37° during spring months in a wide range. In summer season, the tilt angles result in range of 12°-24° which can be describe as a close range. The OTAs for the summer and spring seasons mostly range from 20 °- 25 °. The OTAs can be seen from Figure 41- Figure 44 as change in 39°-53° range for fall and 46°-72° for winter season for 12 radiation models. The methods performed for defining the OTAs obtain 39°-55° range in fall season.

As can be seen from Figure 41- Figure 44 the optimal angle values calculated for 4 different seasons, the average value of all radiation models in winter was 56.76 °. According to the results of the anisotropic models, the average optimal angle value is 57.28 ° that very close to the general average value for winter. As a result of the t-test conducted for the fall season, the median value was found to be 46.04 °, where the winter season is 56.49, for all models. When the results in the are examined, it is seen that the average of the anisotropic models used in the analysis, except for the RM, is 46.52 °. It can be said that the 46.52 ° is very close to the general average found for the fall season. Besides, it can be seen that the mean values of the BM and HM in the t-Test result are statistically equal. Considering the data of all models both isotropic and anisotropic that can be used in the preliminary design for the positioning of the panels, the average angle of inclination for the spring season is 28.19 °. While the difference between the average values obtained from the analysis of KLM and SUM models can be ignored statistically, the OTA values for anisotropic models varies between 24.61 ° - 36.9 ° and on average is 28.22° in spring. During the summer months, the overall average of the models is 19.13 ° and the average values of RM and HDKR are statistically the same according to the t-Test. Tilt Angle values for anisotropic models ranged from 15.96 ° -23.66 °, while the average value was found as 19.82°. As seen in the previous section, Koronakis a isotropic model and KLM an anisotropic model produces higher tilt angle values for all seasons Turkey

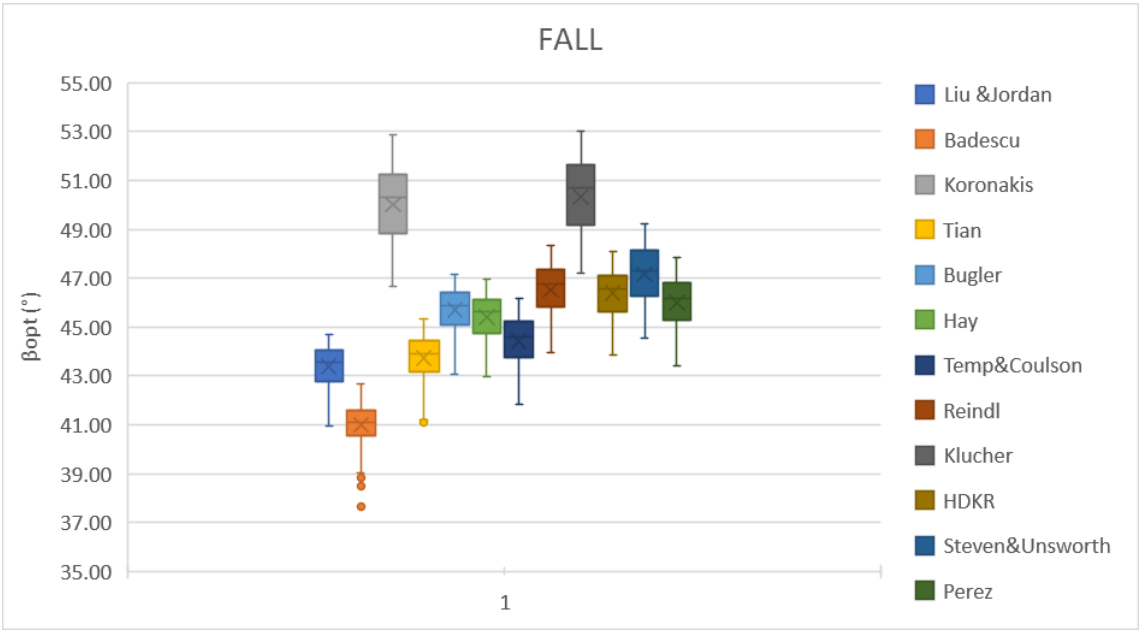

Figure 41 Fall season optimum tilt angles variation for 81 provinces of Turkey

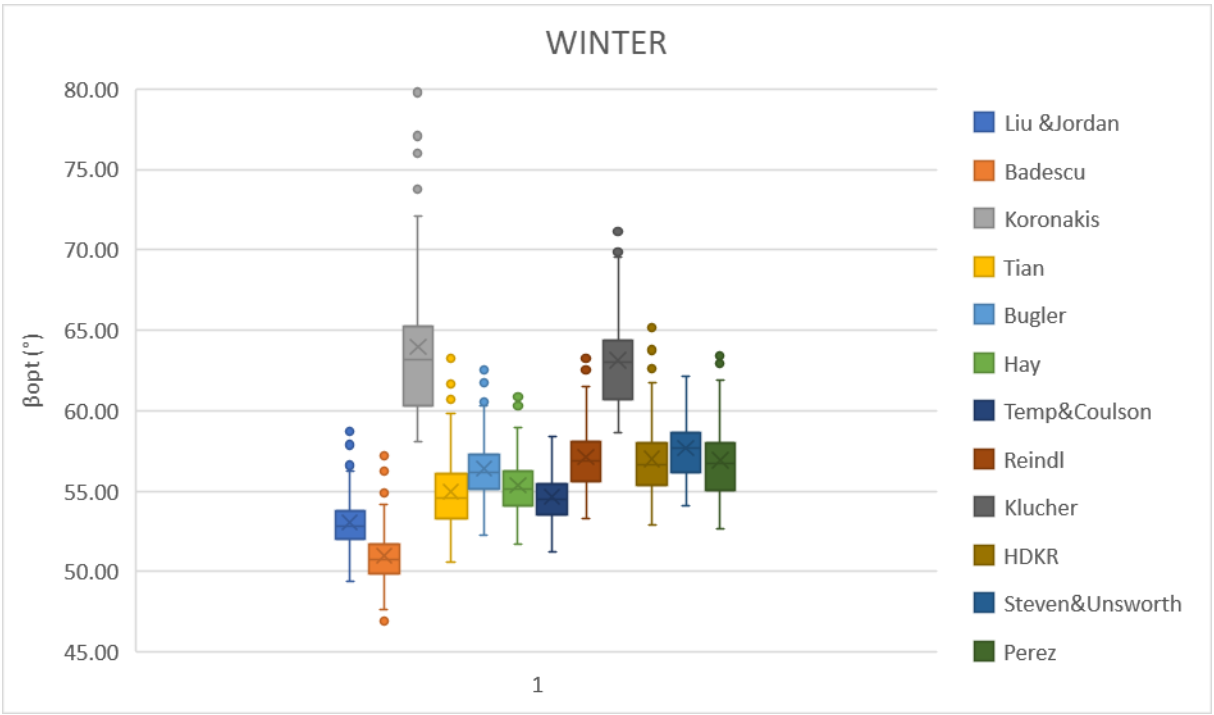

Figure 42 Winter season optimum tilt angles variation for 81 provinces of Turkey

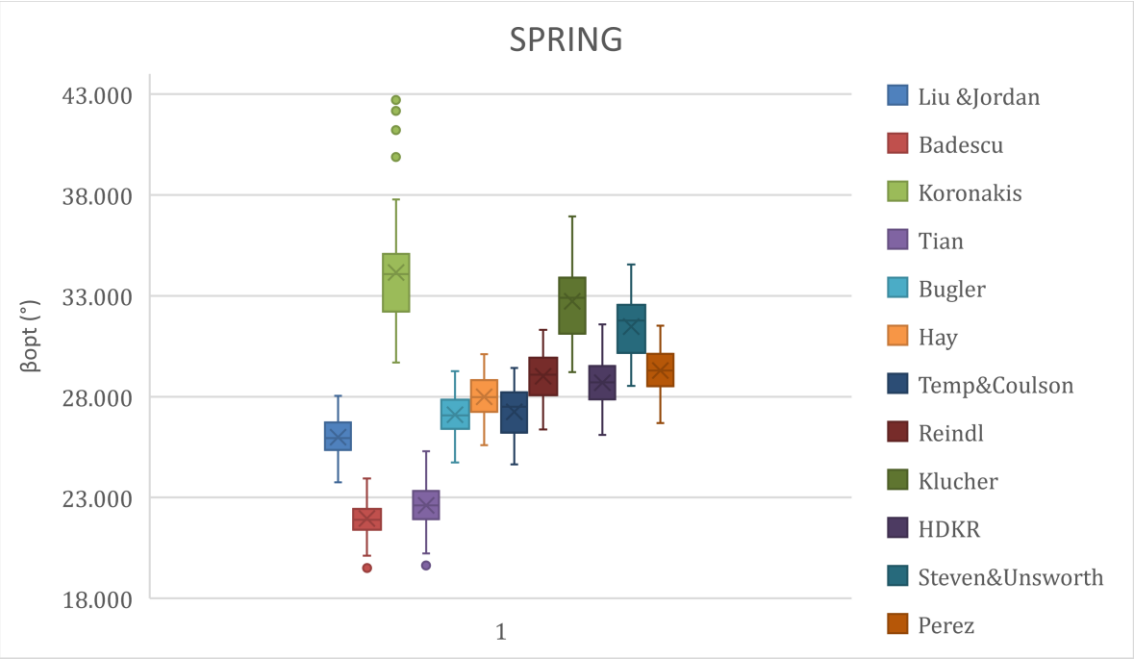

Figure 43 Spring season optimum tilt angles variation for 81 provinces of Turkey

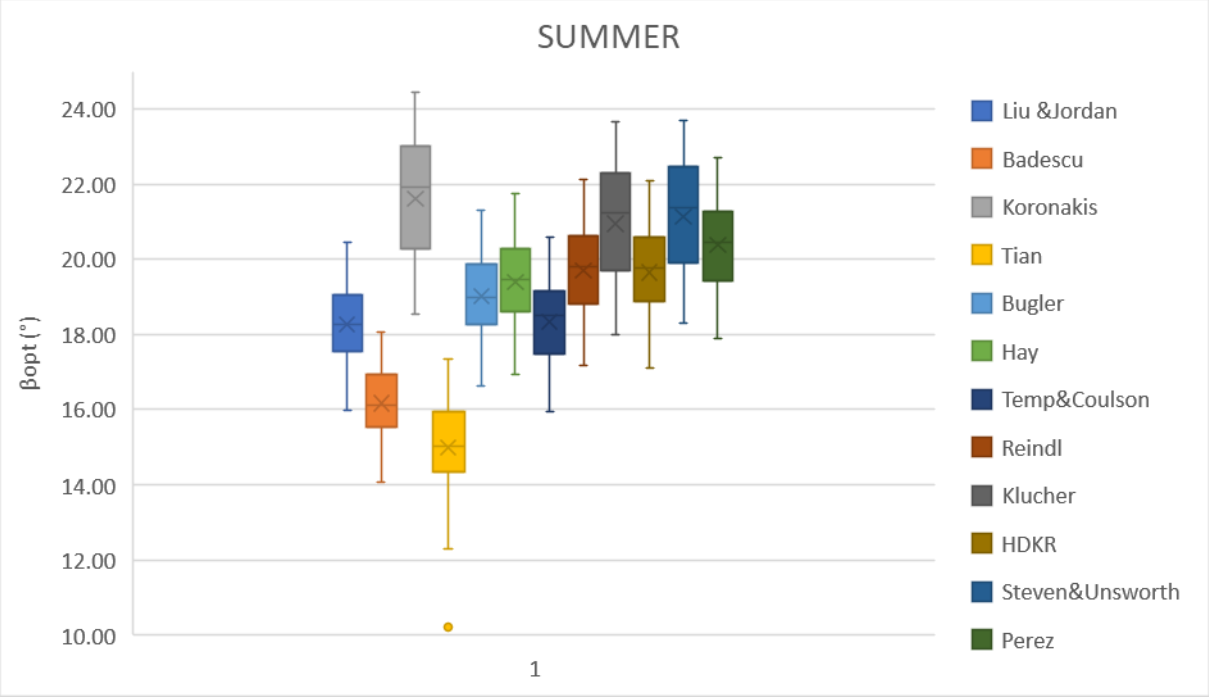

Figure 44 Summer season optimum tilt angles variation for 81 provinces of Turkey

The maps obtained for the isotropic and anisotropic models of the optimum tilt angles obtained for the fall season by taking the average of the monthly angles in September, October, and November are shown in the Figure 45 and Figure 46.

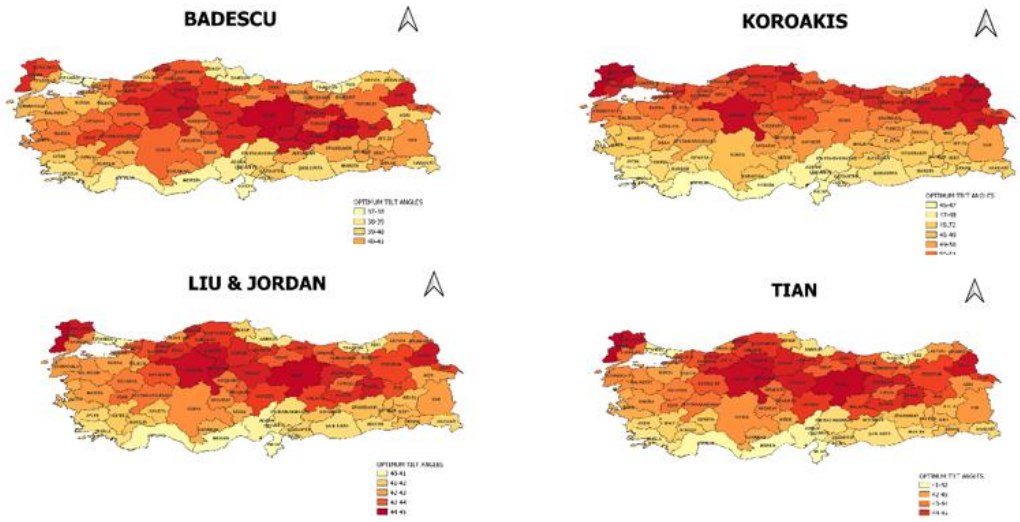

Figure 45 The Map Modelling of Seasonal (Fall) Optimum Tilt Angles of Turkey by Isotropic Models

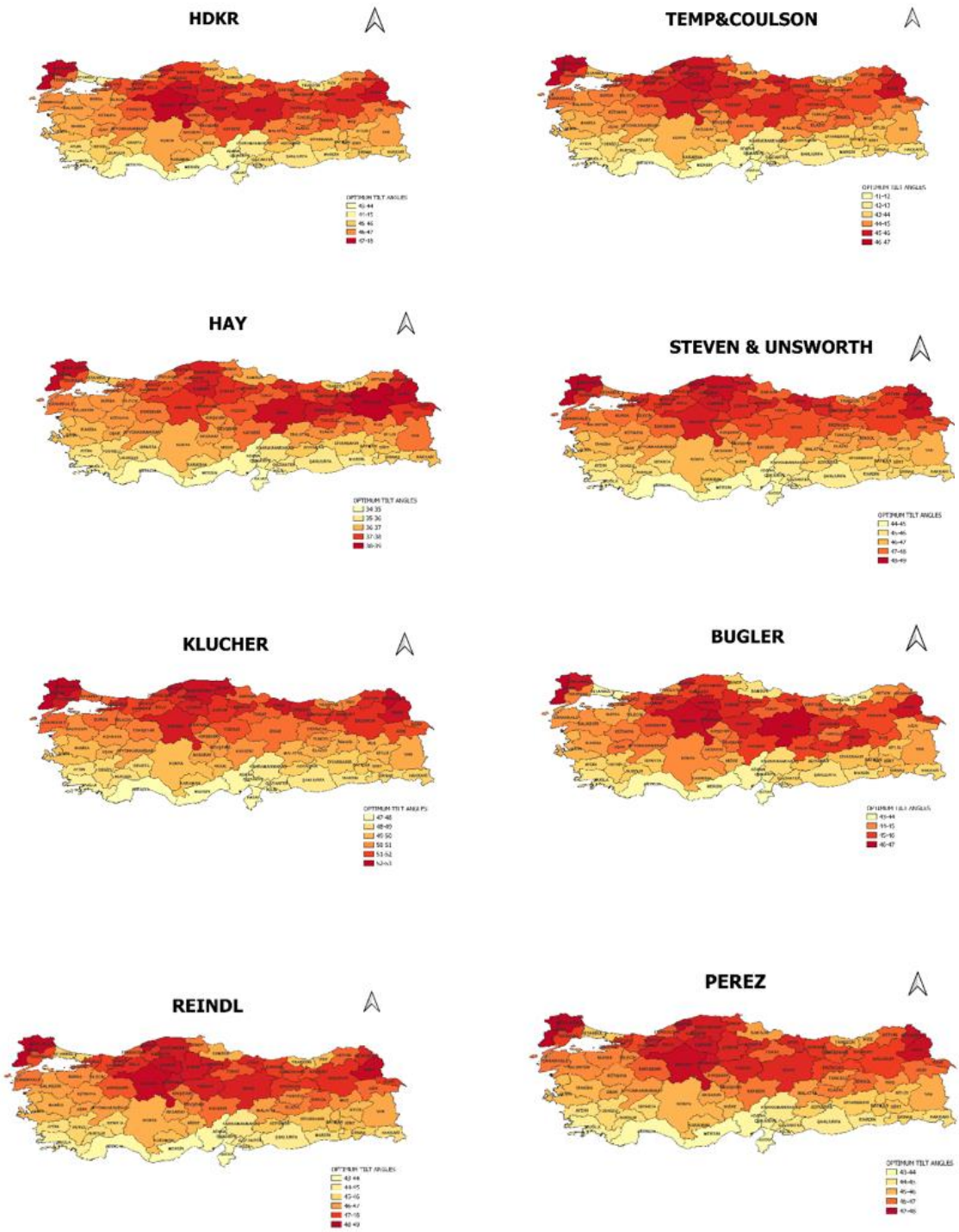

Figure 46 The Map Modelling of Seasonal (Fall) Optimum Tilt Angles of Turkey by Anisotropic Models

The maps obtained by taking the average of the monthly angles in December, January and February for the isotropic and anisotropic models of the optimum tilt angles obtained for the winter season are shown in the Figure 46 and Figure 47.

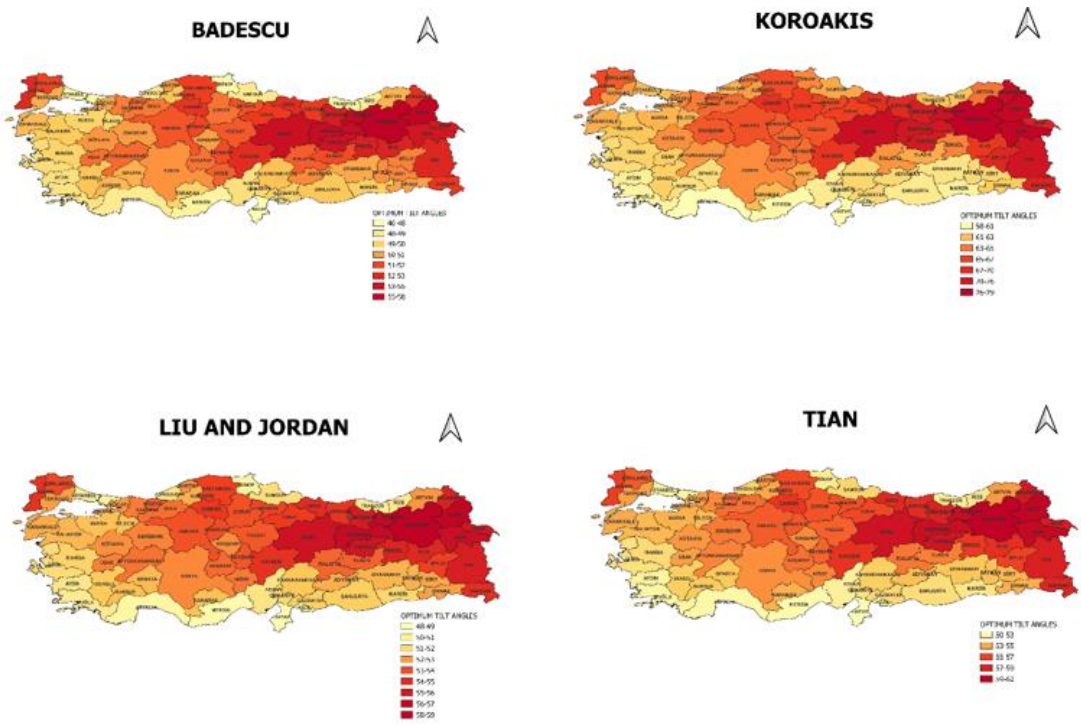

Figure 47 The Map Modelling of Seasonal (Winter) Optimum Tilt Angles of Turkey by Isotropic Models

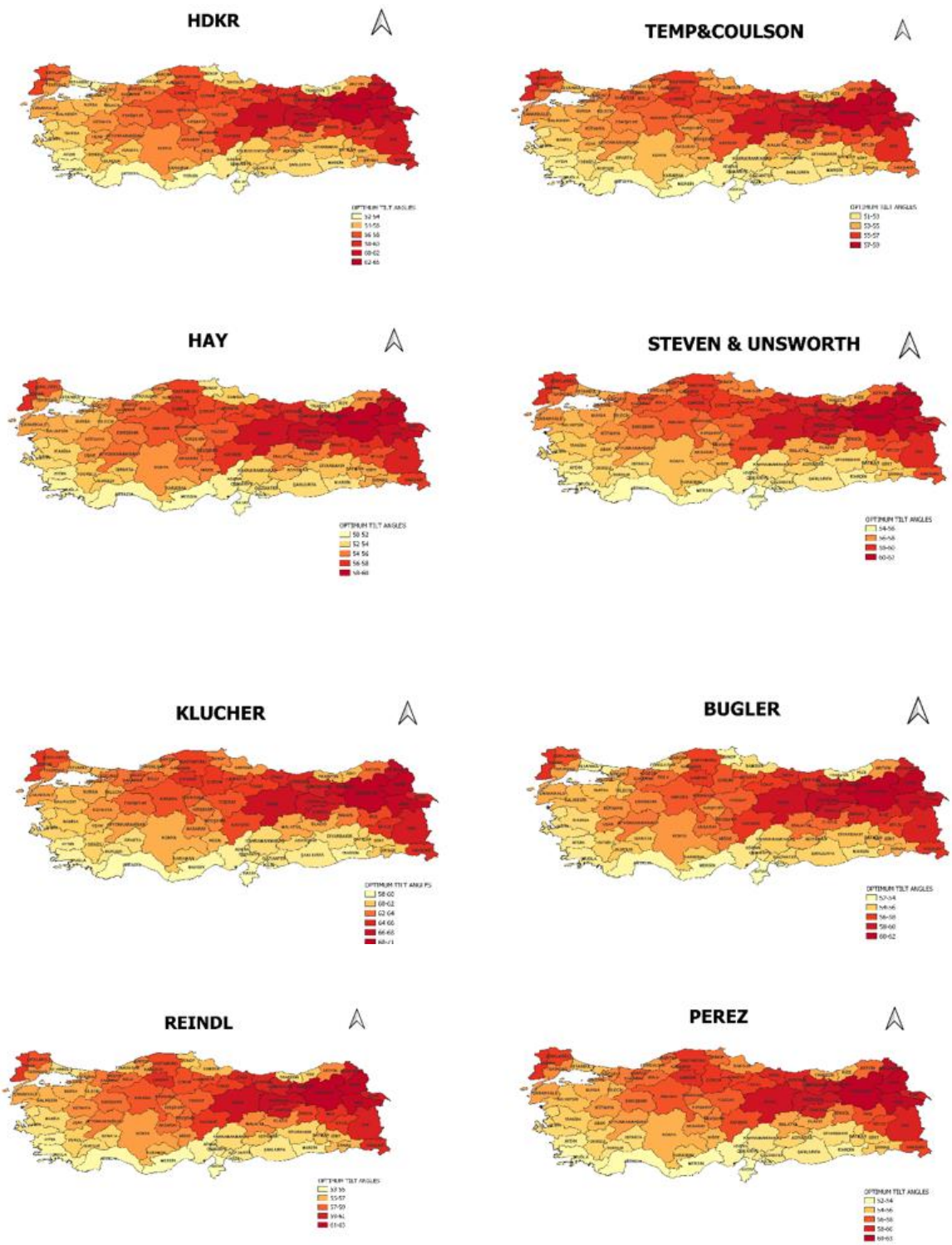

Figure 48 The Map Modelling of Seasonal (Winter) Optimum Tilt Angles of Turkey by Anisotropic Models

The maps obtained by taking the average of the monthly angles in March, April and May for the isotropic and anisotropic models of the OTAs obtained for the spring season are shown in the Figure 49 and Figure 50.

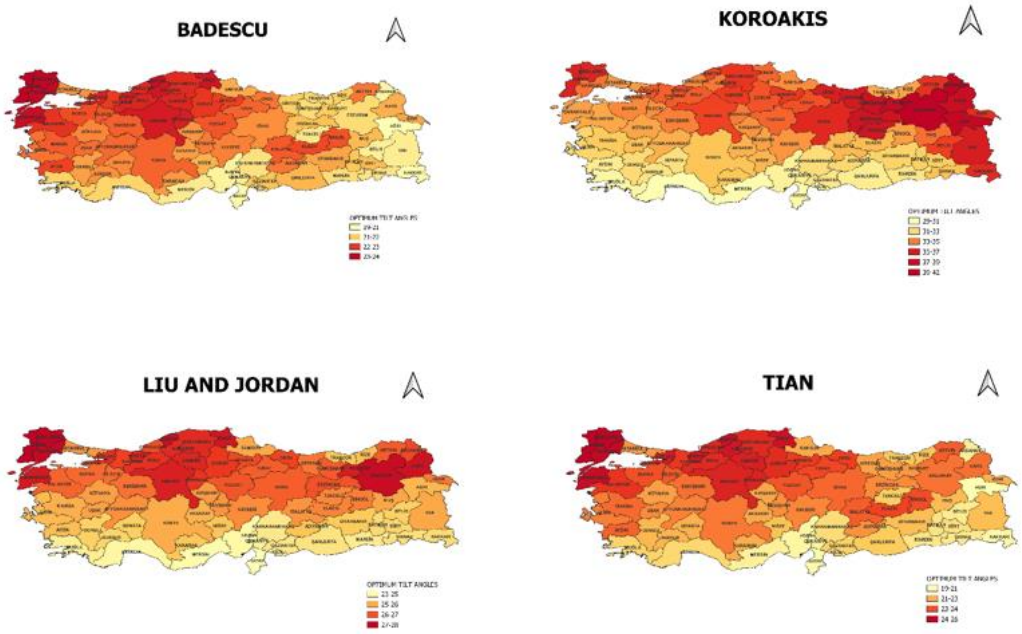

Figure 49 The Map Modelling of Seasonal (Spring) Optimum Tilt Angles of Turkey by Isotropic Models

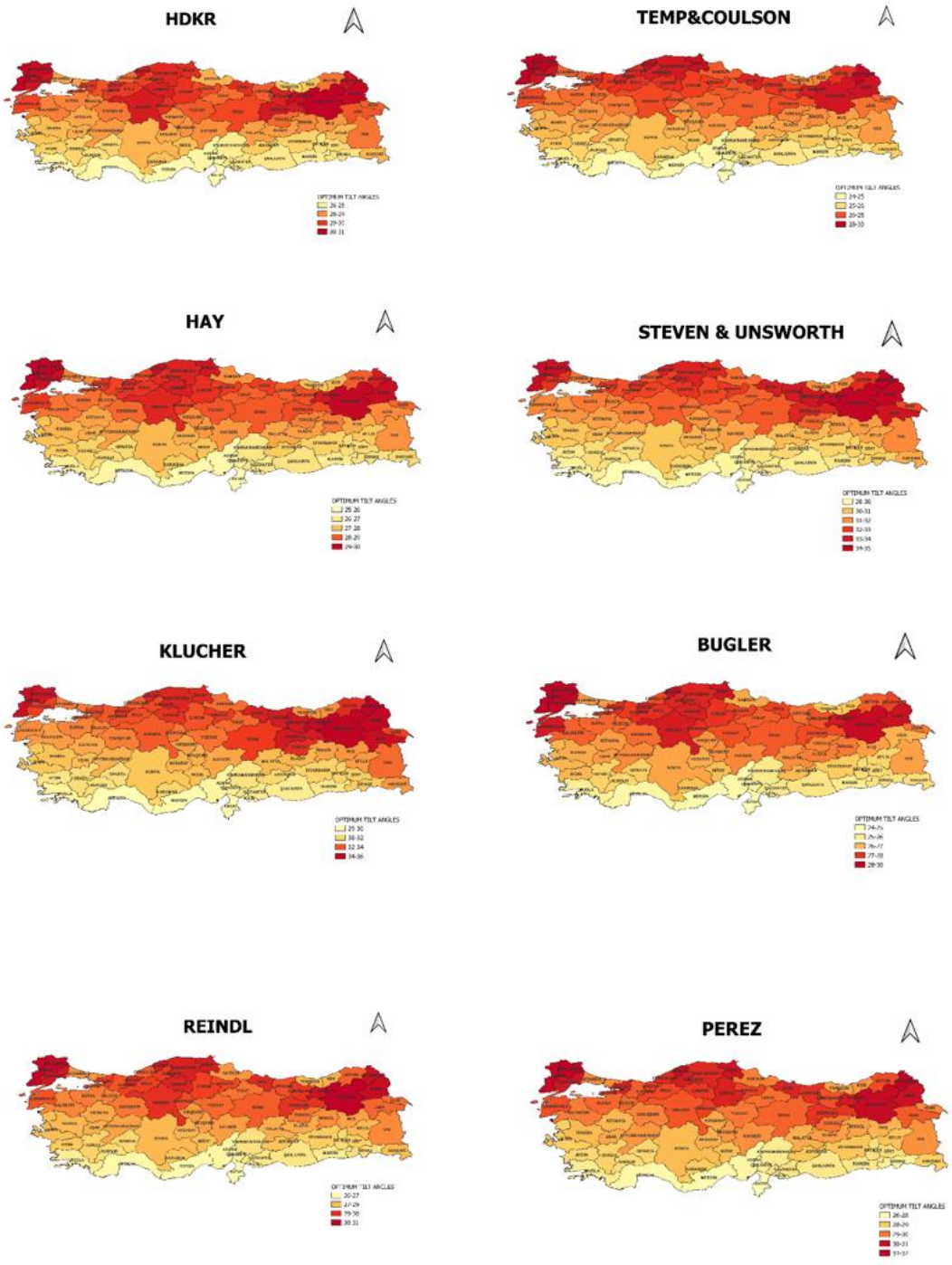

Figure 50 The Map Modelling of Seasonal (Spring) Optimum Tilt Angles of Turkey by Anisotropic Models

The maps obtained by taking the average of the monthly angles in June, July and August for the isotropic and anisotropic models of the OTAs obtained for the winter season are shown in the Figure 51 and Figure 52.

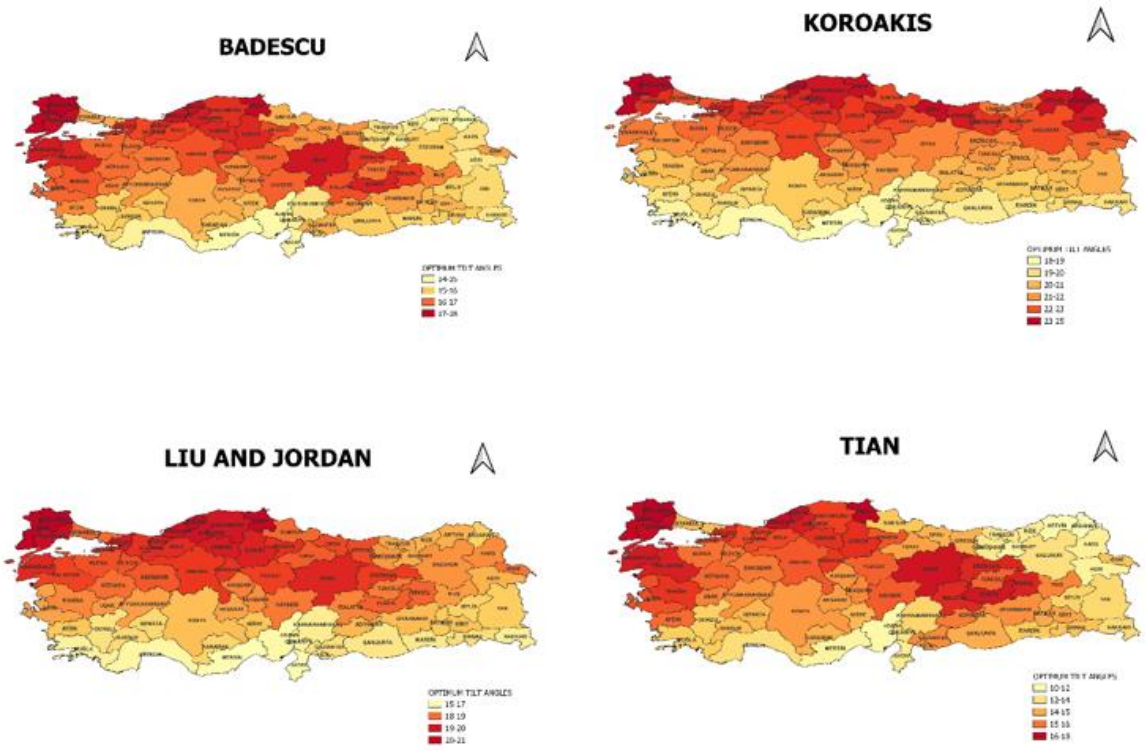

Figure 51 The Map Modelling of Seasonal (Summer) Optimum Tilt Angles of Turkey by Isotropic Models

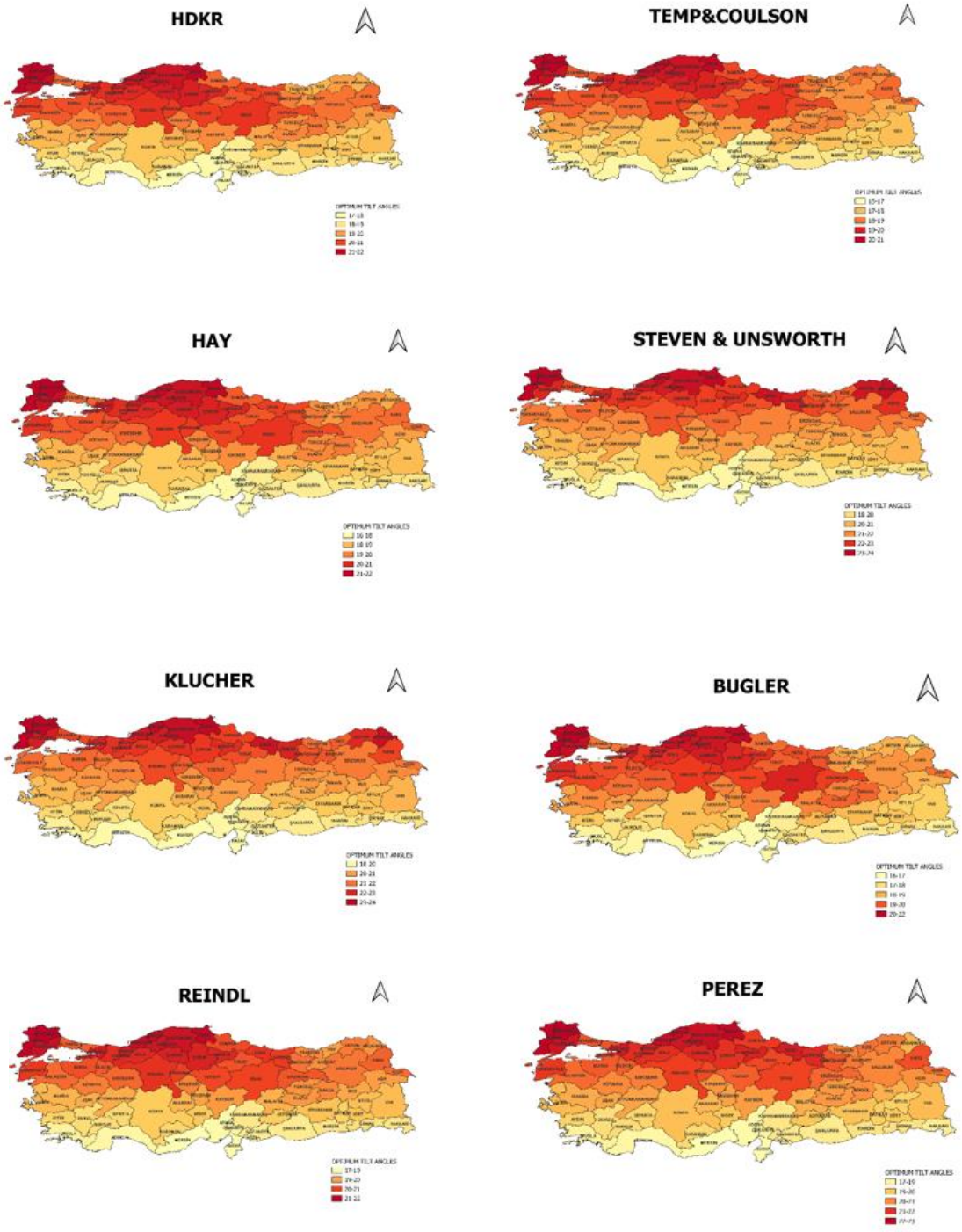

Figure 52 The Map Modelling of Seasonal (Summer) Optimum Tilt Angles of Turkey by Anisotropic Models

3.3. Monthly Variation

In this section, the monthly variation of the tilt angle, for each month, obtained from the 12 radiation models used for provinces of Turkey was implemented as shown in Figure 53. The tilt angles of in the majority of the radiation models used for the 81 cities which having different latitudes of Turkey, the range is start with 51 ° -75 ° in January by continuing to drop to in 8° -20 ° range in June and again rising to 54° -74 ° in December. When the average inclination angle values for each model are examined, if we compare it to 12 months, the angle value is minimum in June.

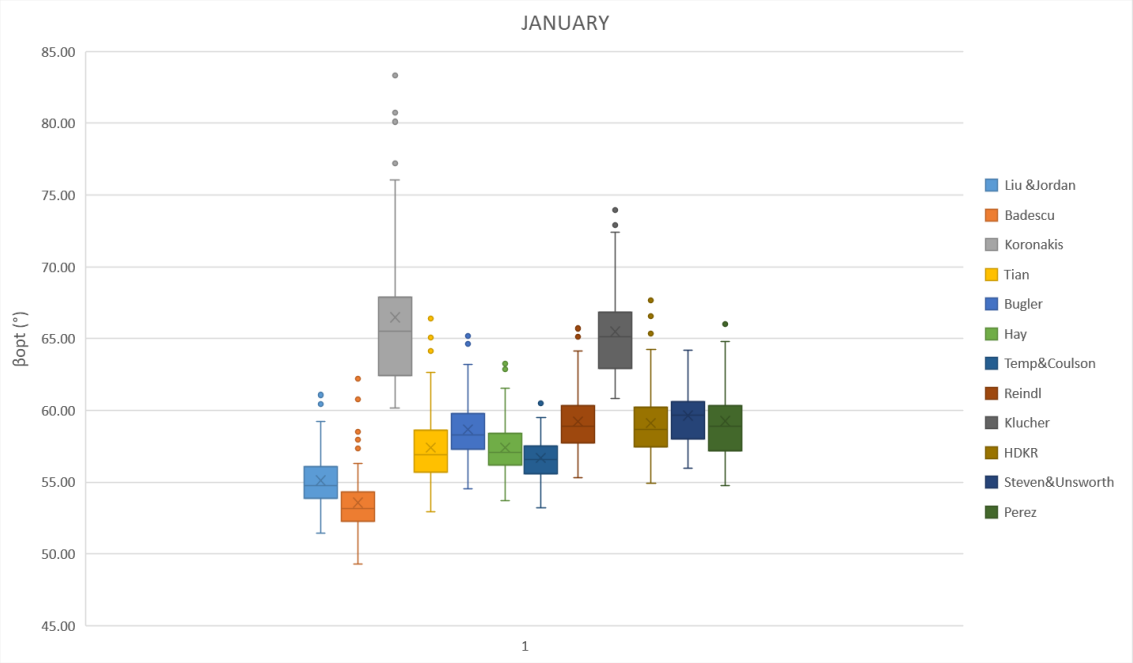

Figure 53 The variation of tilt angles of the models for the provinces of Turkey in January

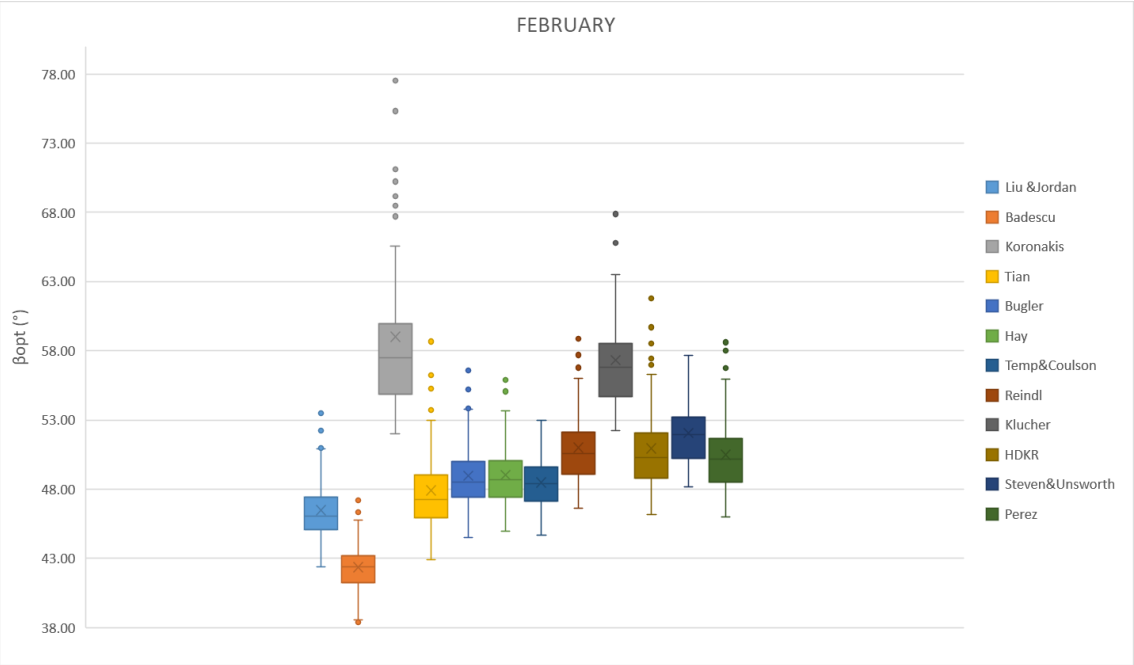

Figure 54 The variation of tilt angles of the models for the provinces of Turkey in February

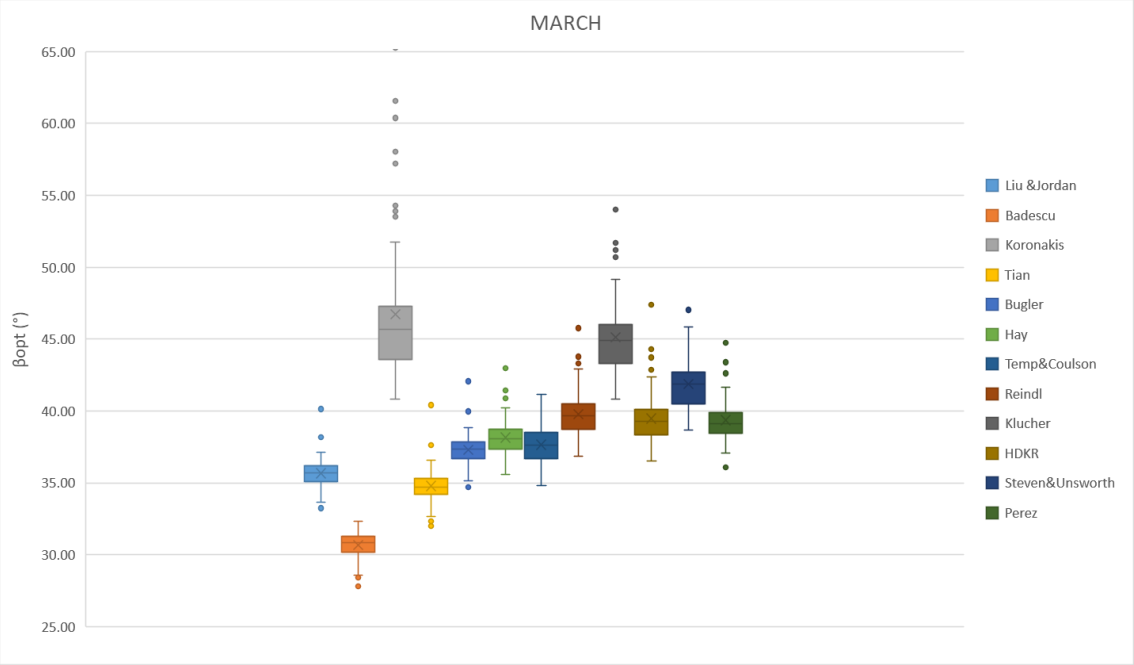

Figure 55 The variation of tilt angles of the models for the provinces of Turkey in March

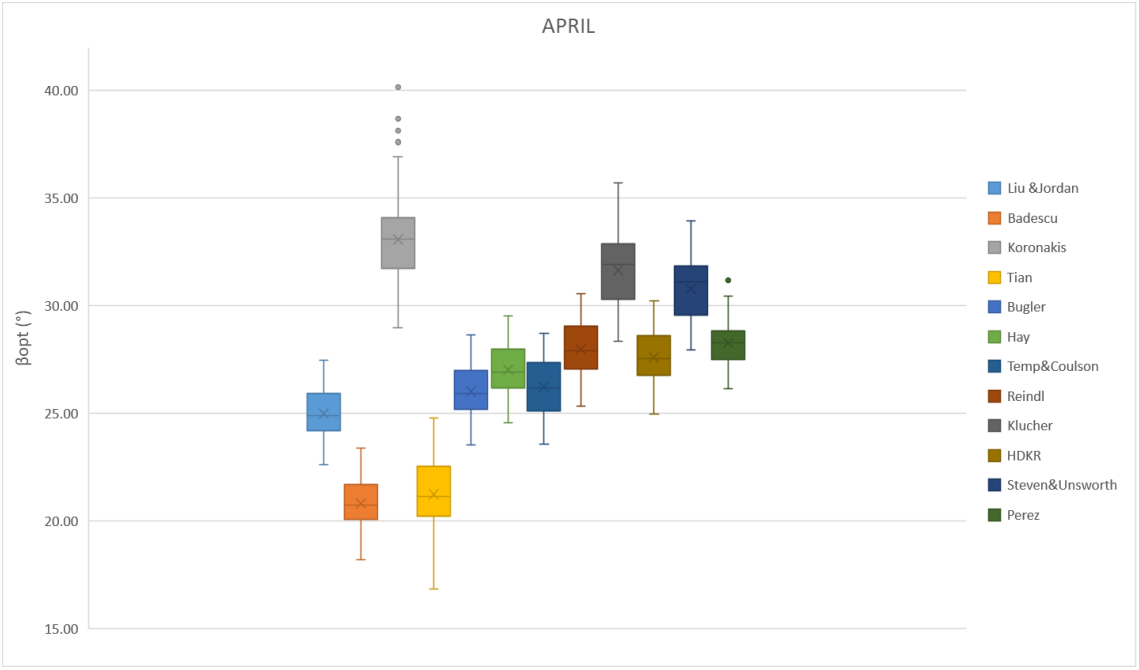

Figure 56 The variation of tilt angles of the models for the provinces of Turkey in April

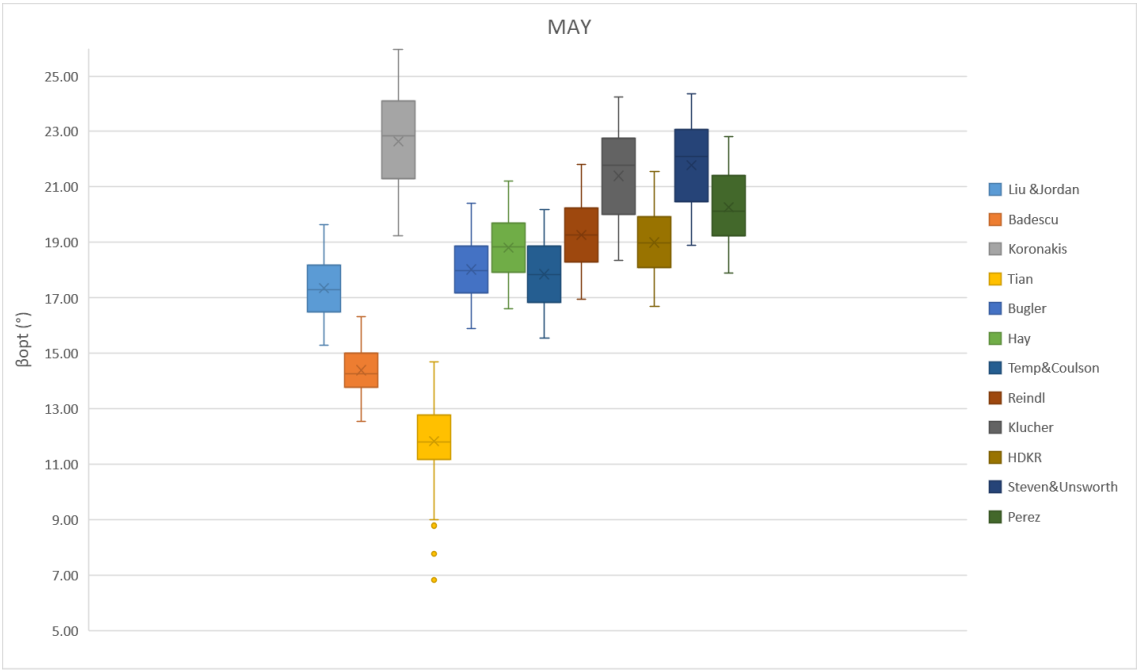

Figure 57 The variation of tilt angles of the models for the provinces of Turkey in May

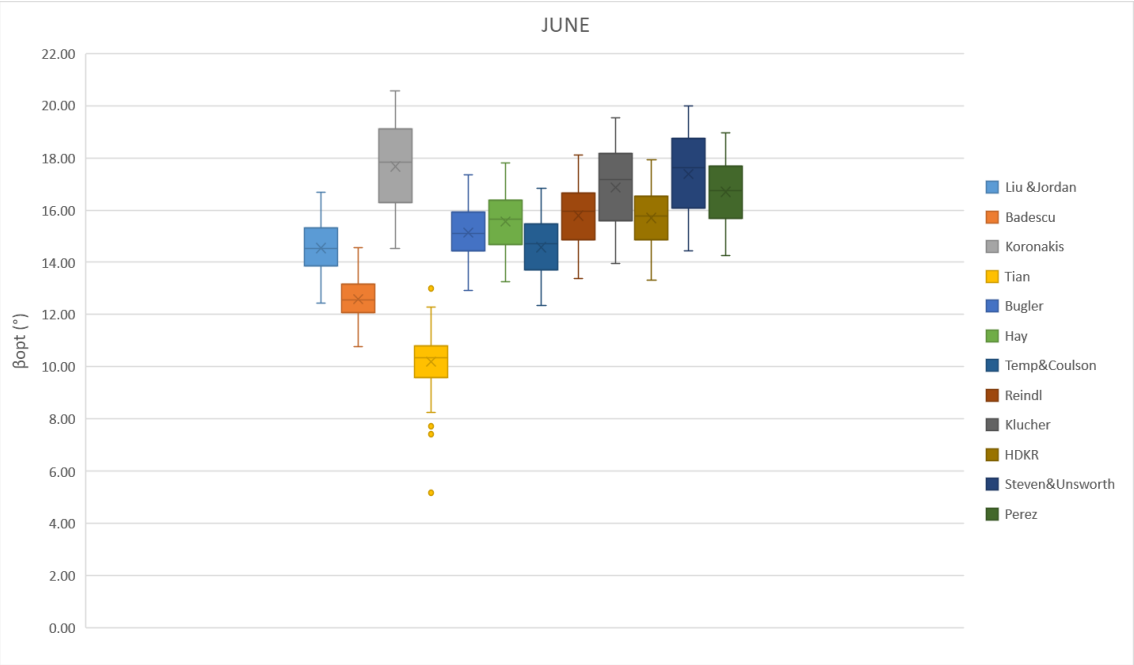

Figure 58 The variation of tilt angles of the models for the provinces of Turkey in June

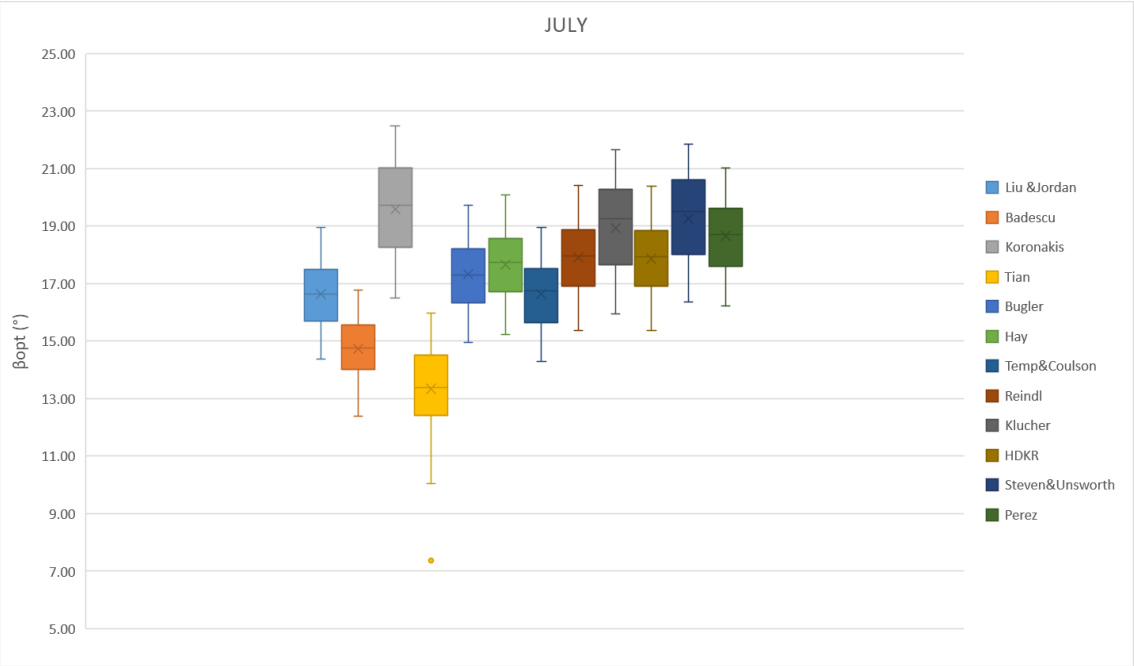

Figure 59 The variation of tilt angles of the models for the provinces of Turkey in July

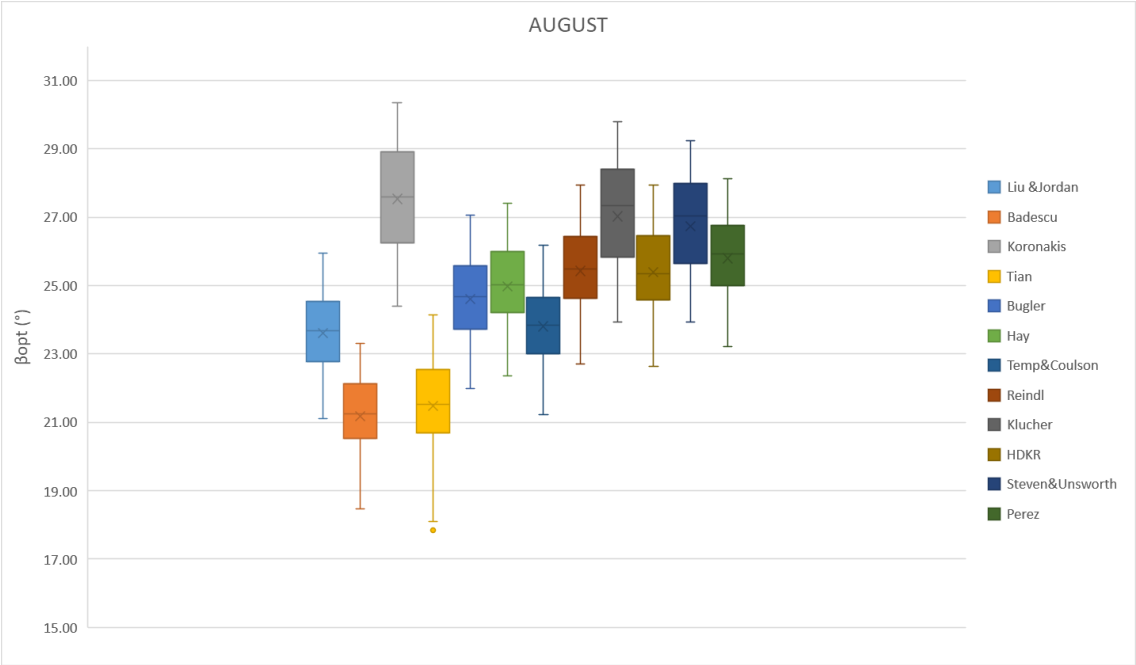

Figure 60 The variation of tilt angles of the models for the provinces of Turkey in August

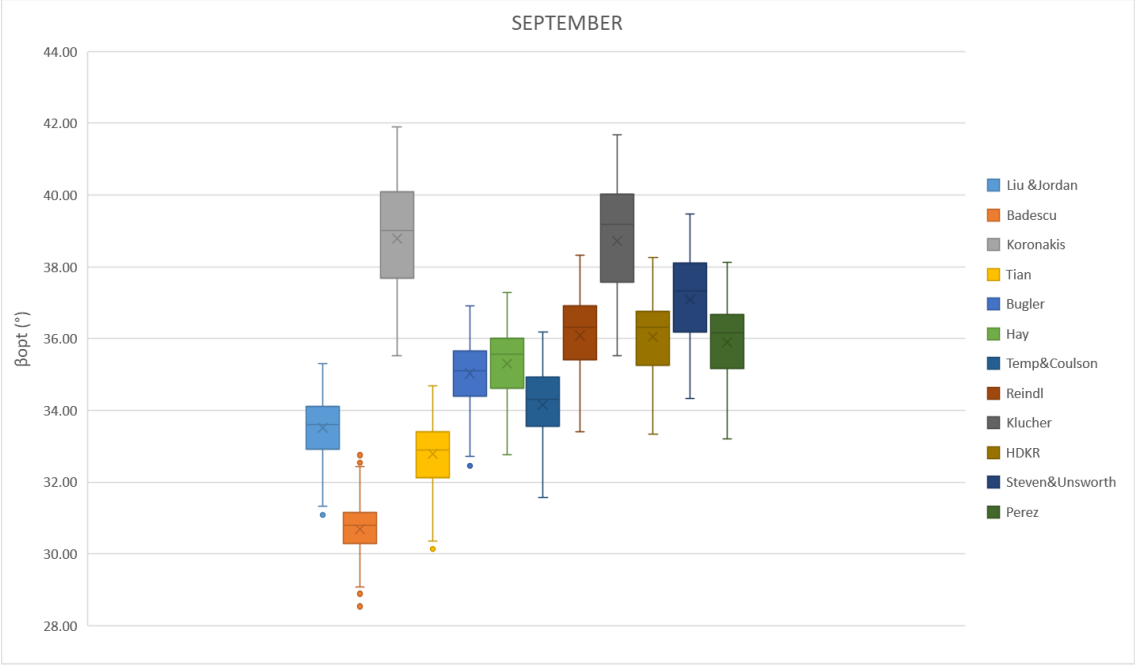

Figure 61 The variation of tilt angles of the models for the provinces of Turkey in September

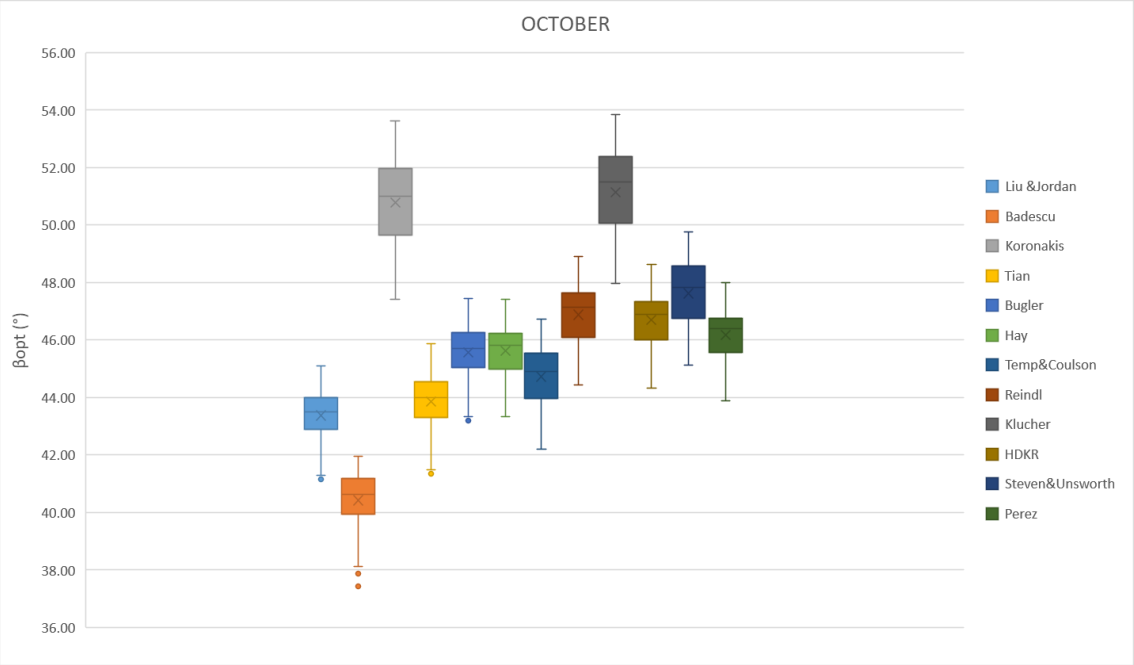

Figure 62 The variation of tilt angles of the models for the provinces of Turkey in October

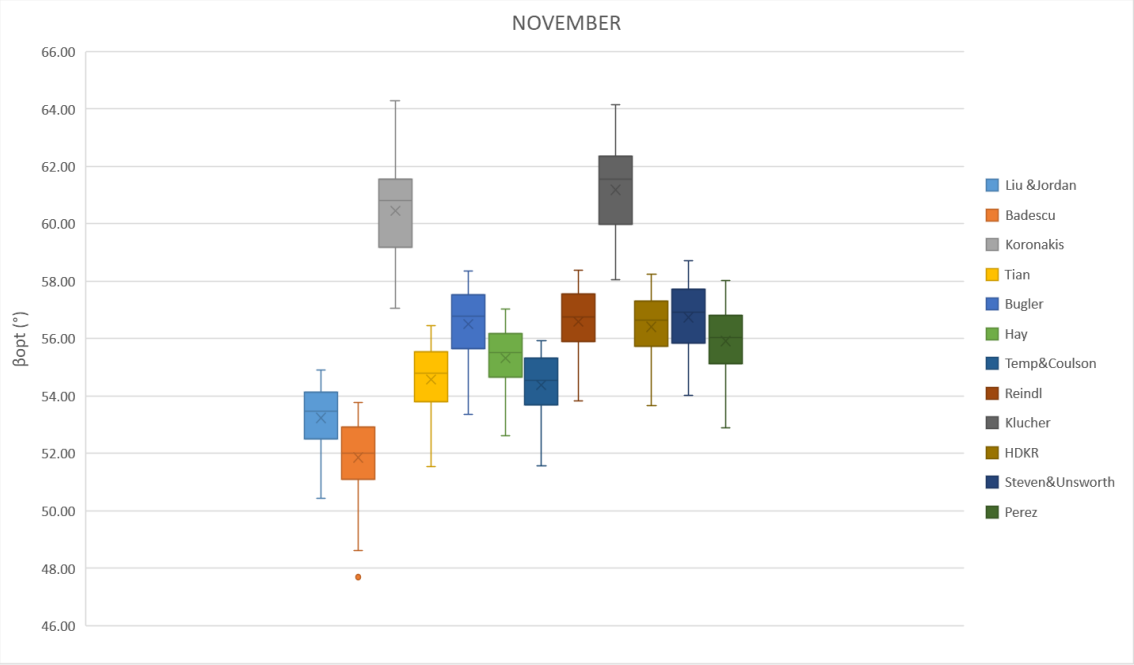

Figure 63 The variation of tilt angles of the models for the provinces of Turkey in November

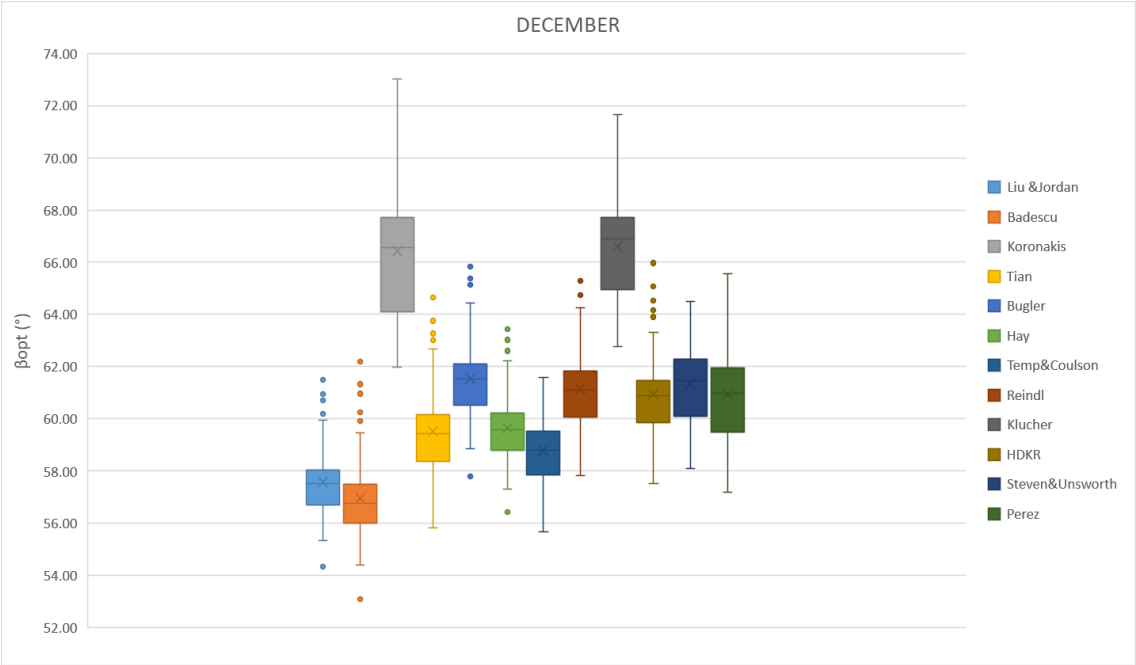

Figure 64 The variation of tilt angles of the models for the provinces of Turkey in December

As presented in figures above, the lines shown as outliers are excessive for most models during February, March and December. In this case, the tilt angle distribution on Turkey is irregular and not clear for February, March and December due to obtained data from NASA. KM and KLM models systematically resulted in high values, as in annual and seasonal variation analyzes. In November, it states that the variation of the tilt angle in each model is achieved at the confidence level of each method.

3.4. Comparison of Using Annual and Monthly Optimum Tilt Angles

Monthly, seasonal, and annual OTAs were obtained by using 12 radiation models for 81 provinces of Turkey. A comparison was made for the radiation obtained using the monthly angle and the radiation obtained using the annual angle. The analysis comparison performed on Eq. 2.41 by using 12 radiation models for 6 provinces with different seasonal and geological characteristics in different regions of Turkey is shown in the Table 8- Table 13.

As can be seen in the Table 8, total annual radiation as 56.32057 kWh/m² is obtained by using the annual OTA with the BAM for the province of İzmir, while total annual radiation as 59.78729 kWh/m² is obtained by using the monthly OTA. An increase of 6% is observed.

Table 8 The comparison of total solar radiation for İzmir, Turkey

İZMİR			
MODEL	**Annual total solar radiation by using Annual Optimum Tilt Angle (kWh/m²)**	**Annual total solar radiation by using Monthly Optimum Tilt Angle (kWh/m²)**	**Percentage (%)**
BADESCU	56.32057	59.78729	6%
KORONAKIS	41.70358	45.26650	9%
LIU&JORDAN	57.32516	60.58391	6%
TIAN	55.41293	59.41886	7%
BUGLER	54.58553	57.63876	6%
TEMP&COULSON	67.16704	71.26460	6%
HAY	63.09147	66.83178	6%
REINDL	64.54783	68.20373	6%
KLUCHER	47.89969	52.21828	9%
HDKR	50.73531	54.08499	7%
STEVEN & UNSWORTH	72.27272	76.83773	6%
PEREZ	66.36437	70.09008	6%

Table 9 The comparison of total solar radiation for Ankara, Turkey

ANKARA			
MODEL	**Annual total solar radiation by using Annual Optimum Tilt Angle (kWh/m²)**	**Annual total solar radiation by using Monthly Optimum Tilt Angle (kWh/m²)**	**Percentage (%)**
BADESCU	55.62641	58.93431	6%
KORONAKIS	39.39959	42.43699	8%
LIU&JORDAN	56.86265	59.80913	5%
TIAN	54.64852	58.51750	7%
BUGLER	54.45975	57.25929	5%
TEMP&COULSON	68.29333	72.14989	6%
HAY	62.93294	66.29759	5%
REINDL	64.74548	67.91369	5%
KLUCHER	46.18592	50.10560	8%
HDKR	50.32019	53.26951	6%
STEVEN & UNSWORTH	74.33756	78.64163	6%
PEREZ	65.14823	68.60981	5%

Table 10 The comparison of total solar radiation for Hatay, Turkey

HATAY			
MODEL	**Annual total solar radiation by using Annual Optimum Tilt Angle (kWh/m²)**	**Annual total solar radiation by using Monthly Optimum Tilt Angle (kWh/m²)**	**Percentage (%)**
BADESCU	59.08231	62.36926	6%
KORONAKIS	42.91541	46.37102	8%
LIU&JORDAN	60.02273	63.16193	5%
TIAN	58.02880	62.00245	7%
BUGLER	57.34710	60.26746	5%
TEMP&COULSON	70.33182	74.35775	6%
HAY	65.75411	69.38961	6%
REINDL	67.22812	70.97130	6%
KLUCHER	49.35699	53.59184	9%
HDKR	52.86326	56.10276	6%
STEVEN & UNSWORTH	75.61118	80.16218	6%
PEREZ	69.00563	72.75000	5%

Table 11 The comparison of total solar radiation for Ağrı, Turkey

AĞRI			
MODEL	**Annual total solar radiation by using Annual Optimum Tilt Angle (kWh/m²)**	**Annual total solar radiation by using Monthly Optimum Tilt Angle (kWh/m²)**	**Percentage (%)**
BADESCU	55.22917	58.59846	6%
KORONAKIS	36.61152	40.45910	11%
LIU&JORDAN	56.53823	59.56652	5%
TIAN	54.01337	58.43223	8%
BUGLER	54.49546	57.48725	5%
TEMP&COULSON	69.81976	73.86742	6%
HAY	62.32218	65.79226	6%
REINDL	64.40911	67.65030	5%
KLUCHER	43.58685	47.83043	10%
HDKR	50.26062	53.45999	6%
STEVEN & UNSWORTH	76.84832	81.55103	6%
PEREZ	61.96222	65.38799	6%

Table 12 The comparison of total solar radiation for Edirne, Turkey

EDİRNE			
MODEL	**Annual total solar radiation by using Annual Optimum Tilt Angle (kWh/m²)**	**Annual total solar radiation by using Monthly Optimum Tilt Angle (kWh/m²)**	**Percentage (%)**
BADESCU	48.67371	51.66992	6%
KORONAKIS	33.68178	36.32741	8%
LIU&JORDAN	49.80605	52.42823	5%
TIAN	47.75418	51.17291	7%
BUGLER	47.58164	50.10109	5%
TEMP&COULSON	60.49820	63.98862	6%
HAY	55.04032	57.98611	5%
REINDL	56.78523	59.52613	5%
KLUCHER	40.03284	43.55379	9%
HDKR	44.28131	46.86662	6%
STEVEN & UNSWORTH	66.19520	70.05607	6%
PEREZ	58.34698	61.44344	5%

Table 13 The comparison of total solar radiation for Sinop, Turkey

SİNOP			
MODEL	**Annual total solar radiation by using Annual Optimum Tilt Angle (kWh/m²)**	**Annual total solar radiation by using Monthly Optimum Tilt Angle (kWh/m²)**	**Percentage (%)**
BADESCU	44.42300	46.97696	6%
KORONAKIS	28.95308	31.63543	9%
LIU&JORDAN	45.24506	47.63227	5%
TIAN	43.28135	46.35659	7%
BUGLER	43.02212	45.33186	5%
TEMP&COULSON	55.56409	58.89233	6%
HAY	50.00501	52.70894	5%
REINDL	51.57515	54.14463	5%
KLUCHER	35.23067	38.69695	10%
HDKR	39.77630	42.17696	6%
STEVEN & UNSWORTH	61.07507	64.85899	6%
PEREZ	53.13605	56.00764	5%

For the province of Ağrı as shown in Table 11, total annual radiation as 76.84832 kWh/m² is obtained when the annual OTA is used with the SUM, while a total annual radiation as 81.55103 kWh/m² is obtained when using the monthly OTA. It can be interpreted that there is an increase of approximately 6% again. The increase rates of other provinces according to the DSR models are also shown in the tables. Although the rate of increase varies on the basis of DSR models and provinces, there is an average increase of 6% for each province.

Since the use of monthly panel angles brings a 6% increase in radiation, it is expected that the electricity production obtained from the panels will increase in this direction. The electricity production efficiency of the panels is affected by the panel properties and environmental factors. However, the increase in radiation cannot be ignored in terms of productivity. Changing the angles monthly after the installation of a facility ensures that the investment made turns into profit sooner. However, considering that changing the monthly panel tilt angle is costly, the cost and feasibility analysis should be investigated in detail.

3.5. Validation And Comparison of Models

The validation of the models was evaluated using data recorded between 1994-1996 at the Ege University İzmir Solar Energy Institute Solar-Meteorology Station ($\phi = 38.415°$) provided by Günerhan and Hepbaşlı (2007). OTAs calculated in the study were used in Equation 2.41 and monthly radiation was calculated for 12 models. Other parameters in the equation were used data from NASA. The monthly radiation values of the applied models are calculated in Table 6-Table 25 below.

In order to obtain a statistically more comprehensive comparison, error measures such as root mean squared error (RMSE), mean bias error (MBE), the coefficient of determination (R2), the scattered index (SI) between measured data and model data are used as follows:

$$RMSE = \sqrt{\frac{1}{N}\sum_{i=1}^{N} \hat{y}_i - y_i \ ^2} \tag{3.1}$$

$$MBE = \frac{1}{N}\sum_{i=1}^{N} \hat{y}_i - y_i \tag{3.2}$$

$$R^2 = 1 - \frac{\sum_{i=1}^{N} (\hat{y}_i - y_i)^2}{\sum_{i=1}^{N} \left(y_i - \frac{1}{N}\sum_{i=1}^{N} y_i \right)} \tag{3.3}$$

$$SI = \frac{RMSE}{\frac{1}{N}\sum_{i=1}^{N} y_i} \tag{3.4}$$

where $\hat{y}_i$ is model response, y_i is measured data and N is the total number of data.

Table 14 The performance of the Liu and Jordan model for İzmir

LIU & JORDAN								
MONTHS	β_{opt}	**Monthly total solar radiation on an optimum tilt (measured) (kWh/m²)**	**Monthly total solar radiation on an optimum tilt (estimated) (kWh/m²)**	**R²**	**RMSE**	**MBE**	**SSE**	**SI**
JANUARY	65.30	2.89795	2.90685					
FEBRUARY	56.40	5.20268	3.30941					
MARCH	42.20	7.51319	4.29191					
APRIL	23.40	6.92460	5.46374					
MAY	6.60	8.94428	6.76703					
JUNE	0.00	9.24434	7.78728	0.795605	1.92761	3.71568	44.58816	0.28595
JULY	1.30	9.98181	8.07328					
AUGUST	16.60	8.08562	6.96459					
SEPTEMBER	35.00	7.96329	5.63537					
OCTOBER	52.20	7.87096	4.56526					
NOVEMBER	63.20	3.11607	3.68073					
DECEMBER	67.40	3.14838	2.89447					

Table 15 The performance of the Badescu model for İzmir

BADESCU								
MONTHS	β_{opt}	**Monthly total solar radiation on an optimum tilt (measured) (kWh/m²)**	**Monthly total solar radiation on an optimum tilt (estimated) (kWh/m²)**	**R²**	**RMSE**	**MBE**	**SSE**	**SI**
JANUARY	65.30	2.89795	2.78644					
FEBRUARY	56.40	5.20268	3.13887					
MARCH	42.20	7.51319	4.11046					
APRIL	23.40	6.92460	5.37731					
MAY	6.60	8.94428	6.75850					
JUNE	0.00	9.24434	7.78728	0.782843	2.00963	4.03860	48.46315	0.29812
JULY	1.30	9.98181	8.07306					
AUGUST	16.60	8.08562	6.93204					
SEPTEMBER	35.00	7.96329	5.51760					
OCTOBER	52.20	7.87096	4.40037					
NOVEMBER	63.20	3.11607	3.55322					
DECEMBER	67.40	3.14838	2.79273					

Table 16 The performance of the Koronakis model for İzmir

KOROAKIS								
MONTHS	β_{opt}	**Monthly total solar radiation on an optimum tilt (measured) (kWh/m²)**	**Monthly total solar radiation on an optimum tilt (estimated) (kWh/m²)**	**R²**	**RMSE**	**MBE**	**SSE**	**SI**
JANUARY	65.30	2.89795	2.34149					
FEBRUARY	56.40	5.20268	2.41772					
MARCH	42.20	7.51319	2.87671					
APRIL	23.40	6.92460	3.52953					
MAY	6.60	8.94428	4.47402					
JUNE	0.00	9.24434	5.80506	0.678286	3.19455	10.20516	122.46197	0.47389
JULY	1.30	9.98181	6.56240					
AUGUST	16.60	8.08562	5.55222					
SEPTEMBER	35.00	7.96329	4.37714					
OCTOBER	52.20	7.87096	3.62162					
NOVEMBER	63.20	3.11607	3.07361					
DECEMBER	67.40	3.14838	2.41945					

Table 17 The performance of the Tian model for İzmir

TIAN								
MONTHS	β_{opt}	**Monthly total solar radiation on an optimum tilt (measured) (kWh/m²)**	**Monthly total solar radiation on an optimum tilt (estimated) (kWh/m²)**	**R²**	**RMSE**	**MBE**	**SSE**	**SI**
JANUARY	65.30	2.89795	2.83586	0.779029	2.02866	4.11544	49.38533	0.30094
FEBRUARY	56.40	5.20268	3.18517					
MARCH	42.20	7.51319	4.09375					
APRIL	23.40	6.92460	5.26021					
MAY	6.60	8.94428	6.68064					
JUNE	0.00	9.24434	7.78728					
JULY	1.30	9.98181	8.06122					
AUGUST	16.60	8.08562	6.84824					
SEPTEMBER	35.00	7.96329	5.46998					
OCTOBER	52.20	7.87096	4.43119					
NOVEMBER	63.20	3.11607	3.60188					
DECEMBER	67.40	3.14838	2.83720					

Table 18 The performance of the Bugler model for İzmir

BUGLER								
MONTHS	β_{opt}	**Monthly total solar radiation on an optimum tilt (measured) (kWh/m²)**	**Monthly total solar radiation on an optimum tilt (estimated) (kWh/m²)**	**R²**	**RMSE**	**MBE**	**SSE**	**SI**
JANUARY	65.30	2.89795	2.80327	0.79432	2.12964	4.53535	54.42426	0.31592
FEBRUARY	56.40	5.20268	3.18850					
MARCH	42.20	7.51319	4.11526					
APRIL	23.40	6.92460	5.23534					
MAY	6.60	8.94428	6.51321					
JUNE	0.00	9.24434	7.47028					
JULY	1.30	9.98181	7.70264					
AUGUST	16.60	8.08562	6.59818					
SEPTEMBER	35.00	7.96329	5.33512					
OCTOBER	52.20	7.87096	4.36681					
NOVEMBER	63.20	3.11607	3.54041					
DECEMBER	67.40	3.14838	2.79083					

Table 19 The performance of the Hay model for İzmir

HAY								
MONTHS	β_{opt}	**Monthly total solar radiation on an optimum tilt (measured) (kWh/m²)**	**Monthly total solar radiation on an optimum tilt (estimated) (kWh/m²)**	**R²**	**RMSE**	**MBE**	**SSE**	**SI**
JANUARY	65.30	2.89795	3.40245	0.803089	1.54000	2.37160	28.45925	0.22845
FEBRUARY	56.40	5.20268	3.79886					
MARCH	42.20	7.51319	4.81270					
APRIL	23.40	6.92460	5.95229					
MAY	6.60	8.94428	7.22496					
JUNE	0.00	9.24434	8.24022					
JULY	1.30	9.98181	8.49986					
AUGUST	16.60	8.08562	7.45773					
SEPTEMBER	35.00	7.96329	6.23700					
OCTOBER	52.20	7.87096	5.22138					
NOVEMBER	63.20	3.11607	4.29045					
DECEMBER	67.40	3.14838	3.39685					

Table 20 The performance of the Temps&Coulson model for İzmir

TEMPS & COULSON								
MONTHS	β_{opt}	**Monthly total solar radiation on an optimum tilt (measured) (kWh/m²)**	**Monthly total solar radiation on an optimum tilt (estimated) (kWh/m²)**	**R²**	**RMSE**	**MBE**	**SSE**	**SI**
JANUARY	65.30	2.89795	3.66118	0.83123	1.26266	1.59432	19.13184	0.18731
FEBRUARY	56.40	5.20268	4.25994					
MARCH	42.20	7.51319	5.39469					
APRIL	23.40	6.92460	6.57319					
MAY	6.60	8.94428	7.84305					
JUNE	0.00	9.24434	8.66672					
JULY	1.30	9.98181	8.76302					
AUGUST	16.60	8.08562	7.70330					
SEPTEMBER	35.00	7.96329	6.49836					
OCTOBER	52.20	7.87096	5.46221					
NOVEMBER	63.20	3.11607	4.43935					
DECEMBER	67.40	3.14838	3.56289					

Table 21 The performance of the Reindl model for İzmir

REINDL								
MONTHS	β_{opt}	**Monthly total solar radiation on an optimum tilt (measured) (kWh/m²)**	**Monthly total solar radiation on an optimum tilt (estimated) (kWh/m²)**	**R²**	**RMSE**	**MBE**	**SSE**	**SI**
JANUARY	65.30	2.89795	3.55361	0.812941	1.47597	2.17848	26.14179	0.21895
FEBRUARY	56.40	5.20268	3.98660					
MARCH	42.20	7.51319	4.99801					
APRIL	23.40	6.92460	6.05460					
MAY	6.60	8.94428	7.24256					
JUNE	0.00	9.24434	8.24022					
JULY	1.30	9.98181	8.50071					
AUGUST	16.60	8.08562	7.49442					
SEPTEMBER	35.00	7.96329	6.34590					
OCTOBER	52.20	7.87096	5.38220					
NOVEMBER	63.20	3.11607	4.43737					
DECEMBER	67.40	3.14838	3.53178					

Table 22 The performance of the Klucher model for İzmir

KLUCHER								
MONTHS	β_{opt}	**Monthly total solar radiation on an optimum tilt (measured) (kWh/m²)**	**Monthly total solar radiation on an optimum tilt (estimated) (kWh/m²)**	**R²**	**RMSE**	**MBE**	**SSE**	**SI**
JANUARY	65.30	2.89795	2.76503	0.734142	2.66720	7.11394	85.36732	0.39566
FEBRUARY	56.40	5.20268	2.96261					
MARCH	42.20	7.51319	3.56224					
APRIL	23.40	6.92460	4.26476					
MAY	6.60	8.94428	5.18075					
JUNE	0.00	9.24434	6.39866					
JULY	1.30	9.98181	7.04731					
AUGUST	16.60	8.08562	6.08279					
SEPTEMBER	35.00	7.96329	4.97754					
OCTOBER	52.20	7.87096	4.18914					
NOVEMBER	63.20	3.11607	3.52580					
DECEMBER	67.40	3.14838	2.79634					

Table 23 The performance of the HDKR model for İzmir

HDKR								
MONTHS	β_{opt}	**Monthly total solar radiation on an optimum tilt (measured) (kWh/m²)**	**Monthly total solar radiation on an optimum tilt (estimated) (kWh/m²)**	**R²**	**RMSE**	**MBE**	**SSE**	**SI**
JANUARY	65.30	2.89795	2.78923	0.782868	2.44901	5.99764	71.97165	0.36330
FEBRUARY	56.40	5.20268	3.10584					
MARCH	42.20	7.51319	3.86983					
APRIL	23.40	6.92460	4.77662					
MAY	6.60	8.94428	5.85840					
JUNE	0.00	9.24434	6.80523					
JULY	1.30	9.98181	7.18369					
AUGUST	16.60	8.08562	6.14994					
SEPTEMBER	35.00	7.96329	5.00528					
OCTOBER	52.20	7.87096	4.18163					
NOVEMBER	63.20	3.11607	3.48535					
DECEMBER	67.40	3.14838	2.78848					

Table 24 The performance of the Steven &Unsworth model for İzmir

STEVEN & UNSWORTH								
MONTHS	β_{opt}	**Monthly total solar radiation on an optimum tilt (measured) (kWh/m²)**	**Monthly total solar radiation on an optimum tilt (estimated) (kWh/m²)**	**R²**	**RMSE**	**MBE**	**SSE**	**SI**
JANUARY	65.30	2.89795	4.27024	0.807825	1.11551	1.24437	14.93241	0.16548
FEBRUARY	56.40	5.20268	4.79346					
MARCH	42.20	7.51319	5.86451					
APRIL	23.40	6.92460	7.10603					
MAY	6.60	8.94428	8.63015					
JUNE	0.00	9.24434	9.44913					
JULY	1.30	9.98181	9.33951					
AUGUST	16.60	8.08562	8.11577					
SEPTEMBER	35.00	7.96329	6.86146					
OCTOBER	52.20	7.87096	5.90283					
NOVEMBER	63.20	3.11607	4.97743					
DECEMBER	67.40	3.14838	4.16049					

Table 25 The performance of the Perez model for İzmir

PEREZ								
MONTHS	β_{opt}	**Monthly total solar radiation on an optimum tilt (measured) (kWh/m²)**	**Monthly total solar radiation on an optimum tilt (estimated) (kWh/m²)**	**R²**	**RMSE**	**MBE**	**SSE**	**SI**
JANUARY	65.30	2.89795	3.49519	0.841613	1.29598	1.67956	20.15475	0.19225
FEBRUARY	56.40	5.20268	4.12766					
MARCH	42.20	7.51319	5.26891					
APRIL	23.40	6.92460	6.44025					
MAY	6.60	8.94428	7.64815					
JUNE	0.00	9.24434	8.57277					
JULY	1.30	9.98181	8.62956					
AUGUST	16.60	8.08562	7.57887					
SEPTEMBER	35.00	7.96329	6.61901					
OCTOBER	52.20	7.87096	5.50076					
NOVEMBER	63.20	3.11607	4.40173					
DECEMBER	67.40	3.14838	3.42558					

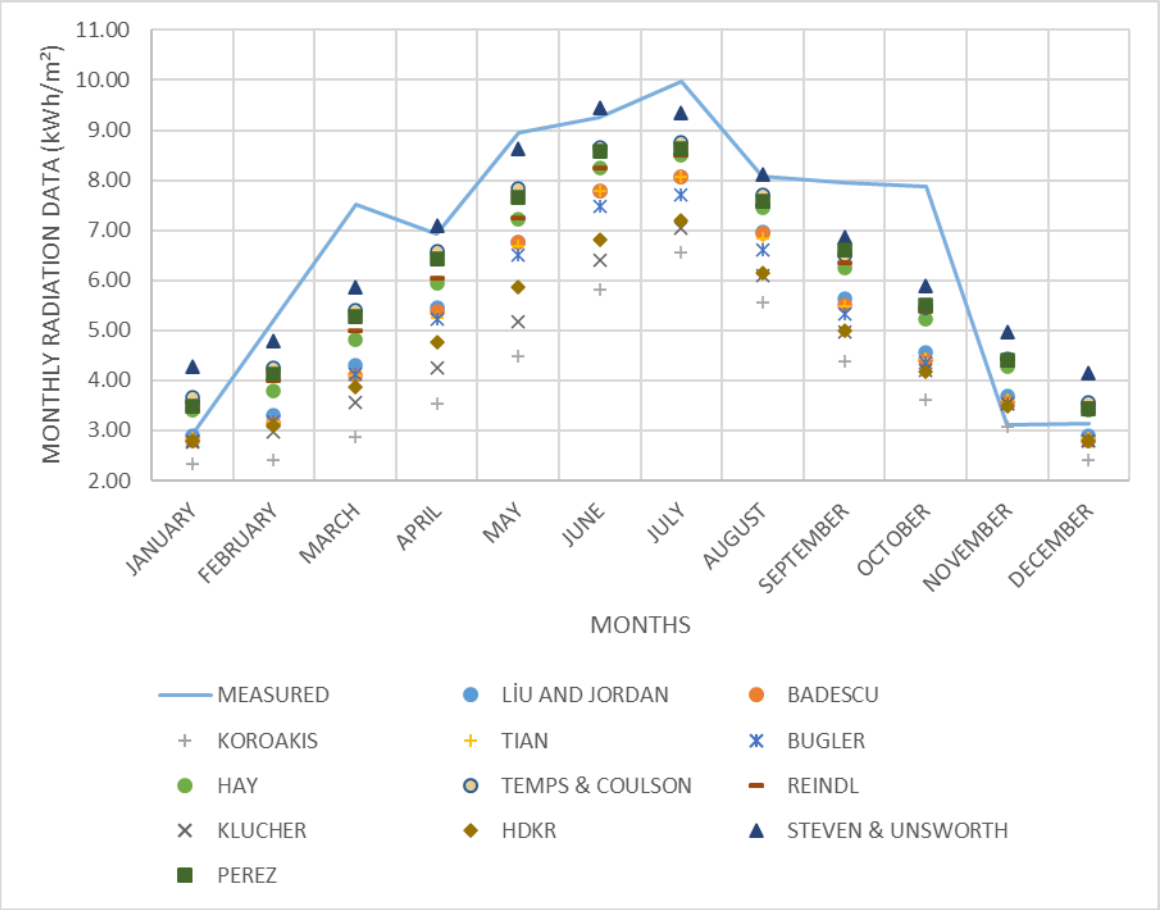

Figure 65 The measured and response of the models

As seen in Table 25 based on the results obtained, it is seen that the model with the highest score explaining the monthly radiation coming to İzmir is the PM. When the R^2 values are compared, the TCM can be said as the second-best model. PM may not be preferred in applications because it requires many parameters when calculating. Therefore, the TCM can be offered as an alternative to the PM for Turkey. The RM is seen as the third best model and the HM as the fourth best model. The difference between SUM and HM does not seem to matter. On the other hand, considering the results in Table 16 the KM seems insufficient to describe the total daily radiation response in İzmir. It is important to note that in order to generalize the overall performance of the model, Turkey needs to measure broader data. This preliminary analysis highlights that there is a significant trend towards accuracy as a result of comparing the data calculated by the models with the recorded datasets.

3.6. The Regression Analysis on Different Radiation Models

Simple regressions have been developed for HM, SUM and PM, RM by using the latitude, longitude and altitude values that are easy to obtain in order to facilitate the acquisition of annual OTAs. In this way, it is aimed to use less and easily available parameters instead of many parameters. Simple regressions developed using latitude, longitude and altitude values are,

$$\begin{aligned}
\beta_{opt,R} &= 10.11515 + 0.70668\phi - 0.01543\lambda + 0.00105z \\
\beta_{opt,Hay} &= 13.34304 + 0.606354\phi - 0.02332\lambda + 0.000974z \\
\beta_{opt,SU} &= 3.75722 + 0.88605\phi + 0.00505\lambda + 0.00085z \\
\beta_{opt,P} &= 7.22814 + 0.77576\phi - 0.00663\lambda - 0.00093z
\end{aligned} \tag{3.5}$$

where z means the altitude of the given location and λ is the longitude. and R^2 are realized as 0.94, 0.85, 0.92 and 0.90 for SUM, RM, HM and PM, respectively. The results of regression analysis given in Table 26, Table 27, Table 28, Table 29. As can be seen from Figure 66 obtained using Eq.3.5., there is a significant improvement in the annual tilt angle evaluation in the SUM.

Table 26 Results of regression analysis for Hay Model

HAY						
	Coefficients	***Standard Error***	***t Stat***	***P-Value***	***R²***	***RMSE***
Constant	13.34304	1.470798535	9.071972368	8.7137E-14	0.92	0.04520
Longitude	-0.02332	0.012712012	-1.83441384	0.070455474		
Latitude	0.60635	0.035374377	17.1410388	5.29328E-28		
Altitude	0.00097	0.000116407	8.367037183	1.99467E-12		

Table 27 Results of regression analysis for Perez Model

PEREZ						
	Coefficients	***Standard Error***	***t Stat***	***P-Value***	***R²***	***RMSE***
Constant	7.22814	1.263559256	5.720458261	1.93298E-07	0.90	0.07380
Longitude	-0.00663	0.010920857	-0.60683613	0.545744855		
Latitude	0.77576	0.030390037	25.52689359	2.53769E-39		
Altitude	0.00093	0.000100005	9.313897637	2.98219E-14		

Table 28 Results of regression analysis for Reindl Model

REINDL						
	Coefficients	***Standard Error***	***t Stat***	***P-Value***	***R²***	***RMSE***
Constant	10.11515	1.472540381	6.869180834	1.46893E-09	0.85	0.08043
Longitude	-0.01543	0.012727067	-1.212398118	0.229066887		
Latitude	0.70668	0.03541627	19.95350295	3.68809E-32		
Altitude	0.00105	0.000116544	9.040710113	1.001E-13		

Table 29 Results of regression analysis for Steven & Unsworth Model

STEVEN & UNSWORTH						
	Coefficients	***Standard Error***	***t Stat***	***P-Value***	***R²***	***RMSE***
Constant	3.75722	1.046857741	3.589047279	0.000581408	0.94	0.04097
Longitude	0.00505	0.009047921	0.558116041	0.578384377		
Latitude	0.88605	0.025178119	35.19139828	3.27921E-49		
Altitude	0.00085	8.28537E-05	10.20159807	5.97209E-16		

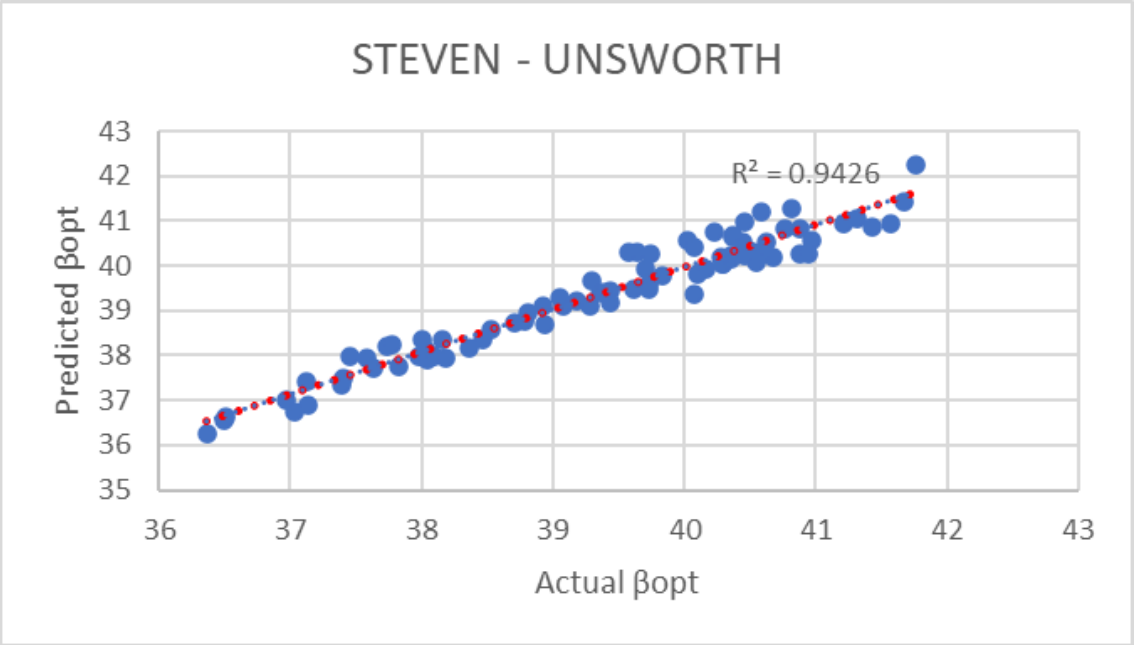

Figure 66 The performance of Steven & Unsworth model

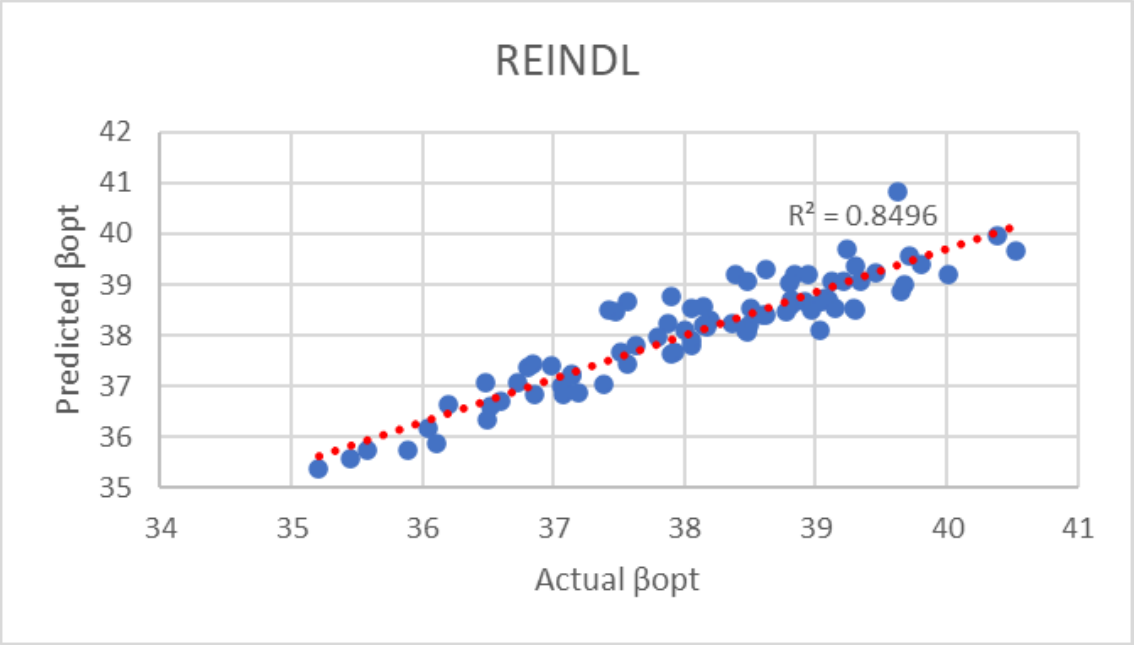

Figure 67 The performance of Reindl model

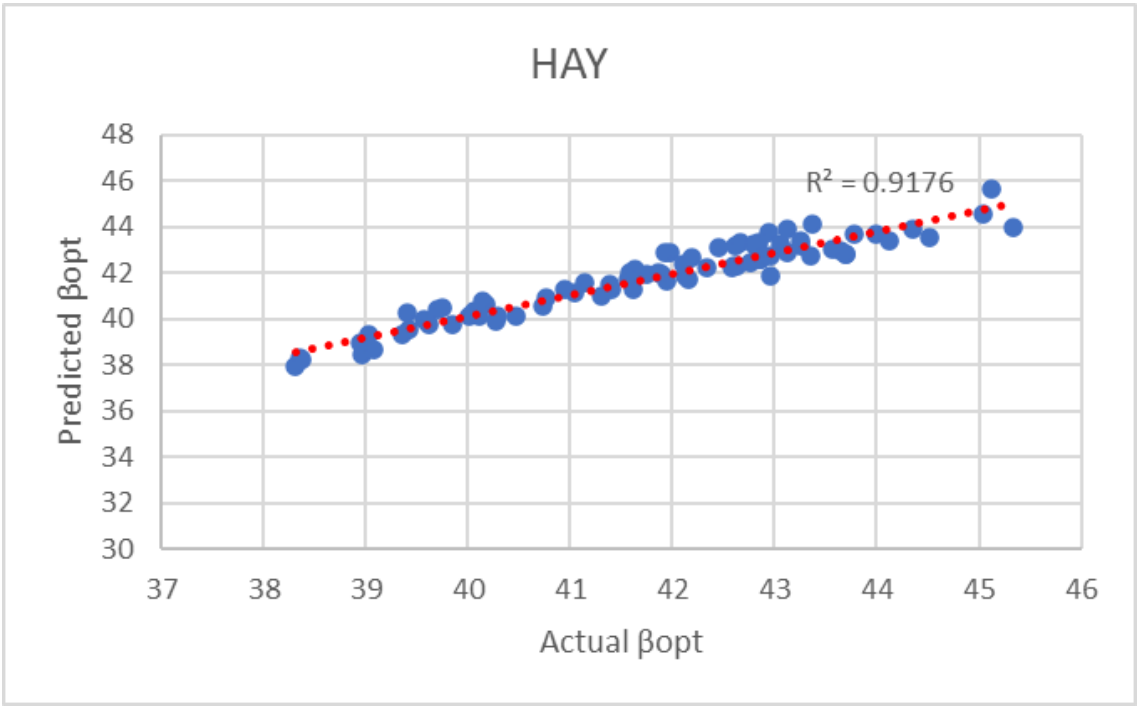

Figure 68 The performance of Hay model

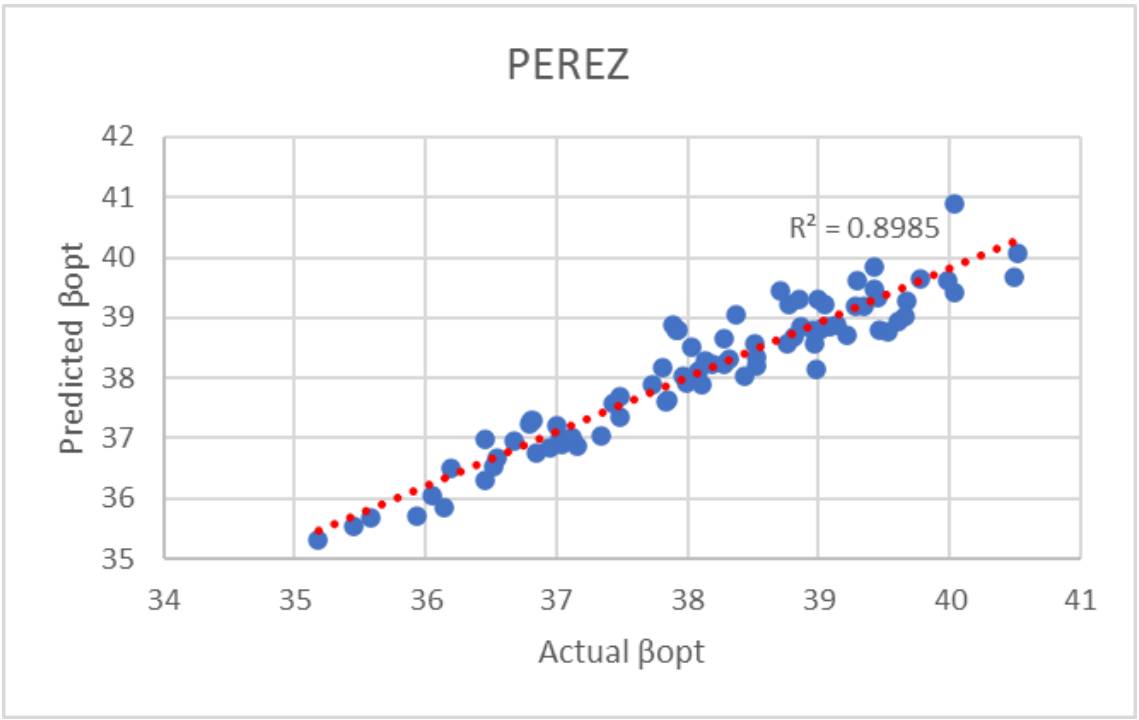

Figure 69 The performance of Perez model

Beside that as can be seen in the analyzes performed, many input parameters are required for the use of the models. For this reason, while the OTA of any model for example Liu & Jordan model, which has simple equation, is known, the regression analysis has been studied in order to obtain the OTA of another model by using the latitude angle.

The simple regression analysis performed by using the OTAs and latitude angles of 81 provinces of Turkey for TCM, KLM, SUM, and PM in each other with R^2 values change between 0.91- 0.99 and results are given in Eq. 3.6. and statistical results are given in Table 30.

$$\begin{aligned}
\beta_{opt,K} &= -14.7384 + 0.524628\phi + 1.020632\beta_{opt,LJ} \\
\beta_{opt,P} &= -4.998 + 0.327985\phi + 0.859996\beta_{opt,LJ} \\
\beta_{opt,TC} &= -1.55942 + 0.354062\phi + 0.676886\beta_{opt,LJ} \\
\beta_{opt,SU} &= -5.96096 + 0.494119\phi + 0.736179\beta_{opt,LJ}
\end{aligned} \tag{3.6}$$

Table 30 Results of regression analysis

PEREZ-LIU&JORDAN	**Standard Error**	**t Stat**	**P-Value**	**R^2**	**RMSE**
	0,934771902	-5,348688386	8,59459E-07	0,97	0,223983
	0,037163284	23,14100205	1,12201E-36		
	0,023314446	14,06789898	4,2321E-23		
KLUCHER-LIU&JORDAN	**Standard Error**	**t Stat**	**P-Value**	**R^2**	**RMSE**
	2,131703243	-6,913899279	1,14826E-09	0,91	0,510784
	0,084749117	12,0429849	1,77965E-19		
	0,053167494	9,867451497	2,26873E-15		
TEMPS&COULSON-LIU&JORDAN	**Standard Error**	**t Stat**	**P-Value**	**R^2**	**RMSE**
	0,224420581	-6,948643241	9,86395E-10	0,99	0,053774
	0,008922183	75,86551428	7,54362E-75		
	0,005597346	63,25537221	8,66317E-69		
STEVEN&UNSWORTH-LIU&JORDAN	**Standard Error**	**t Stat**	**P-Value**	**R^2**	**RMSE**
	0,224420581	-6,948643241	9,86395E-10	0,96	0,280475
	0,008922183	75,86551428	7,54362E-75		
	0,005597346	63,25537221	8,66317E-69		

4. CONCLUSION

One of the most important factors affecting the usability and efficiency of solar energy systems is the OTA of PV panel. The OTA is one of the important factors in increasing the efficiency of the panels. The OTA ensures that the panels receive maximum solar radiation. In the light of this inspiration, OTAs for 81 different provinces of Turkey have been extensively studied in this study using 12 radiation model which are 4 isotropic model and 8 anisotropic radiation models.

The monthly average solar radiation data for 2001-2020 years obtained from NASA POWER Project. Data were performed for each model by using the Golden Ratio Search Method. The acquired monthly average tilt angles converted to annual and seasonal OTAs. Radiation values were compared with TSMS data to compare the accuracy and reliability of the data obtained from the NASA POWER Project. It was concluded that the data were statistically compatible with each other.

In the light of the analyses results, the differences between the cities are due to the difference in latitude and altitude values, and the geographical features of the region are an important factor at different tilt angles. Maximum yield was expressed with geographic and climatic dependencies using anisotropic models. The existence of a new mathematical model was investigated by multivariate regression analysis. Annual and seasonal distribution maps of Turkey were created with the angle values obtained from the analyzes. It has been shown that the angle values increase gradually from the south to the north of Turkey.

The annual OTA is range between 28° and 48° by using different radiation models. Seasonal average OTAs, OTAs for summer and spring seasons mostly vary between 20°-25°. It has been observed that it varies between 39°-53° for fall and 46°-72° for winter. While the monthly average OTAs vary between 51° -75° in January at the beginning of the year, it continues to decrease to 8° -20° in June in the middle of the year and rises again to 54° -74° in December at the end of the year.

When the 12 models used in the analysis for the whole of Turkey were analyzed, it was observed that the results of the KM, which is an isotropic model, and the KLM, RM, SUM, PM, which are anisotropic models, showed a linear relationship with the latitude value. Considering the linear relationship with the latitude of the SUM, also the RM can be said as a viable alternative to this model in Turkey.

As a result of the analyzes made, it is not possible to comment on which model gives the most accurate results for Turkey. Real field data is needed to determine which model is the most accurate for Turkey. The analysis made with the real field data taken for the province of Izmir, it can be concluded that the PM is a suitable model for İzmir. Due to the large number of parameters in the application of the PM, the TCM, which is also highly accurate, can be used as an alternative. If we had real field data for 81 provinces in Turkey, it could be interpreted which model is the best for each province and which model is the best for the whole of Turkey.

In future studies,

- The effects of climatic conditions such as wind, precipitation and humidity on solar radiation values can be examined.
- It can also evaluate the effects of the heights of the measuring stations on the measured solar radiation.
- It can be suggested that an efficiency analysis should be made on the effects of generation, which affects the OTA, on storage optimization in off-grid systems, the solar tracking system that has not been studied much in Turkey, and techno-economic activities.
- Since the data used in this study is satellite data, some results could not be obtained properly, and analysis with more accurate data from meteorology stations may result in clear results.
- In order to determine the accuracy of the models for 81 provinces in Turkey, real field measurements should be made.

REFERENCES

Ajder, A., Durusu, A., Nakir, İ. Impact of Climatic Conditions on PV Array's Optimum Tilt Angle. EJOSAT, 13 **(2018)** 84.

Badescu, V., 3D isotropic approximation for solar diffuse irradiance on tilted surfaces, Renewable Energy, 26 **(2002)** 221.

Bakirci, K., General models for optimum tilt angles of solar panels: Turkey case study, Renewable and Sustainable Energy Reviews, 16 **(2012)** 6149.

Benghanem, M., Optimization of tilt angle for solar panel: Case study for Madinah, Saudi Arabia, Applied Energy, 88 **(2011)** 1427.

Berisha, X., Zeqiri, A., and Meha, D., Solar Radiation-The Estimation of the Optimum Tilt Angles for South-Facing Surfaces in Pristina, preprints **2017**.

Brent, R. P., Algorithms for minimization without derivatives. Englewood Cliffs, NJ: Prentice-Hall, **1973**.

Bugler, J. W., The determination of hourly insolation on an inclined plane using a diffuse irradiance model based on hourly measured global horizontal insolation, Solar Energy, 19 **(1977)** 477.

Bulut, H. and Büyükalaca, O., Simple model for the generation of daily global solar-radiation data in Turkey, Applied Energy, 84 **(2007)** 477.

Chapra, S. C. and Canale, R. P., Numerical methods for engineers, Seventh edition. New York, NY: McGraw-Hill Education, **2015**.

Cooper, P. I., The absorption of radiation in solar stills, Solar Energy, 12 **(1969)** 333.

Çağlar A. Farklı Derece-Gün Bölgelerindeki Şehirler İçin Optimum Eğim Açısının Belirlenmesi. Süleyman Demirel Üniversitesi Fen Bilimleri Enstitüsü Dergisi, 22 **(2018)** 849.

Danandeh, M. A. and Mousavi G , S. M., Solar irradiance estimation models and optimum tilt angle approaches: A comparative study, Renewable and Sustainable Energy Reviews, 92 **(2018)** 319.

Diez-Mediavilla, M., Miguel, A., and Bilbao, J., Measurement and comparison of diffuse solar irradiance models on inclined surfaces in Valladolid (Spain), Energy Conversion and Management, 46 **(2005)** 2075.

Duffie, J. A. and Beckman, W. A., Solar engineering of thermal processes, Vol. 3, Wiley, **1980**.

El-Sebaii, A. A., Al-Hazmi, F. S., Al-Ghamdi, A. A., and Yaghmour ,S. J., Global, direct and diffuse solar radiation on horizontal and tilted surfaces in Jeddah, Saudi Arabia, Applied Energy, 87 **(2010)** 568.

Ertekin, C. and Yaldız, O., Estimation of monthly average daily global radiation on horizontal surface for Antalya (Turkey), Renewable Energy, 17 **(1999)** 95.

Ertekin, C., Evrendilek, F., and Kulcu, R., Modeling Spatio-Temporal Dynamics of Optimum Tilt Angles for Solar Collectors in Turkey, Sensors, 8 **(2008)** 2913.

Gunerhan H. and Hepbasli A., "Determination of the optimum tilt angle of solar collectors for building applications, Building and Environment, 42 **(2007)** 779.

Güneş Panellerinin Tarihçesi, GunesDukkan.com. https://www.gunesdukkan.com/blog/gunes-panellerinin-tarihcesi **(accessed May 30, 2020).**

Hay, J. E., Calculation of monthly mean solar radiation for horizontal and inclined surfaces, Solar Energy, 23 **(1979)** 301.

H. Hottel and B. Woertz, Performance of flat-plate solar-heat collectors, Trans. ASME (Am. Soc. Mech. Eng.) (United States), 64 **(1942)** 64.

History of Solar Energy: Timeline & Invention of Solar Panels | EnergySage, Solar News, May 03, 2018. https://news.energysage.com/the-history-and-invention-of-solar-panel-technology/ **(accessed May 30, 2020)**.

Iqbal, M., An Introduction to Solar Radiation. Elsevier, **2012**.

Kabala, Z. J., Sensitivity analysis of a pumping test on a well with wellbore storage and skin, Advances in Water Resources, 24 (2001) 483.

Kacira, M., Simsek, M., Babur, Y., and Demirkol, S., Determining optimum tilt angles and orientations of photovoltaic panels in Sanliurfa, Turkey, Renewable Energy, 29 **(2004)** 1265.

Kallioğlu, M. A., Optimization of tilt angle for solar panel, 2nd International Energy & Engineering Conference 12-13 October 2017, Gaziantep, Turkey, **2017**, p. 8.

Kennedy, J. and Eberhart, R., Particle swarm optimization, Proceedings of ICNN'95 - International Conference on Neural Networks, 4 **(1995)** 1942.

Kılıç, A. and Öztürk, A., Güneş enerjisi, Kipaş Dağıtımcılık, **1983**.

Kiefer, J., Sequential minimax search for a maximum, American Mathematical Society, 4 **(1953)** 502.

Klucher, T. M., Evaluation of models to predict insolation on tilted surfaces, Solar Energy, 23 **(1979)** 111.

Koronakis, P. S., On the choice of the angle of tilt for south facing solar collectors in the Athens basin area, Solar Energy, 36 **(1986)** 217.

Liu, B. and Jordan, R., Daily insolation on surfaces tilted towards equator, *ASHRAE J.*, 10 **(1961)** 526.

Menges, H. O., Ertekin, C., and Sonmete, M. H., Evaluation of global solar radiation models for Konya, Turkey, Energy Conversion and Management, 47 **(2006)** 18.

Mousavi Maleki, S., Hizam, H., and Gomes, C., Estimation of Hourly, Daily and Monthly Global Solar Radiation on Inclined Surfaces: Models Re-Visited, Energies, 10 **(2017)** 134.

Muneer, T., Solar radiation model for Europe, Building Services Engineering Research and Technology, 11 **(1990)** 153.

NASA POWER | Data Access Viewer, https://power.larc.nasa.gov/data-access-viewer/ **(accessed July 28, 2021).**

Oğulata, R. T. and Oğulata, S. N., Solar radiation on Adana, Turkey, Applied Energy, 71 **(2002)** 351.

Oğulata, R. T., Energy sector and wind energy potential in Turkey, Renewable and Sustainable Energy Reviews, 7 **(2003)** 469.

Orgill, J. F. and Hollands, K. G. T., Correlation equation for hourly diffuse radiation on a horizontal surface, Solar Energy, 19 **(1977)** 357.

Perez, R., Ineichen, P., Seals, R., Michalsky, J., and Stewart, R., Modeling daylight availability and irradiance components from direct and global irradiance, Solar Energy, 44 **(1990)** 271.

Reindl, D. T., Beckman, W. A., and Duffie, J. A., Evaluation of hourly tilted surface radiation models, Solar Energy, 45 (1990) 9.

Skartveit, A. and Olseth, J. A., A model for the diffuse fraction of hourly global radiation, Solar Energy, 38 **(1987)** 271.

Smith, C. J., Forster , P. M., and Crook, R., An all-sky radiative transfer method to predict optimal tilt and azimuth angle of a solar collector, Solar Energy, 123 **(2016)** 88.

Stanciu, C. and Stanciu, D., Optimum tilt angle for flat plate collectors all over the World – A declination dependence formula and comparisons of three solar radiation models, Energy Conversion and Management, 81 **(2014)** 133.

Steven, M. D. and Unsworth, M. H., The angular distribution and interception of diffuse solar radiation below overcast skies, Quarterly Journal of the Royal Meteorological Society, 106 **(1980)** 57.

Şahin , A. U., A Particle Swarm Optimization Assessment for the Determination of Non-Darcian Flow Parameters in a Confined Aquifer, Water Resource Manage, 32 **(2018)** 751.

Şenpınar, A. Güneş açilarina bağli olarak optimum sabit güneş paneli açisinin hesaplanmasi, Fırat Üniversitesi Doğu Araştırmaları Dergisi, 4 **(2006)** 36.